

UNCLASSIFIED

AD NUMBER
ADB243646
NEW LIMITATION CHANGE
TO Approved for public release, distribution unlimited
FROM Distribution authorized to U.S. Gov't. agencies only; Proprietary Info; Oct 98 Other requests shall be referred to USAMRMC, Ft. Detrick, MD 21702-5012
AUTHORITY
USAMRMC ltr, 23 Aug 2001

THIS PAGE IS UNCLASSIFIED

AD _____

GRANT NUMBER DAMD17-97-1-7344

TITLE: Pathogenesis of Germline and Somatic NF1 Rearrangements

PRINCIPAL INVESTIGATOR: Karen Stephens, Ph.D.

CONTRACTING ORGANIZATION: University of Washington
Seattle, Washington 98195

REPORT DATE: October 1998

TYPE OF REPORT: Annual

PREPARED FOR: U.S. Army Medical Research and Materiel Command
Fort Detrick, Maryland 21702-5012

DISTRIBUTION STATEMENT: Distribution authorized to U.S. Government agencies only (proprietary information, Oct 98). Other requests for this document shall be referred to U.S. Army Medical Research and Materiel Command, 504 Scott Street, Fort Detrick, Maryland 21702-5012.

The views, opinions and/or findings contained in this report are those of the author(s) and should not be construed as an official Department of the Army position, policy or decision unless so designated by other documentation.

1 9 9 9 0 4 1 5 0 3 4

NOTICE

USING GOVERNMENT DRAWINGS, SPECIFICATIONS, OR OTHER DATA INCLUDED IN THIS DOCUMENT FOR ANY PURPOSE OTHER THAN GOVERNMENT PROCUREMENT DOES NOT IN ANY WAY OBLIGATE THE U.S. GOVERNMENT. THE FACT THAT THE GOVERNMENT FORMULATED OR SUPPLIED THE DRAWINGS, SPECIFICATIONS, OR OTHER DATA DOES NOT LICENSE THE HOLDER OR ANY OTHER PERSON OR CORPORATION; OR CONVEY ANY RIGHTS OR PERMISSION TO MANUFACTURE, USE, OR SELL ANY PATENTED INVENTION THAT MAY RELATE TO THEM.

LIMITED RIGHTS LEGEND

Award Number: DAMD17-97-1-7344
Organization: University of Washington
Location of Limited Rights Data (Pages):

Those portions of the technical data contained in this report marked as limited rights data shall not, without the written permission of the above contractor, be (a) released or disclosed outside the government, (b) used by the Government for manufacture or, in the case of computer software documentation, for preparing the same or similar computer software, or (c) used by a party other than the Government, except that the Government may release or disclose technical data to persons outside the Government, or permit the use of technical data by such persons, if (i) such release, disclosure, or use is necessary for emergency repair or overhaul or (ii) is a release or disclosure of technical data (other than detailed manufacturing or process data) to, or use of such data by, a foreign government that is in the interest of the Government and is required for evaluational or informational purposes, provided in either case that such release, disclosure or use is made subject to a prohibition that the person to whom the data is released or disclosed may not further use, release or disclose such data, and the contractor or subcontractor or subcontractor asserting the restriction is notified of such release, disclosure or use. This legend, together with the indications of the portions of this data which are subject to such limitations, shall be included on any reproduction hereof which includes any part of the portions subject to such limitations.

THIS TECHNICAL REPORT HAS BEEN REVIEWED AND IS APPROVED FOR PUBLICATION.

N. M. ...
4-2-99

REPORT DOCUMENTATION PAGE

Form Approved
OMB No. 0704-0188

Public reporting burden for this collection of information is estimated to average 1 hour per response, including the time for reviewing instructions, searching existing data sources, gathering and maintaining the data needed, and completing and reviewing the collection of information. Send comments regarding this burden estimate or any other aspect of this collection of information, including suggestions for reducing this burden, to Washington Headquarters Services, Directorate for Information Operations and Reports, 1215 Jefferson Davis Highway, Suite 1204, Arlington, VA 22202-4302, and to the Office of Management and Budget, Paperwork Reduction Project (0704-0188), Washington, DC 20503.

1. AGENCY USE ONLY (Leave blank)	2. REPORT DATE October 1998	3. REPORT TYPE AND DATES COVERED Annual (30 Sep 97 - 29 Sep 98)	
4. TITLE AND SUBTITLE Pathogenesis of Germline and Somatic NF1 Rearrangements		5. FUNDING NUMBERS DAMD17-97-1-7344	
6. AUTHOR(S) Stephens, Karen, Ph.D.			
7. PERFORMING ORGANIZATION NAME(S) AND ADDRESS(ES) University of Washington Seattle, Washington 98195		8. PERFORMING ORGANIZATION REPORT NUMBER	
9. SPONSORING / MONITORING AGENCY NAME(S) AND ADDRESS(ES) U.S. Army Medical Research and Materiel Command Fort Detrick, Maryland 21702-5012		10. SPONSORING / MONITORING AGENCY REPORT NUMBER	
11. SUPPLEMENTARY NOTES			
12a. DISTRIBUTION / AVAILABILITY STATEMENT Distribution authorized to U.S. Government agencies only (proprietary information, Oct 98). Other requests for this document shall be referred to U.S. Army Medical Research and Materiel Command, 504 Scott Street, Fort Detrick, Maryland 21702-5012.		12b. DISTRIBUTION CODE	
13. ABSTRACT (Maximum 200 words) We have determined that novel germline and somatic chromosome rearrangements involving the NF1 gene are common in specific subsets of NF1 patients. Patients with facial abnormalities and an early age of onset of dermal neurofibromas often carried a germline microdeletion of 1-2 Mb that deleted an NF1 allele and flanking DNA. Over 3/4 of these microdeletions had chromosomal breakpoints that mapped to the same small interval. These data suggest that microdeletions tend to occur at specific sites and they alter the expression of unknown genes that predisposes the patients to early tumor development. Identification of these sites is in progress. In related studies, we determined that leukemic cells of NF1 children with malignant myeloid disorders commonly undergo double mitotic recombination events at common breakpoint intervals. This results in a cell without functional NF1 alleles and a large interstitial chromosome segment that may be altered in as yet unknown ways. Both of these remarkable rearrangements appear to contribute to tumor development.			
14. SUBJECT TERMS Neurofibromatosis microdeletions, tumorigenesis, mitotic recombination		15. NUMBER OF PAGES 109	
		16. PRICE CODE	
17. SECURITY CLASSIFICATION OF REPORT Unclassified	18. SECURITY CLASSIFICATION OF THIS PAGE Unclassified	19. SECURITY CLASSIFICATION OF ABSTRACT Unclassified	20. LIMITATION OF ABSTRACT Limited

Figure 1 has been withdrawn from this draft per Principal Investigator. Pages of the draft have been renumbered and resubmitted to Journal.

Figure 3 is a photo of cell chromosomes. This figure is in color and is difficult to reproduce for this draft manuscript per Principal Investigator. Refer to reprint when published.

FOREWORD

Opinions, interpretations, conclusions and recommendations are those of the author and are not necessarily endorsed by the U.S. Army.

___ Where copyrighted material is quoted, permission has been obtained to use such material.

___ Where material from documents designated for limited distribution is quoted, permission has been obtained to use the material.

ky X Citations of commercial organizations and trade names in this report do not constitute an official Department of Army endorsement or approval of the products or services of these organizations.

NA In conducting research using animals, the investigator(s) adhered to the "Guide for the Care and Use of Laboratory Animals," prepared by the Committee on Care and use of Laboratory Animals of the Institute of Laboratory Resources, national Research Council (NIH Publication No. 86-23, Revised 1985).

ky X For the protection of human subjects, the investigator(s) adhered to policies of applicable Federal Law 45 CFR 46.

NA In conducting research utilizing recombinant DNA technology, the investigator(s) adhered to current guidelines promulgated by the National Institutes of Health.

NA In the conduct of research utilizing recombinant DNA, the investigator(s) adhered to the NIH Guidelines for Research Involving Recombinant DNA Molecules.

NA In the conduct of research involving hazardous organisms, the investigator(s) adhered to the CDC-NIH Guide for Biosafety in Microbiological and Biomedical Laboratories.

Karen Stephens 10/26/98
PI - Signature Date

Table of Contents

Cover page	1
SF298 form	2
Foreword	3
Table of contents	4
I. Introduction	5
II. Body	
A. Progress during year 1 on Technical Objective 1	6
B. Progress during year 1 on Technical Objective 2	7
C. Progress during year 1 on Technical Objective 3	14
III. Conclusions	
III. Conclusions	15
IV. References	15
Appendices	
A. Abstracts from this research	17
B. Manuscript	19-61
Maruyama K, Weaver M, Leppig KA, Farber R, Aylsworth A, Ortenberg J, Rubenstein A, Immken L, Haan E, Curry C, and Stephens K. <i>NF1</i> microdeletions with clustered breakpoints identified by a quantitative PCR gene dosage assay. <i>Am J Hum Genet</i> , submitted.	
C. Manuscript	62-85
Stephens K, Weaver M, Leppig KA, Maruyama K, Davis EM, Espinosa III R, Freedman MH, Emanuel P, Side L, LeBeau MM, Shannon K. Tumor suppressor inactivation by double mitotic recombination at clustered breakpoints. In preparation; draft attached.	
D. Manuscript	86-108
Shen S, Battersby S, Weaver M, Clark E, Lutz EM, Stephens K, Harmar AJ. Mapping of the human serotonin transporter and carboxypeptidase D genes to a 1 Mb YAC/PAC contig on 17q11.1: hemizyosity in a patient with a deletion spanning the adjacent neurofibromatosis 1 gene. In preparation; draft attached.	

I. Introduction

Neurofibromatosis type 1 is a common autosomal dominant tumor-susceptibility disorder (1). The causal gene, NF1, encodes the protein neurofibromin which can function as a tumor suppressor by negatively regulating ras and thereby disrupting signal transduction and growth control (2, 3, 4). Virtually every affected individual develops benign cutaneous neurofibromas, while the development of other tumors such as malignant myeloid disorders are a less common complication (5, 6).

The subject of this research project is to investigate the genetic mechanisms and pathology underlying both germline and somatic microdeletions involving the NF1 gene. Our published and preliminary data indicated that NF1 patients with germline microdeletions spanning one NF1 allele may be predisposed to early onset of cutaneous neurofibromas. The identification and mapping of NF1 microdeletions will determine the size of the microdeletions and address their putative contribution to the excessive tumor burden of these patients. We have also demonstrated that the leukemic cells of NF1 children with malignant myeloid disorders show loss of heterozygosity at NF1 and adjacent loci. Preliminary data suggested that LOH in these tumors can arise by a novel mechanism. The analyses of additional patients/tumors will address the molecular nature of these somatic rearrangements and their contribution to malignancy.

Hypotheses to be tested:

1. Deletion of a critical region (gene) contiguous to NF1 predisposes individuals to an early onset and/or large numbers of cutaneous neurofibromas.
2. A novel chromosomal rearrangement in a malignant precursor cell, which results in somatic interstitial uniparental disomy (or interstitial isodisomy), is a frequent event in leukemic cells of NF1 patients with malignant myeloid disorders. Such rearrangements may contribute to the development of these tumors in children with NF1.

Background:

In 1992 we reported the first NF1 patient with a submicroscopic deletion spanning the entire NF1 gene and flanking contiguous genetic material (7). This patient carried a de novo deletion estimated at 7.4 cM and had abnormal facial features, mental retardation, and an excessive number of cutaneous neurofibromas. The identification of additional microdeletion patient (both de novo and familial) by us (8, 9, 10) (and Appendix B) and other investigators (11, 12, 13, 14) have demonstrated that NF1 microdeletion patients have a consistent phenotype of abnormal facial features and early onset (<age 10 yr) or large numbers (>85 centile) of cutaneous neurofibromas for their age. These observations on selected patients suggested that deletion of a novel gene contiguous to NF1 predisposed to tumorigenesis. NF1 contiguous gene deletions may also account for other features observed in some of our patients including Madelung deformity, skin and skeletal features consistent with a connective tissue disorder and neoplasms at a young age (7, 8, 9, 10). To test this hypothesis, patients need to be screened for NF1 microdeletions regardless of their phenotype, the extent of the deletions need to be mapped, and phenotype/genotype studies performed. To facilitate screening for NF1 microdeletions we developed a PCR-based NF1 gene dosage assay (see manuscript Appendix B; Technical Objective 1).

Children with NF1 are at 200-500 increased risk of developing malignant myeloid disorders (1, 6, 15). Approximately 50% of primary leukemic cells show loss of constitutional heterozygosity (LOH) at the NF1 locus. We recently discovered a patient whose LOH resulted from a novel somatic rearrangement - interstitial isodisomy most likely resulting from double mitotic recombination. The novelty of this rearrangement prompted us to map the LOH regions in leukemic cells of other NF1 children to investigate the frequency, mechanism, and pathology of such rearrangements.

II. Body

Section A. Technical Objective 1: To identify additional patients with large germline NF1 deletions.

- Task 1: Months 1-6: develop and optimize an *NF1* gene dosage PCR assay for detecting deletions at the 5' end of the gene.
- Task 2: Months 4-7: assay the ~105 DNA samples currently in the lab for 3' *NF1* deletions.
- Task 3: Months 1-25: obtain pathological tissue samples or purified DNA from NF1 clinic patients; perform the 5' and 3' *NF1* gene dosage PCR assays for all samples; calculate the *NF1* gene dosage to identify deletion patients.
- Task 4: Months 20-25: Determine the frequency of *NF1* deletions. Write a manuscript on deletion screening protocol and frequency.

Progress during year 1 on Technical Objective 1

The timeline for accomplishing Objective 1 was altered for two important reasons. First, we chose to focus on and complete Objective 3 (see below) because samples were available earlier than expected and the results were so exciting. Second, we chose to wait for delivery of a new instrument which will permit development of an automated gene dosage PCR assay for the 5' end of the *NF1* gene.

To date, we have chosen appropriate primers and determined amplification conditions for a segment of *NF1* exon 5, which will be utilized for the assay of *NF1* gene dosage at the 5' end of the gene. Initial attempts to develop an assay for *NF1* exon 1 failed. We were unable to identify primers for specific amplification of the expressed *NF1* gene on chromosome 17q11.2, rather than the numerous pseudogenes located on other autosomes. Primers and multiplex amplification conditions were also determined for the disomic control gene, APP. We are just beginning to focus on the collection of patient tissues or purified DNAs from our clinical collaborators; samples for 20 individuals have been collected to date.

NOTE: The new strategy described in the following paragraph is proprietary information and not for publication or distribution.

In the next 2 months, we will assess the use of the Applied Biosystems Inc. 7700 Tac-Man instrument for use as a automated *NF1* gene dosage assay. This instrument measures real time quantitative PCR from 96 samples simultaneously. We will assess a new methodology using a fluorescent dye called SyberGreen which quantitatively binds to the minor groove of the double stranded DNA product. This method should permit us to utilize the primers and conditions we have already established for the 5' and 3' *NF1* gene dosage assays (exons 5 and 32, respectively). This methodology will be validated using the same *NF1* disomic and monosomic samples that were evaluated in our manual gene dosage assay (see manuscript in Appendix B). If the automated assay is as sensitive and specific as the manual one, we will develop automated assays for *NF1* exon 5 also.

END of proprietary information.

Section B. Technical Objective 2: Identify a critical deletion region associated with early onset of neurofibromas.

- Task 1: Months 1-12: Map the location of additional loci to the *NFI* region by somatic cell hybrid analysis; identify any physical intervals that lack markers.
- Task 2: Month 13-14: Write a manuscript describing the physical map of the *NFI* region; assess the need for identification and mapping of new marker loci to certain physical intervals. If necessary, obtain YACs, PACs, cosmids of the intervals.
- Task 3: Months 14-20: Perform FISH to confirm that the large physical clones map to the interval of interest. Make a plasmid library, screen for single copy clones, sequence, and design primers to map new markers on somatic cell hybrid panels to the critical interval.
- Task 4: Months 1-30: construct hybrid cell lines from lymphoblasts of newly identified deletion patients; delineate the extent of the deletions by genotyping of regional markers on hybrid lines.
- Task 5: Months 20-36: determine if there is a correlation between deletion extent and age of onset of neurofibromas; write a manuscript of study results; assess whether an *NFI* gene dosage PCR assay or FISH assay to detect deletion of the critical region has sufficient predictive value to warrant development of a diagnostic test.

NOTE: The following data regarding progress on Technical Objective 2 is proprietary information and not for publication or distribution.

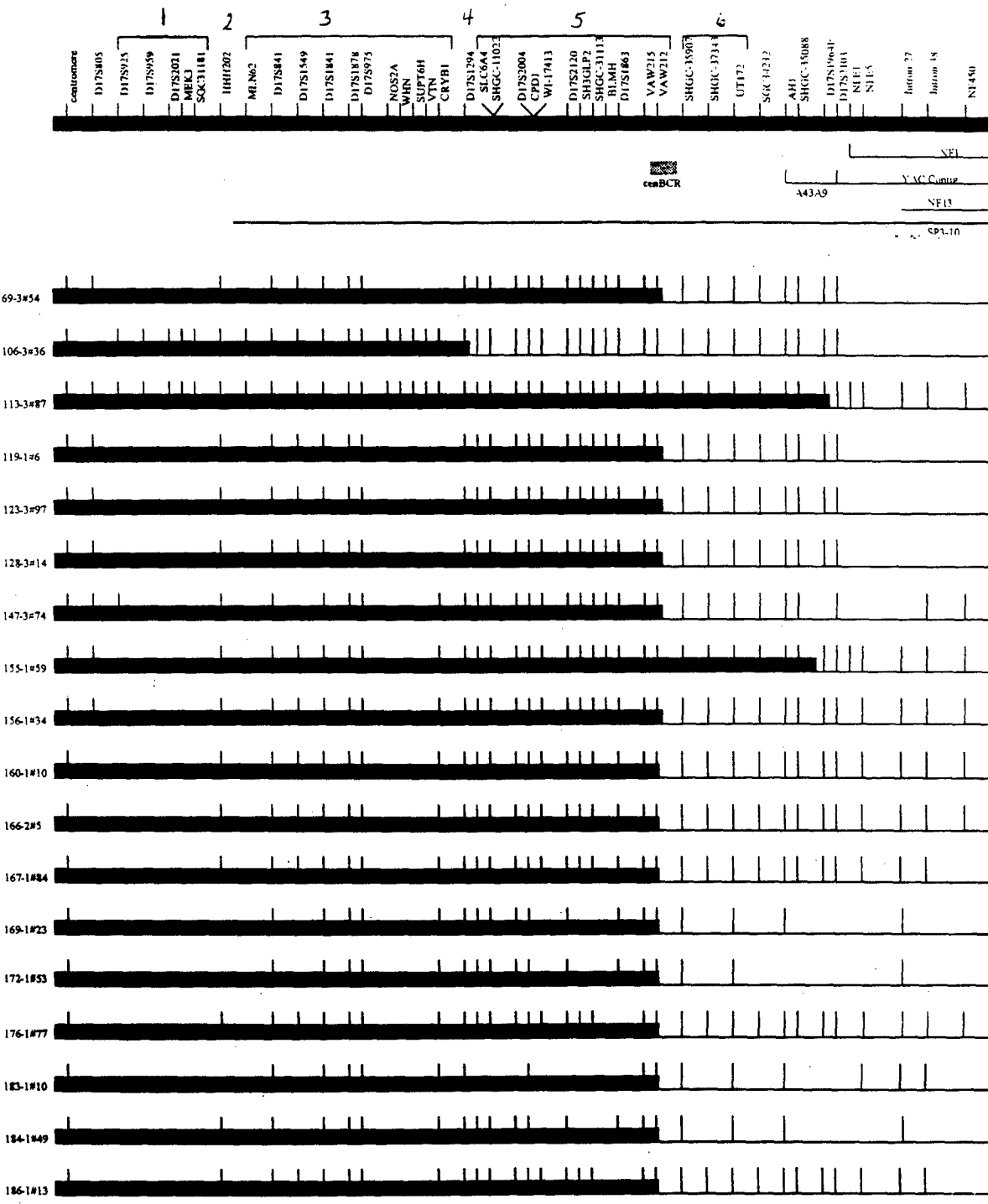
Progress during year 1 on Technical Objective 2:

We have made significant progress on Objective 2; a manuscript that describes mapping of the serotonin transporter and carboxypeptidase D genes in the *NFI* region is in Appendix D.

Using a mapping panel of somatic cell hybrid lines from 18 probands with *NFI* microdeletions, we have mapped >50 new loci to the *NFI* region for a total of >85 loci (Figures 1-4). Remarkably, we found that both the centromeric breakpoints and the telomeric breakpoints were clustered in common marker intervals (Figures 1A and 1B, following pages). For 15 of the 18 probands, the centromeric breakpoints were between markers in intervals 5 and 6, which was defined as the centromeric breakpoint cluster region (cenBCR). For 14 of the 18 probands, the telomeric breakpoints mapped between markers SH3GLP1 and D17S1880, which was defined as the telBCR. Somatic cell hybrid lines were constructed during year 1 for 4 of these 18 patients.

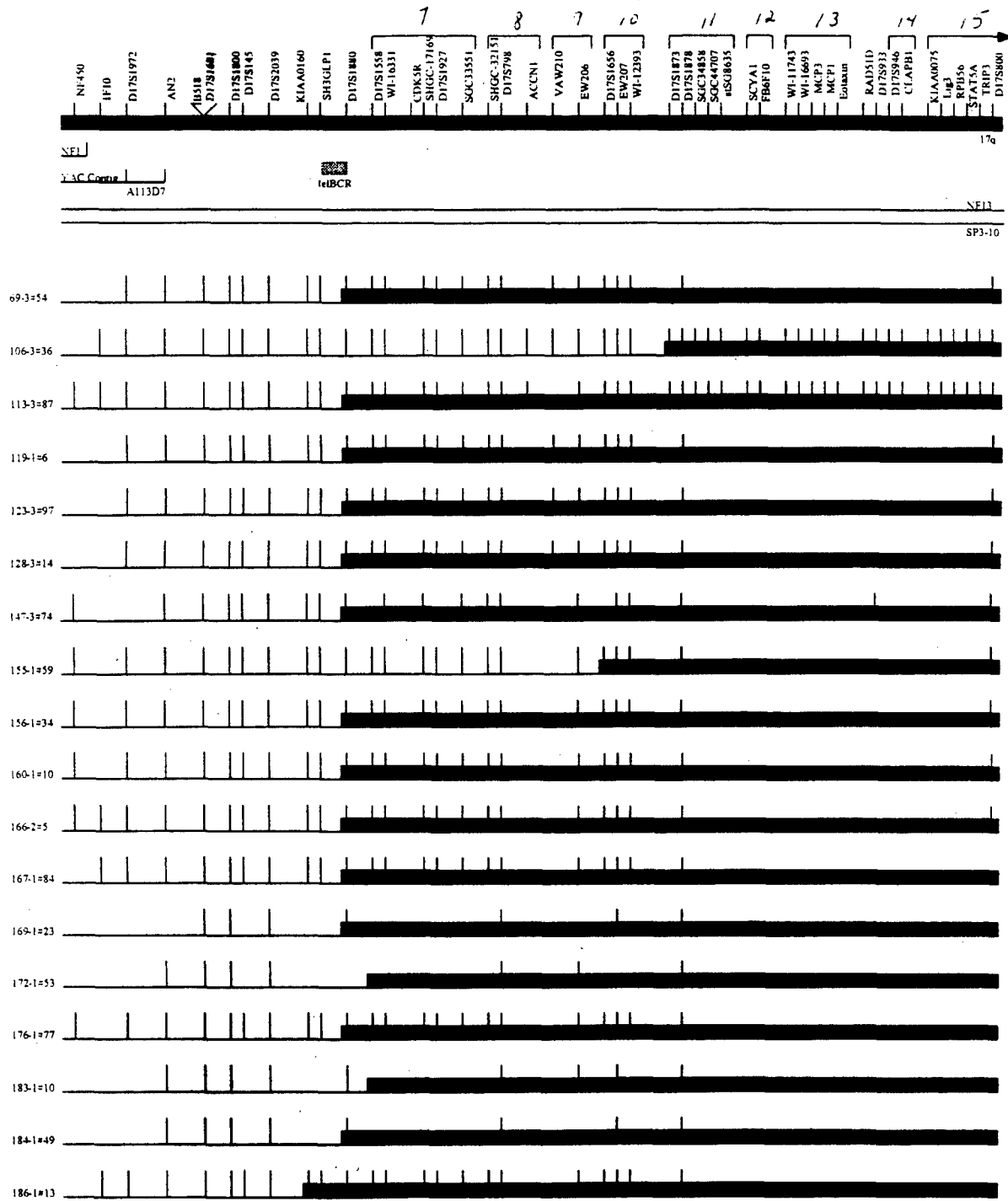
Among the ~85 loci mapped to date, 40 are known genes or expressed sequence tag sites (ESTs) in the *NFI* microdeletion region (Figures 1-4). In collaboration with Dr. Anthony Harmar's laboratory, we have mapped the serotonin transporter (SLC6A4) and the carboxypeptidase D (CPD1) genes to the to marker region 5, which is just centromeric to the cenBCR. These 2 genes are deleted in patient UWA106-3#36 who carries the largest microdeletion identified to date (Figures 1,2 and Shen et al. manuscript in Appendix D). Because these genes are not deleted in other patients, it is considered unlikely that they make a major contribution to the *NFI* microdeletion tumor phenotype. As described in Shen et al., we have identified a marker within 15 kb of the centromeric breakpoint of patient UWA106-3. Efforts to clone this breakpoint are in progress and should provide important information about the mechanism(s) of germline *NFI* microdeletions.

FIGURE 1A.



proprietary information

FIGURE 1B.



proprietary information

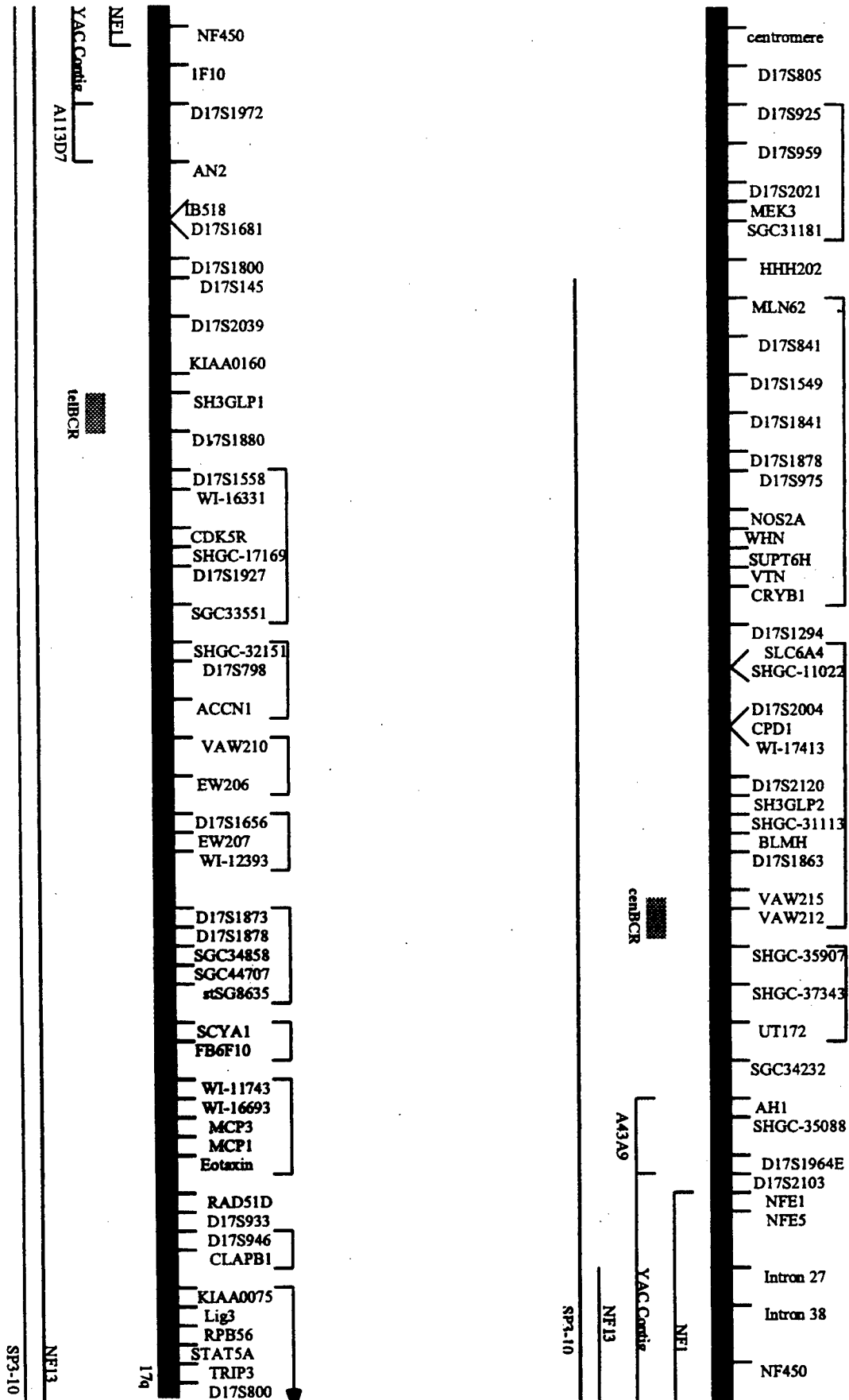


Figure 2.

Proprietary Information

SP3-10

NEI3

17q

SP3-10

A43A9

NF13

YAC Centric

NEI

Figure 3

Proprietary Information

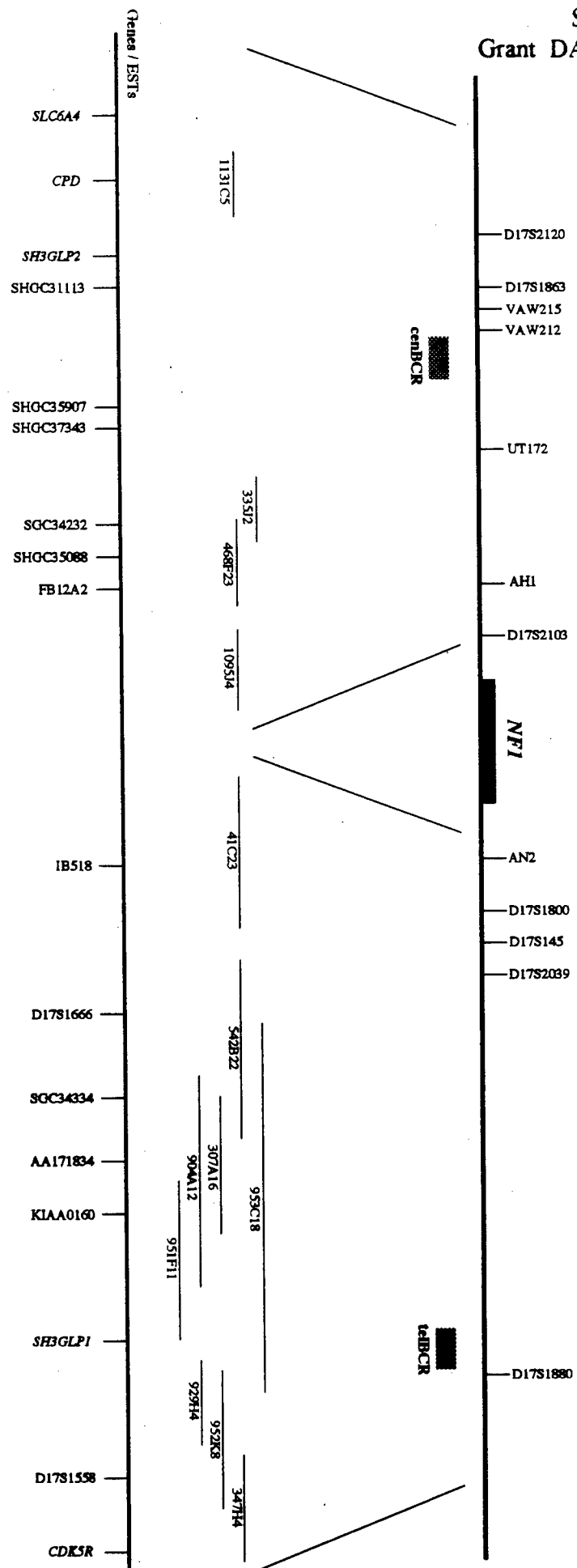
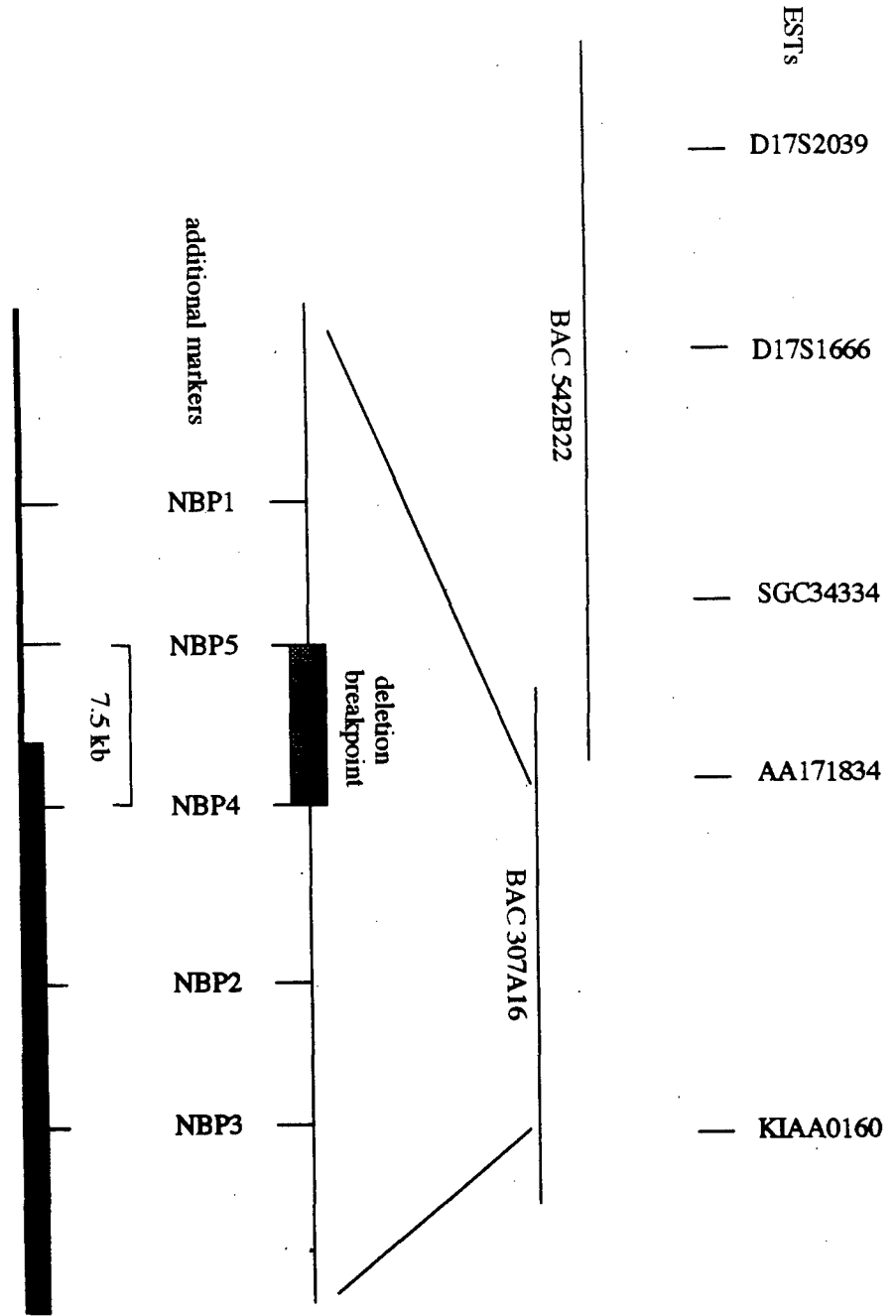


Figure 4.

proprietary information

Patient 186-#13 - Telomeric Breakpoint Mapping



Proprietary information continued:

The clustering of breakpoints at the cenBCR and telBCR suggest that these regions carry recombination prone sequences. To identify such sequences, Dr. Michael Dorschner (a postdoctoral fellow) has focused initially on cloning the telBCR. As depicted in Figure 3, we have constructed a contig of BAC clones across the telBCR by screen a human BAC library with markers we had previously mapped to this region. We will map and sequence the telomeric breakpoint in patient UWA69-3. This sequence information will then be utilized to first, determine how close all the breakpoints are that map to the telBCR, and second, to 'jump over' or cross the novel joint of the deletion in patient 69-3 and thereby obtain sequence information for the cenBCR.

We are also mapping the telomeric breakpoint of patient 186-1 because early studies suggested it disrupted the gene KIAA0160. This was confirmed and Dr. Dorschner is now within 7.5 kb of mapping this breakpoint of patient 186-1, which does not map within the telBCR (Figure 1 & 4). Cloning of this breakpoint will provide an alternative method for 'jumping' across the novel DNA sequences to the cenBCR in case unexpected difficulties arise in our initial strategy of crossing from the telBCR in patient 69-3 as described above. In addition, patient 186-1 is a somatic mosaic for the *NFI* microdeletion; cloning of this breakpoint will permit accurate determination of the levels of mosaicism that resulted in her extraordinarily severe tumor burden and facilitate a comparison of somatic versus germline *NFI* microdeletion breakpoints.

Legend of Figure 1. Physical map of the *NFI* region defined by analysis of *NFI* microdeletions. The top line is a non-scaled schematic of loci in the chromosome 17 *NFI* region; the relative positions of markers in bracketed intervals are unknown. Estimates of physical distances include the YAC contig at 700 kb and the location of UT172, estimated at about 1.5 Mb centromeric to *NFI*(6, 16). A schematic of the deleted chromosome 17 homolog is shown for each proband. Thin lines are deleted regions, thick lines are not deleted, and vertical marks indicate the loci assayed by PCR amplification of somatic hybrid cell lines carrying the single deleted chromosome 17 homolog. Data showing the presence of all loci in the hybrid lines carrying the undeleted chromosome 17 for each patient are not shown. *NFI* exon 32 was assayed by the gene dosage assay. P1-9, a 65 kb probe spanning *NFI* exons 2-11 assayed by FISH was deleted (data not shown).

Legend of Figure 2. Detailed physical map of the *NFI* microdeleted region. This is a larger and more legible version of the map described and depicted in Figure 1.

Legend of Figure 3. Physical contig map of the *NFI* microdeletion region. The upper line represents a map of the *NFI* region showing a few anchor loci and the cenBCR and telBCR; numbered segments in the center are BAC clones that we have mapped to date; the lower line depicts genes and ESTs mapped to the region.

Legend of Figure 4. Mapping of the telomeric deletion breakpoint of patient 186-1 (deleted hybrid#13). The telomeric breakpoint of this patient does not map to the common telBCR. ESTs and BACs were mapped to the region, additional markers developed, and we are now within 7.5 kb of this telomeric breakpoint.

Note: End of proprietary information.

Section C: Technical Objective 3: To determine if somatic uniparental disomy (UPD) of the *NF1* region is a frequent event in leukemic tumor tissue and to investigate somatic mechanisms of uniparental disomy.

- Task 1: Months 1-12: obtain additional tumor samples and determine their *NF1* gene dosage by the gene dosage PCR assay; confirm by *NF1* FISH that tumors predicted to undergo LOH by UPD have two *NF1* alleles, while those predicted to result from LOH by deletion have one *NF1* allele; determine the frequency of UPD-LOH.
- Task 2: Months 10-25: Map the extent of each uniparental disomy region; assay normal tissue for mosaicism for the UPD of the *NF1* region; write a manuscript addressing mechanisms of UPD-LOH.

Progress during year 1 on Technical Objective 3:

Technical Objective 3, Tasks 1 and 2, have been achieved and a nearly completed manuscript draft, which will be submitted in the next month as an original article to the journal *Nature Genetics* is in Appendix C of this report. Because the results of this study were so remarkable and novel, we decided to focus on this aim earlier during the study period than was anticipated in the original Statement of Work.

A brief summary of the results detailed in the attached manuscript "Tumor suppressor inactivation by double mitotic recombination at clustered breakpoints" follow.

The patterns of LOH at chromosome 17 loci were analyzed to gain insight into the mechanisms leading to allelic loss of *NF1* in primary leukemia cells of *NF1* children. Analysis of bone marrows from 11 unselected cases showed that LOH occurred by two distinct mechanisms, each of which resulted in loss of the normal *NF1* allele. Three tumors (30%) had interstitial microdeletions between D17S1294 and D17S250, an estimated distance of 22 cM or 17 Mb that spanned the normal *NF1* gene at chromosome 17q11.2. The remaining 8 cases (70%) resulted from isodisomy for a 50 Mb chromosomal segment harboring a defective *NF1* allele. In at least 4 of these cases, the isodisomic segment was interstitial to the chromosome 17q arm and estimated to be 55 Mb in length.

Although somatic isodisomy of varying extent commonly leads to LOH in tumors, we believe this is the first report of interstitial isodisomy. We propose that interstitial isodisomy arose by a double mitotic recombination event between non-sister chromatids during the S/G2 phase of the cell cycle of an ancestral cell. Remarkably, the isodisomic breakpoints in all 8 cases examined were in a 2.7 cM centromeric interval between D17S959 and D1294, an estimated physical length of 5.3 Mb. The telomeric breakpoints in 4 cases mapped to a 9.6 cM interval flanked by D17S1822/D17S1830 and D17S928, an estimated physical length of 7.2 Mb. The clustering of the both LOH breakpoints suggests the existence of recombination-prone sequences in these regions of chromosome 17. While functional inactivation of neurofibromin is apparently sufficient for the myeloproliferative phenotype, these data suggest a putative role of modifying gene(s) on chromosome 17 that may contribute to the development of acute leukemia.

We have also mapped the LOH region in different tissues from a child with juvenile monomyelocytic leukemia, who later developed a T cell lymphoma. We have demonstrated that the mechanism of LOH was by an interstitial deletion and that the LOH regions were identical in length in the B cells, lymph node, and sorted cells from the node (data not shown). This demonstrates that both tumors arose from a single hematopoietic malignant clone. This study was performed in collaboration with Drs. Laurence Cooper and Eric Sievers at the Fred

Hutch Cancer Research Center (Seattle) and Dr. Kevin Shannon (UCSF). A manuscript is in the early stages of preparation.

III. Conclusions

We have determined that both germline and somatic rearrangements involving the *NF1* gene are common in specific subsets of NF1 patients. Among NF1 patients with the selected phenotype of facial dysmorphism and early onset of cutaneous neurofibromas, germline microdeletions of 1-2 Mb in size spanning one entire *NF1* allele are a predominant mechanism of rearrangement. Although not yet understood, the clustering of both the centromeric and telomeric microdeletion breakpoints to small marker intervals suggests that recombination-prone sequences flank the *NF1* gene. These breakpoint cluster sequences may be low copy number repeats that predispose to recombination or they may affect expression of nearby novel gene(s) in a manner that modifies the NF1 phenotype by reducing the age of onset and increasing the severity of cutaneous neurofibromas. Cloning of *NF1* centromeric and telomeric breakpoint cluster regions and screening unselected NF1 patients for deletions will help us understand the mechanisms and biological relevance to the NF1 phenotype of such germline rearrangements.

We determined that interstitial isodisomy for a large 50 Mb region of chromosome 17q is a predominant and novel mechanism of LOH in primary leukemic cells of NF1 children with malignant myeloid disorders. Unexpectedly, we again demonstrated that both the centromeric and telomeric recombination breakpoints map to common breakpoint intervals. Albeit the breakpoint intervals are significantly different from those of the germline microdeletions. These data suggest that sequences which are recombination-prone in a hematopoietic progenitor clone are located at these sites or the recombination events select for growth of the progenitor clone. Interestingly, we identified two patients with somatic microdeletions in leukemic cells that mapped to the same intervals as the germline microdeletions in the patients described above. Together these data suggest that chromosome 17 carries sequences that are recombinogenic in both germline and somatic tissues and that are significant and novel mechanisms of *NF1* gene inactivation.

IV. References

1. J. J. Mulvihill, in *The Neurofibromatoses: A pathogenetic and Clinical Overview* S. M. Huson, R. A. C. Hughes, Eds. (Chapman & Hall Medical, London, 1994) pp. 487.
2. D. A. Largaespada, C. I. Brannan, N. A. Jenkins, N. G. Copeland, *Nat Genet* 12, 137-43 (1996).
3. L. Side, et al., *N Eng J Med* 336, 1713-1720 (1997).
4. T. Jacks, et al., *Nature Genet* 7, 353-61 (1994).
5. V. M. Riccardi, *Semin Dermatol* 12, 266-73 (1993).
6. K. Shannon, et al., *N Engl J Med* 330, 597 (1994).
7. L. M. Kayes, V. M. Riccardi, W. Burke, R. L. Bennett, K. Stephens, *J Med Genet* 29, 686-90 (1992).
8. L. M. Kayes, et al., *Am J Hum Genet* 54, 424-36 (1994).
9. K. A. Leppig, et al., *Cytogenet Cell Genet* 72, 95-8 (1996).
10. K. Leppig, et al., *Am J Med Genet* 73, 197-204 (1997).

11. M. H. Cossen, et al., *Human Mutation* 9, 458-464 (1997).
12. B.-L. Wu, M. Austin, G. Schneider, R. Boles, B. Korf, *Am J Med Genet* 59, 528-535 (1995).
13. B. L. Wu, G. H. Schneider, B. R. Korf, *Am J Med Genet* 69, 98-101 (1997).
14. M. C. Valero, I. Pascual Castroviejo, E. Velasco, F. Moreno, C. Hernandez Chico, *Hum Genet* 99, 720-6 (1997).
15. D. Miles, et al., *Blood* 88, 4314-4320 (1997).
16. D. A. Marchuk, et al., *Genomics* 13, 672-80 (1992).

Appendices A, B, C, and D are attached.

Program Nr: 205

Double mitotic recombination at common breakpoint intervals leading to interstitial isodisomy and LOH. K. Stephens¹; M. Weaver¹; K. Leppig¹; M. Maruyama¹; L. Side²; E. Davis³; R. Espinoza III²; M. Le Beau²; K. Shannon³ 1) Univ of Washington, Seattle, WA; 2) Univ of Chicago, Chicago, IL; 3) Univ of California, San Francisco, CA.

Leukemic cells of children with neurofibromatosis 1 (NF1) who develop malignant myeloid disorders commonly show loss of constitutional heterozygosity (LOH) of the normal NF1 allele at 17q11.2 and cytogenetically normal chromosomes 17. Mapping the LOH region revealed that the predominant mechanism is interstitial isodisomy. FISH and quantitative PCR analyses of 11 cases, whose bone marrows had LOH at the NF1 locus, showed that in 8 cases the leukemic cells were disomic for NF1, while the remaining 3 cases were monosomic. In each of the 8 NF1 disomic cases, a large interstitial 17q segment had undergone LOH with the breakpoints mapping to common intervals. The proximal LOH breakpoints mapped centromeric to NF1 between D17S1878 and D17S975, while the distal LOH breakpoints were subtelomeric and bounded by D17S928 and D17S1822/D17S1830. Together these data indicate that the leukemic cells were isodisomic for an ~50 Mb interstitial 17q segment which carried the mutated NF1 allele, thereby resulting in LOH and functional loss of NF1. Interstitial isodisomy most likely arose by a double mitotic recombination during the S/G2 cell cycle of a hematopoietic progenitor cell, which gave rise to the malignant clone. The high frequency and common recombination breakpoint intervals of these novel rearrangements imply that along with NF1, additional chromosome 17 loci play a role in development of malignant myeloid disorders in NF1 children, perhaps by favoring growth of the malignant clone. Because cases of maternal and paternal isodisomic regions were both observed, genomic imprinting is unlikely to be a factor. Bone marrow cells in the remaining 3 cases showed NF1 LOH, NF1 monosomy, and small LOH regions of 1-2 Mb spanning the NF1 locus, indicating that they arose by small interstitial deletions. These studies demonstrate that critical genetic loci and mechanisms underlying neoplasia may not be detected if LOH analyses are not performed in conjunction with physical mapping.

48th Annual Meeting of Am Soc Hum Genet
Denver, CO Oct 27-31, 1998

ABSTRACT

A novel and frequent mechanism of loss of heterozygosity in malignant myeloid cells of NF1 children: Double mitotic recombination at common breakpoint intervals

K Stephens¹, M Weaver¹, K Leppig¹, K Maruyama¹, L Side³, EA Davis², R Espinosa III²,
M Le Beau², K Shannon³

¹University of Washington, ²University of Chicago, ³University of California, San Francisco
¹Depts Medicine and Laboratory Medicine, Mail Box 357720, University of Washington, Seattle, WA
98195

Ph 206-543-8285; Fax 206-685-4829, millie@u.washington.edu

Leukemic cells of NF1 children with malignant myeloid disorders commonly show loss of constitutional heterozygosity (LOH) at the NF1 gene and flanking loci. We have found that a novel mechanism of LOH is employed, which involves an apparent double mitotic recombination at common breakpoint intervals. Quantitative PCR and FISH analyses of leukemic cells revealed that, despite showing LOH at NF1, these cells harbor two NF1 alleles. NF1 LOH in conjunction with NF1 disomy was detected in 9 out of 11 cases analyzed. Six of these cases were further studied by genotypic analyses of loci spanning chromosome 17. In each of these 6 cases, a large interstitial region of the q arm of chromosome 17 showed LOH. The LOH breakpoints mapped to common intervals. The centromeric LOH breakpoint in 5 of 6 cases mapped centromeric to NF1 between D17S1878 and D17S975. The breakpoint of the remaining case mapped to an adjacent interval bounded by D17S1878 and D17S959. Similarly, 4 of the 6 cases had LOH breakpoints close to the telomere in intervals bounded by D17S928 and D17S1822/D17S1830. The other 2 cases had breakpoints within this region, but it is unclear if they map in the same interval due to lack of informative markers. Together, these data are consistent with a mechanism whereby the LOH region originated by a double mitotic recombination event in a hematopoietic progenitor cell that gave rise to the malignant clone. The high frequency of this rearrangement in leukemic cells of NF1 children implies that it either has biological significance, such as selecting for growth of the malignant clone, or is favored due to recombination-prone sequences in specific regions of chromosome 17.

*National Neurofibromatosis Foundation International
Consortium for the Molecular Biology of NF1 + NF2
6/7 - 6/10/98 Aspen, CO*

APPENDIX B.

Submitted to
Am J Hum Genet

NF1 microdeletions with clustered breakpoints identified by quantitative PCR

K. Maruyama¹, M. Weaver¹, K.A. Leppig², R. Farber⁴, A. Aylsworth⁵, J. Ortenberg⁶, A. Rubenstein⁷, L. Immken⁸, E. Haan⁹, C. Curry¹⁰, and K. Stephens^{1,3}

Departments of Medicine¹, Pediatrics², and Laboratory Medicine³, University of Washington, Seattle, WA

Departments of Pathology⁴ and Pediatrics⁵, University of North Carolina, Chapel Hill, NC

⁶Montreal Children's Hospital, McGill University, Montreal, Canada

⁷Department of Neurology, Mount Sinai School of Medicine, New York, NY

⁸Applied Genetics, Inc., Austin, TX

⁹Department of Medical Genetics, Women's & Children's Hospital, North Adelaide, Australia

¹⁰Valley Children's Hospital, Fresno, CA

Running title: *NF1* gene dosage assay

Corresponding author: Karen Stephens, PhD, University of Washington,
Medical Genetics Box 357720, Seattle, WA 98195
Ph: 206-543-8285; FAX: 206-695-4829; millie@u.washington.edu

Summary

Individuals affected with neurofibromatosis type 1 are at increased risk for developing benign and malignant tumors. Affected patients with a microdeletion spanning the *NF1* gene are remarkable for an early age of onset of dermal neurofibromas, greater numbers of dermal neurofibromas relative to their age, and certain abnormal facial features. Previously, we hypothesized that the deletion of a novel gene contiguous with *NF1* predisposed these patients to early onset tumorigenesis. To facilitate screening large numbers of patients for microdeletions, we developed a quantitative gene dosage assay for a segment of *NF1* exon 32. Thirty patients of selected phenotype were screened by the assay which predicted that 21 were disomic at *NF1*, 6 monosomic at *NF1*, and 3 were of "intermediate" *NF1* zygosity. Fluorescent *in situ* hybridization and somatic cell hybrid analyses provided physical confirmation that the 6 apparent monosomic patients were deleted for about 1- 2 Mb, which spanned an entire *NF1* allele and contiguous flanking regions. All of the centromeric and telomeric microdeletion breakpoints were clustered in two discrete marker intervals. The centromeric breakpoints mapped between D17S1294 and UT172, while the telomeric deletion breakpoints mapped between D17S1800 and D17S798. These data suggest the presence of recombination-prone sequences that flank the *NF1* locus. The development and application of PCR-based gene dosage assays for loci across a deleted region will provide rapid identification and genotyping of patients with microdeletions for detection of genotype/phenotype correlations.

Introduction

Individuals affected with neurofibromatosis type 1 (NF1) are at increased risk for developing benign and malignant tumors. Essentially all NF1 patients develop benign tumors of peripheral nerves, called neurofibromas, which are most commonly of the discrete cutaneous type (Huson 1994; Riccardi 1992). Population-based studies have shown that cutaneous neurofibromas increase in number with age, but generally do not appear before the second decade of life (Huson et al. 1988; Huson 1994). About one-third of NF1 patients also develop a plexiform neurofibroma(s), a diffuse, benign peripheral nerve tumor, which can be severe due to hypertrophy of adjacent normal tissues (Huson 1994; Riccardi 1992). Only about 5% of patients develop nodular neurofibromas, which have major peripheral nerve trunk involvement and can result in neurological symptoms (Huson 1994). Other tumors epidemiologically-associated with the NF1 disorder include optic pathway glioma, neurofibrosarcoma, malignant myeloid disorders, pheochromocytoma, and neurohumoral-secreting tumors in the duodenum and the ampulla of Vater, and possibly other soft tissue sarcomas and carcinomas (Mulvihill 1994; Zoller et al. 1995; Zoller et al. 1997). In addition to having an increased risk for certain types of neoplasms, NF1 subjects also have an increased risk of developing a second malignancy. The risk for NF1 patients is 8-20% compared to the 4% risk of the general population (Mulvihill 1994).

Genetic and biochemical analyses of primary leukemic cells of children with NF1 and malignant myeloid disorders has provided definitive evidence that neurofibromin, the product of the *NF1* gene, functions as a tumor suppressor by negative regulation of ras (Miles et al. 1997; Shannon et al. 1994; Side et al. 1997). Consistent with these data, homozygous inactivation of *NF1* has been detected in a variety of tumors from NF1 patients, including benign dermal

neurofibromas (Colman et al. 1995; Sawada et al. 1996; Serra et al. 1997) malignant peripheral nerve sheath tumors (Legius et al. 1993; Skuse et al. 1989), pheochromocytomas (Xu et al. 1992), and neuroblastomas (Martinsson et al. 1997; The et al. 1993). In addition, human malignant tumor cells, cell lines, and tissues of neurofibromin-deficient mice were constitutive for activated ras, which promoted cell proliferation (Basu et al. 1992; Bollag et al. 1996; DeClue et al. 1992; Kim et al. 1995; Martin et al. 1990; Xu et al. 1990). Like humans, mice with *NF1* haplo-insufficiency are predisposed to develop tumors, in particular pheochromocytomas and myeloid leukemias (Brannan et al. 1994; Jacks et al. 1994; Tischler et al. 1995).

Additional functions for the ubiquitously-expressed neurofibromin protein are implied by the heart malformation and ganglion hyperplasia of neurofibromin-deficient mice (Brannan et al. 1994), the interaction of neurofibromin with tubulin and microtubules (Xu and Gutmann 1997), and the array of clinical findings, other than tumor development, commonly found in NF1 patients. For example, NF1 patients typically develop cafe-au-lait macules, axillary and/or inguinal freckling, and Lisch nodules of the iris. Bony abnormalities and learning disabilities occur in a significant subset of patients (Gutmann and Collins 1995; Huson 1994; Riccardi 1992).

The cloning of the *NF1* gene (Cawthon et al. 1990; Marchuk et al. 1991; Viskochil et al. 1990; Wallace et al. 1990) held the promise of identifying specific mutant alleles that predisposed a patient to develop certain clinical manifestations of NF1, particularly for the more severe manifestations such as plexiform neurofibromas, optic glioma, sphenoid dysplasia, kyphoscoliosis, or malignancy. Such correlations could provide clues to other functions of neurofibromin and have predictive value for a subset of patients. However, an estimated 80% of NF1 patients had germline mutations dispersed throughout the gene that predicted premature

truncation of neurofibromin (Heim et al. 1995; Shen et al. 1996; Upadhyaya et al. 1997).

Among these patients, no correlation between *NF1* genotype and phenotype has been detected.

In contrast, a consistent phenotype has been observed in patients with an *NF1* microdeletion. Our initial reports that *de novo NF1* microdeletion patients were remarkable for an early age at onset of dermal neurofibromas (<age 10 yr), an increased number of neurofibromas relative to their age (>85 percentile), and a mildly dysmorphic facies (Kayes et al. 1994; Kayes et al. 1992) have subsequently been confirmed by us and other investigators (Ainsworth et al. 1997; Cnossen et al. 1997; Leppig et al. 1996; Valero et al. 1997; Wu et al. 1995). Studies of families segregating an *NF1* deletion demonstrated that it is co-inherited with the dysmorphic facies and early onset of neurofibromas (Cnossen et al. 1997; Leppig et al. 1997; Wu et al. 1997). These studies strengthen the argument that an *NF1* microdeletion is the primary cause of the remarkable tumor phenotype of these patients.

The molecular basis for the early onset of dermal neurofibromas in *NF1* microdeletion patients is unknown. In general, it can be attributed to (1) hemizyosity of the *NF1* gene alone, (2) hemizyosity of both *NF1* and a novel contiguous gene(s), or (3) inactivation or activation of a novel gene at the deletion breakpoint. These possibilities cannot be distinguished currently because the number of deletion patients is relatively small and information regarding tumor number, age at tumor onset, and/or the physical delineation of the deletions were not always evaluated and/or reported. It appears unlikely that neurofibromin haplo-insufficiency alone could account for early onset of tumorigenesis. In a population-based study of *NF1* patients of undetermined genotype, about 14% of subjects developed dermal neurofibromas before 10 years of age (Huson et al. 1988; Huson 1994). Yet, approximately 80% of *NF1* patients carry mutations that predict haplo-insufficiency of neurofibromin due to premature protein termination

(Upadhyaya et al. 1997). In addition, patients with *NF1* mutations predicting premature translation termination do not typically have early onset or large numbers of neurofibromas. The germline *NF1* microdeletions mapped to date have an estimated length of 0.7 - 2 Mb, which, even accounting for the large 350 kb *NF1* gene, makes it highly probable that multiple unknown contiguous genes are also deleted (Kayes et al. 1994; Kayes et al. 1992; Leppig et al. 1997; Leppig et al. 1996). Testing the possibility that the early onset of tumorigenesis is caused by activation or inactivation of a gene at the deletion breakpoint awaits finer mapping studies. At least one out of 8 probands, however, is known to have unique deletion breakpoints (Kayes et al. 1994).

To date, *NF1* deletion studies were limited primarily to patient cohorts of selected phenotype and utilized inefficient methods for deletion detection. *NF1* hemizyosity has been detected by densitometry of *NF1* fragments on Southern blots, conventional nonquantitative PCR, absence of biparental allelic inheritance in patients with sporadic NF1 disease, or unexpected apparent homozygosity at multiple intragenic and extragenic polymorphic sites (Ainsworth et al. 1997; Cnossen et al. 1997; Colman et al. 1996; Kamei et al. 1992; Kayes et al. 1994; Kayes et al. 1992; Valero et al. 1997). These methods are neither robust nor sensitive. Physical confirmation of an *NF1* deletion in some patients was obtained by somatic cell hybrid analysis and fluorescence in situ hybridization (FISH) (Kayes et al. 1994; Leppig et al. 1997; Leppig et al. 1996; Riva et al. 1996; Wu et al. 1997; Wu et al. 1995). Although definitive, such physical mapping methods are not applicable for screening a large cohort of patients.

In the present study, we describe a rapid and sensitive method for detecting microdeletion patients that employs a quantitative *NF1* gene dosage assay. Of 30 patients of selected phenotype screened by the assay, 6 had gene dosage values that predicted *NF1*

hemizyosity. Physical mapping confirmed an *NF1* microdeletion in these patients and revealed that their breakpoints mapped to common marker intervals. This assay will facilitate identifying contiguous gene(s) that may contribute to the phenotype of *NF1* microdeletion patients and is generally applicable to investigating genotype/phenotype correlations of any contiguous gene syndrome.

Subjects and Methods

Human Subjects. DNA from 11 *bona fide NF1* hemizygotes, as determined by somatic cell hybrid analysis and FISH, were used as positive controls. Nine of these patients have been described previously, UWA106-3, UWA119-1, UWA123-3, UWA128-3, and UWA69-3 (Kayes et al. 1994; Kayes et al. 1992), UWA160-1 (Leppig et al. 1996), UWA166-1, UWA166-2, and UWA169-1 (Leppig et al. 1997). DNAs from 21 unrelated unaffected subjects were used as positive controls, including the 4 grandparents of 5 families of The Centre d'Etudes du Polymorphisme Humain (families K-1331, K-1333, K-1340, K-1341, and K-1029 from the Coriell Cell Repositories, Camden, NJ) and one anonymous blood donor (sample C101). This study was approved by the University of Washington Institutional Review Board.

UWA147-3 (referred by L.I.) is a male of Mexican heritage born at term to a gravida 3 para 2-3 mother at age 23 years and a father of 25 years; parents had a negative family history of neurofibromatosis. Birth weight was 8 lb 2 oz; body length 19 in. Three café au lait spots were noted at birth. At nine months, when first evaluated by a clinical geneticist, he was not yet sitting - he did roll over, transfer objects, bear weight and babble. Height, weight and head circumference were all within normal limits. Facies were marked by telecanthus, downslanting palpebral fissures and inner canthal distance at 97th percentile, broad nose, micrognathia, and

courseness. He had a mild pectus carinatum superiorly with excavatum caudally and cubitus valgus. Multiple café au lait spots were present. His teeth were noted to be very large.

At 24 months, on reexamination, he had 3 words. He had begun walking at 21 months. Growth was still normal. His facial skin was now replete with brown patches and reddish tan raised lesions, also present on scalp along with a sebaceous nevus; axillary and inguinal freckling were present. His front teeth appeared to be fused. Overall, his facial appearance was suggestive of the Noonan syndrome. At age 6 he has poor muscle tone, hypotonia, and is not yet reliably continent of urine and stool.

Patient UWA167-1 (referred by C.C.) is a now 5 year old Caucasian male who was the product of a first pregnancy to a 22 year old mother and a 27 year old father. The duration of the pregnancy was 35.5 weeks, and there were no prenatal complications. His birth weight was 3.0 kg and he was thought to look mildly "puffy" at birth. He required supplemental oxygen for 36 hours and had mild jaundice delaying hospital discharge. A cardiac murmur was noted at two months of age and an echocardiogram revealed an atrial septal defect at the fossa ovalis and mild to moderate pulmonic stenosis. Despite significant gastroesophageal reflux, he experienced good weight gain. Initial evaluation at 4 months of age revealed mild bilateral ptosis, nail hypoplasia, and unexplained hepatomegaly. At 9 months of age, he had 3-4 café au lait macules that by age 4 had increased in number to 15-20 macules, along with early inguinal and axillary freckling. By age 4, he had at least seven cutaneous neurofibromas, one with an overlying tuft of hair. There were several hypopigmented spots, including a large nevus anemicus on the left shoulder and neck.

At 17 months of age, patient UWA167-1 began having infantile spasms. An MRI scan at this time revealed a poorly formed rostrum of the corpus callosum and abnormal increased signal

density in the frontal subcortical white matter, temporal lobe, and periauricular white matter. His seizures ceased abruptly at approximately age two.

At his current age, he is mildly developmentally delayed, particularly in the area of expressive language. His phenotype is significant for mild ptosis, blue eyes without obvious Lisch nodules, a long philtrum, sloping trapezius muscles without real neck webbing, pectus carinatum deformity, cardiac murmur, hirsutism especially over the lower back, diastasis recti, cubitus valgus, and hyperextensibility of finger and elbow joints. His hepatomegaly had resolved. Evolution of his phenotype is shown in Figure 6A-B.

Patient UWA172-1 (referred by A.R.) is now a 35 year old female with multiple dermal neurofibromas, facial anomalies, large hands and feet, and a negative family history of NF1. She had surgery for a symptomatic optic glioma at the age of 7 years with subsequent loss of light perception in the right eye. She had subtotal removal of a large C1 cervical plexiform neurofibroma at age 23 and removal of a plexiform neurofibroma of the left arm at age 29. The patient graduated from high school and is employed. Age at onset of dermal neurofibromas is not unknown.

Patient UWA176-1 (referred by J.O.) is a 13 year old female who was given a clinical diagnosis of NF1 with the Noonan phenotype based on her dermatological findings, facial dysmorphism, and somewhat webbed neck. Complications from NF1 included multiple sites of bony dysplasia including the cervical spine, which was fused for stability, and congenital dislocation of the radial head and overgrowth of the ulna relative to radius (Madelung deformity). In addition, she had plexiform neurofibromas on the right hand and lumbosacral spine, and significant learning disabilities/academic difficulties. The age of onset of dermal neurofibromas is not known; family history was negative for NF.

Patient UWA183-1 (referred by E.H.) is now a 13 year old Caucasian male who was the product of the first pregnancy of unrelated parents, mother aged 15 yrs and father aged 21 yrs. He was born at 40 weeks gestation with birth weight 2.88 kg after a normal pregnancy, prolonged labor associated with meconium stained liquor, and normal delivery. The umbilical cord contained two vessels. At birth, he had polycythemia associated with tachypnoea and brief hypoglycemia and received a partial exchange transfusion. He presented at 10 months of age with a lump in the pinna of the left ear that extended into the neck below, and the scalp above and behind the ear. Multiple cafe au lait patches were noted. A diagnosis of neurofibromatosis was made. The lump was removed at 14 months and shown to be a plexiform neurofibroma. Mild pulmonary valve stenosis and developmental delay were documented at this time. The parents were examined and father had a single café au lait patch while mother had no features of neurofibromatosis. CT of the head and neck at 18 months of age demonstrated that the plexiform neurofibroma extended into the left temporal region and extensively infiltrated the neck in the submandibular region.

He was referred to the Genetics Clinic at 21 months of age. He had a distinctive craniofacial appearance with broad and high forehead, triangular facies, striking pale blue eyes, telecanthus, widely set eyes, epicanthic folds, mild ptosis, broad nasal bridge, long philtrum, dental malocclusion with open anterior bite, small chin, low set left ear with brown pigmentation of skin within the pinna and abnormal hair growth over the plexiform neurofibroma, which was palpable in the region of the left ear and in the neck below the mandible. He had multiple café au lait patches and axillary freckling. Mild-moderate pulmonary valve stenosis had been documented on echocardiography. His developmental functioning was at a 10-12 month level. A diagnosis of neurofibromatosis-Noonan syndrome was made; karyotype was normal.

At 5 years 11 months his abilities were assessed to be in the lower end of the borderline range on the Wechsler Preschool and Primary Scale of Intelligence. His verbal abilities were significantly better than his non-verbal abilities. Excision of the plexiform neurofibroma from the left neck, left side of tongue and left pinna was performed at 6 years of age.

At 12.5 years of age, he had borderline intelligence and attended a normal school, with special classes for some subjects. He had mild intermittent asthma. He had height 150.8 cm (25-50th centile), weight 38 kg (25th centile) and head circumference 55.2 cm (50th-98th centile). There were a broad high forehead, small epicanthic folds, telecanthus (inner canthal distance 36 mm, 97th centile), widely set eyes (interpupillary distance 59 mm, 75th-97th centile) and broad nasal bridge. Facial asymmetry was present with unequal palpebral fissure lengths (right 30 mm, left 25 mm), reduced facial soft tissue on the left, chin point deviated to left and the left ear was enlarged, low set and there was brown pigmented skin within the pinna. The chin was small and the inferior margin of the mandible was irregular. Within the mouth there were palatal scoliosis, neurofibroma tissue evident within the left side of the tongue, slight tilt of the occlusal plane upwards to the left and severe malocclusion class II with left cross-bite. Eye examination documented visual acuities of 6/9 on the right and 6/12 on the left, mild hypermetropia, mild amblyopia, divergent strabismus and Lisch nodules. He had minor webbing of the neck, numerous café au lait patches, axillary and inguinal freckling, 10 small cutaneous neurofibromas and pes planus with wide feet. There was a 30-40 dB conductive hearing loss on the left, in part the result of chronic serious otitis media. The pulmonary stenosis had progressed and was moderate in degree. There was no chest wall deformity. His phenotype is shown in Figures 6C-E.

Patient UWA184-1 (referred by A.S.A.) is a 10 year old female who presented in infancy with dysmorphic features including coarse facies, feeding problems, sleep disorder, congestion, hypertonia, mild hepatosplenomegaly that later normalized, four café au lait spots greater than 5 mm, and 2 freckles. She subsequently was found to have an immunodeficiency (treated with IgG infusions since age 3 years), global developmental delays in the borderline range, and diffuse abnormalities of CNS white matter development by MRI. She developed increasing numbers of café au lait spots, intertriginous freckling, and by age 5 years, small cutaneous nodules compatible with neurofibromas over the trunk and thighs. Neither parent had significant features of NF1 and the extended family history was negative for neurofibromatosis.

NF1 gene dosage assay. Primers (5' → 3') consisted of L14(ATCTAGTATTTTTGAGGCCTCAG) and L15(CAGATATGCTATAGTACAGAAGG), which produced a 310 bp segment of *NF1* exon 32 (Cawthon et al. 1990); (Li et al. 1995). The primers L14 and L15 were screened against a human/rodent somatic cell hybrid panel (NIGMS Panel #2, Coriell Cell Repositories, Camden, NJ). Primers APP580F (GCCAGTTGTATATTATTCTTG TG) (Celi et al. 1994) and APP810R (AAGCAGCAATCTGTACAGTAA) amplified a 232 bp segment of exon 18 of the amyloid beta precursor protein gene (*APP*), a single copy gene on chromosome 21 that was used as a control for disomy.

The internal standard (I.S.) for *NF1* was generated by two successive polymerase chain reactions (Celi et al. 1994; Celi et al. 1993). The genomic DNA from normal subject C101 was amplified with primers L14 and L15 and the product re-amplified with primers L14 and L15del, a mutagenic reverse primer designed to introduce a 20 bp subterminal deletion in the amplified product. The sequence of primer L15del was

CAGATATGCTATAGTACAGAAGG[JTCACATTTCCAGAAGCC, where the 23 bases identical to the nonmutagenic primer L15 are underlined and the position of the 20 bp gap deletion is bracketed. The *NFI* I.S. and the genomic alleles are amplified by the same primers, L14 and L15, but the I.S. product is 20 bp smaller for electrophoretic resolution. An I.S. for the *APP* gene was constructed similarly by amplification with primers APP580F and APP810R (Celi et al. 1994) followed by re-amplification with APP580F and the mutagenic reverse primer APP768del, AAGCAGCAATCTGTACAGTAA[JTCTCTAAAGCATCTGAAATAC (brackets and underline, as before). For stability and convenience the I.S. fragments were cloned into *Sma*I linearized pUC19, whose ends were modified by addition of a T by a 2 hr incubation at 75 °C in 50 mM KCl, 10 mM Tris-HCl, pH 8.3, 1.5 mM MgCl₂, 0.001 % (w/v) gelatin, 1 mM dTTP, and 5 µl of AmpliTaq polymerase (Applied Biosystems, Foster City, CA). The amplified products were purified by Qiagen PCR purification kit (Qiagen, Chatsworth, CA), ligated into pUC19 by T4 ligase, and transformed into *E. coli* DH5α using standard methods. Prior to use in the gene dosage assay, the plasmids pKM204 and pKM201, harboring the *NFI* and *APP* I.S. respectively, were linearized with *Eco*RI. Although the effect of linearized I.S. plasmids on the yield of this assay was not tested specifically, we believe it gave a more consistent performance. To confirm equimolar quantities, titration experiments were performed with the two linearized I.S. plasmids. After the optimal concentrations were determined, the two plasmids harboring the I.S. were mixed and stored in aliquots at -20 °C for future assays.

The *NFI* gene dosage assay was performed in a volume of 25 µl and contained 50 ng genomic DNA of the patient (10 ng/µl in 10 µg/ml yeast tRNA), an equimolar quantity of each internal standard (0.05 pg of each linearized pKM204 and pKM201), 0.5 µM each primer pair L14/L15 and APP580F/APP810R, 0.025 µM γ-³²P radiolabeled primers L14 and APP580F, 200

μ M each dNTP (Pharmacia, Piscataway, NJ), and 2.5 Units of AmpliTaq DNA polymerase (Applied Biosystems, Foster City, CA). Hot start PCR was performed by heating genomic DNA of the subject, I.S. plasmids for *NF1* and *APP*, and primer sets L14/L15 and APP580F/APP810R for 4 min at 94 °C. After addition of an aliquot containing the remaining reagents, the reaction was amplified by 22 cycles of 1 min 94 °C, 1.5 min 55 °C, 1.5 min 72 °C. The last cycle was followed by a 5 min extension at 72 °C. Subsequently, AmpliTaq Gold (Perkin-Elmer, San Francisco, CA) was used successfully instead of the manual hot start protocol. After addition of an equal volume of loading dye buffer (95 % formamide, 0.05 % xylene cyanol FF, 0.05 % bromophenol blue, 20 mM EDT, pH 8.0), 20 μ l of the reaction was electrophoresed through a 1 mm thick 6% polyacrylamide gel with 7M urea in 1X TBE (8.9 mM Tris, 8.9 mM boric acid, 0.2 mM EDTA, pH 8.0) for two hours at 25 V/cm at constant. The gel was partially dried, exposed to a phosphor screen and the products quantified with a GS-250 PhosphorImager (Bio-Rad, Hercules, CA). After adjusting for the background, the *NF1* gene dosage was calculated as described in Figure 1.

Deletion mapping. FISH of chromosomes prepared from immortalized lymphoblasts was performed as described previously with probe P1-9, which harbors about 65 kb of *NF1* exons 2-11 (Leppig et al. 1996). A minimum of 20 scorable metaphase cells with both homologues of chromosome 17 clearly identifiable were analyzed for each patient; symmetrical signals on both chromatids of one homolog of chromosome 17 was scored as an intact *NF1* locus, while lack of signal on both chromatids was scored as an *NF1* deletion. Human/rodent somatic cell hybrid lines carrying only one human chromosome 17 homolog were constructed as described previously (Kayes et al. 1994). Deletion mapping was performed by amplification of DNA from rodent/human hybrid cell lines or from DNA of peripheral blood cells for some polymorphic

loci. *NFI* intragenic loci included exon 5 (Hoffmeyer and Assum 1994), intron 27b (Li et al. 1995; Xu et al. 1991), and intron 38 (Lazaro et al. 1993). *NFI* flanking marker were D17S33 (Ainsworth and Rodenhiser 1991) and D17S57 (Rodenhiser et al. 1993), UT172 (Shannon et al. 1994), CRYB1, D17S975, D17S798, D17S1294, and D17S1800. The marker locations were as previously described (Kayes et al. 1994). D17S975, D17S1294, UT172, D17S1800, and D17S798 were determined by analysis of a somatic cell hybrid mapping panel of *NFI* microdeletions (K. Stephens, unpublished data). Plasmids carrying the terminal segments of an *NFI* YAC contig (pAH1 and pAN2; (Marchuk et al. 1992) were sequenced in part using a pYAC4 vector-specific primer (ACTGGGTTGGAAGGCAAGAG) to design primers for locus-specific amplification. The AH1 locus was amplified as a product of about 238 bp using primers AH1-9600-F: GATGGATATCAGGTACCGACAG and AH1-9600-R: GAGTCAGTCTGCTGAGTTTGCA. The AN2 locus was amplified as a product of about 335 bp with primers AN2-517-F: GGCCAAGTATCAATACACGTG and AN2-517-R: GCTCATCATACTGCAGTACAG. Both loci were amplified from 250 ng of DNA in a reaction of 100 μ M each primer, 1.5 mM MgCl₂, 10% glycerol, 200 μ M each dNTP, 1 Unit Taq polymerase and buffer (Boehringer Mannheim) for 1 min at 94°C, and 35 cycles of 1 min 10 sec at 94°C, 2 min at 58°C, and 2 min at 72°C.

Results

The *NF1* gene dosage assay.

The *NF1* gene dosage assay is a modification of an assay originally designed and validated for detection of trisomy 21 (Celi et al. 1994). The method is a competitive PCR, which employs two types of internal controls to minimize the random nature of amplification. The first type of control establishes a competitive reaction by the addition of two DNA segments, termed internal standards (I.S.). The first I.S. shares the same primer binding sequences as the target *NF1* gene, while the second I.S. shares primer binding sequences with a disomic reference gene on another autosome. The second type of internal control is the disomic reference gene. The disomic reference gene and the target gene are co-amplified from patient genomic DNA under the assumption that any factor which affects the quantity or quality of the target gene will affect the reference gene in the same manner. Therefore, the *NF1* gene dosage can be determined by normalization to the disomic reference gene. See the appendix for a brief consideration of the theoretical aspects of gene dosage PCR.

Examples of the *NF1* dosage assay of genomic DNA from a disomic control subject and an *NF1* hemizygous subject are depicted in Figure 1. In this example, the *NF1* dosage for the unaffected disomic control subject was 0.93, close to the expected value of unity, and the gene dosage for the hemizygous control subject was 0.5, as expected.

Because multiple autosomes carry *NF1*-related sequences that have a high degree of homology with the expressed *NF1* locus on chromosome 17 (Cummings et al. 1996; Legius et al. 1992; Purandare et al. 1995; Regnier et al. 1997), it was critical to choose primers for the gene dosage assay that specifically amplified only the expressed *NF1* locus. For this reason, primers L14 and L15 were screened against a panel of human monochromosomal somatic cell

hybrids. These data confirmed that only the expressed *NF1* locus on chromosome 17 was amplified under the defined conditions of the assay (data not shown).

Equivalency of amplification efficiencies

In the multiplexed PCR reaction, the amplification efficiency was exponential for both *NF1* and *APP* genes and their respective internal standard sequences from cycle 18 through cycle 25 (Figure 2). As the number of cycles increased, however, there was a change in the ratio of the products from the genomic target genes to the products from their internal standards (Figure 3). For cycles less than 20, the high background relative to the signal resulted in a greater variation among the three replicate reactions. For cycles greater than 20, the background was less than 10 % of the product signal (data not shown) and variation among replicates was minimal. The ratio of products amplified from the genomic DNA to those from the internal standards remained constant from cycles 20-23 for both *NF1* and *APP* (Figure 3A, 3B). After the plateau was reached, however, the ratio of products amplified from genomic DNA to internal standards increased slightly for *NF1* and decreased for *APP*, resulting in a higher *NF1/APP* ratio (Figure 3C). Therefore, subsequent gene dosage assays were terminated at 22 or 23 cycles.

Variability within and among gels

To study the effect of variation due to the stochastic nature of PCR, 28 replicate *NF1* gene dosage assays were performed for 22 cycles with genomic DNA from an unaffected control subject and another 28 replicate assays with genomic DNA from an *NF1* hemizygous subject. Although absolute amounts of product varied among the 28 reactions, the ratio of the products amplified from the genomic genes to those from the internal standards remained quite similar, as did the final *NF1/APP* ratio (data not shown). For an unaffected subject, the mean *NF1/APP* ratio was 1.04 ± 0.08 sd (one standard deviation). As expected from the model, the mean for

UWA166-1, an *NF1* hemizygous subject, was 0.51 ± 0.068 sd. When replicate reactions were electrophoresed through gels prepared independently, both the mean and standard deviation remained the same, indicating that the gel electrophoresis and quantitation by phosphorimaging does not introduce any significant variation.

To mimic variation in the reaction samples, assays with varying ratios of genomic DNA to internal standards were performed using genomic DNA from an unaffected subject. Although the product output varied along with the input of genomic genes and internal standards, the *NF1/APP* ratio remained constant at the optimal 22 cycles (data not shown).

Distribution of *NF1* gene dosage values among control subjects.

To determine if the *NF1* gene dosage values constituted two distinct distributions, disomic and monosomic control subjects were assayed. Twenty-one unaffected control individuals (presumed disomic at *NF1*) gave a mean gene dosage value of 0.98 ± 0.08 sd (Figure 4). Eleven affected *NF1* hemizygous control subjects gave a mean gene dosage value of 0.45 ± 0.04 sd. The outlier values for each distribution did not overlap. To approximate a 95% confidence interval, the range of values for disomy or monosomy were set at the mean ± 2 sd. This gave a gene dosage value range of 0.82 - 1.14 as indicative of *NF1* disomy and a range of 0.37 - 0.53 for *NF1* monosomy.

Identification of patients with *NF1* microdeletions by the gene dosage assay

Genomic DNA from 30 probands was screened to test the utility of the gene dosage assay. To increase the probability that this group included at least one patient with an *NF1* deletion, it was limited to subjects whose phenotype, in our judgement, was suggestive of an *NF1* microdeletion. Based on their clinical findings, the patients were categorized into one of

four general phenotypic classes (Table 1). Of the 30 probands screened, 21 had gene dosage values between 0.82 and 1.14, which was consistent with *NF1* disomy and 6 had values of 0.42 to 0.47, consistent with *NF1* monosomy (Table 1; Figures 4 and 5). For the 3 remaining patients, the *NF1* zygosity was classified as "intermediate" because the mean dosage from duplicate assays of these subjects was 0.67, 0.80, and 0.78 (Table 1, Figure 4).

Confirmation and mapping of *NF1* deletions

To confirm the presence of a deletion and to determine if it extended beyond *NF1* exon 32, the *NF1* region of the 6 putative deletion patients was physically mapped. FISH with the *NF1* probe P1-9 of lymphoblasts from 4 patients (UWA176-1, UWA147-3, UWA167-1, UWA183-1) revealed hybridization signals on both chromatids of only one chromosome 17 homolog (data not shown). These data confirmed deletion of at least *NF1* exons 2 through 11 (~65 kb). To facilitate finer deletion mapping, each patient's chromosome 17 homologs were segregated into rodent cell lines. Genotypic analysis of each homolog confirmed that these 6 patients carried one chromosome 17 that was deleted for the *NF1* gene and significant flanking sequences (Figure 5).

Remarkably, both the centromeric and telomeric breakpoints of all 6 patients mapped to the same marker intervals (Figure 5). The deleted region between D17S1294 and D17S798 has an estimated genetic length of 2.67 cM on the sex-averaged chromosome 17 map. Because recombination is greater in males than females between these two markers; genetic lengths were 5.38 cM and 0 cM, respectively. The physical length of the region is unknown but is estimated between 700 - 1500 kb based on the size of the 700 kb YAC contig and the 1.5 Mb estimated distance between UT172 and *NF1* (Marchuk et al. 1992; Shannon et al. 1994) (Figure 5). The physical size of the breakpoint cluster regions, designated cenBCR and telBCR, are unknown.

Discussion

We have developed a quantitative *NF1* gene dosage PCR assay, which proved to be a rapid and sensitive screening technique to identify patients with *NF1* deletions. This assay predicted that 6 patients were monosomic at the *NF1* exon 32 locus (Table 1, Figure 5). These predictions were confirmed by FISH and somatic cell hybrid analyses, which mapped the microdeletions at about 1.5-2 Mb that spanned an *NF1* allele (Figure 5). Twenty-one of the patients screened were apparently disomic at *NF1* exon 32 (Table 1). The possibility that these patients are deleted for *NF1* sequences other than exon 32 cannot be excluded. The *NF1* zygosity for the remaining 3 patients was classified as "intermediate" because of *NF1* dosage values of 0.67, 0.805, and 0.785. Two of these patients may be disomic at *NF1*; their values are slightly less than the lower end of the disomic gene distribution of 0.82. Alternatively, all 3 "intermediate" dosage patients, particularly the one with a dosage of 0.67, may be mosaic for an *NF1* deletion. Mosaicism for large *NF1* deletions has been reported previously [Colman, 1996 #30; Ainsworth, 1997 #345].

Remarkably, physical mapping revealed that the six *NF1* microdeletion patients appeared to carry similar, if not identical, *NF1* deleted alleles. The centromeric and telomeric deletion breakpoints mapped to common marker intervals, which were designated as the breakpoint cluster regions cenBCR and telBCR (Figure 5). The physical length of either BCR is unknown; although D17S1800 and D17S798 that flank the telBCR are tightly linked loci without intervening recombination events. The similarity of the breakpoints awaits their cloning and sequencing. However, these data suggest that the cenBCR and telBCR may harbor recombination-prone sequences. Homologous recombination between flanking low copy number repeat sequences are responsible for the dystrophin deletion hotspot, the Smith-Magenis

syndrome microdeletion, and the reciprocal deletion and duplication events that causes hereditary neuropathy with liability to pressure palsies or Charcot-Marie-Tooth disease type 1A, respectively (Chance et al. 1994; Chen et al. 1997; Pizzuti et al. 1992). In the latter example, the 1.5 Mb rearrangements result from recombination between flanking 24 kb CMT1A-REP sequences. Within the CMT1A-REP, about 75% of the deletion breakpoints map to a 456 bp region near a mariner transposon-like element, which is postulated as the site of a double strand break that initiates the recombination event (Reiter et al. 1998; Reiter et al. 1996). Alternatively, the BCRs may reflect the inactivation of a gene or the creation a novel gene fusion, which contributes to the phenotype of the *NF1* microdeletion patients.

Because the patients screened were selected by phenotype, it is not unexpected that the clinical findings of the 6 *NF1* microdeletion patients were similar to those described in our previous microdeletion patients (Kayes et al. 1994; Kayes et al. 1992; Leppig et al. 1997; Leppig et al. 1996). All 6 fulfilled the *NF1* diagnostic criteria, had abnormal facial features, and no prior family histories of *NF1* (Table 1; Materials and Methods). The faces of the 6 *NF1* microdeletion patients were generally described as coarse and/or resembling the face of patients with Noonan syndrome (Allanson 1987). Features which together gave the gestalt of the Noonan syndrome facies included telecanthus, ptosis, broad nasal bridge, and downslanting palpebral fissures. Facial photographs of subjects UWA167-1 and UWA 183-1 in Figure 6 show a striking similarity to photographs of other microdeletion patients (Kayes et al. 1994; Leppig et al. 1997). Like previous *NF1* microdeletion patients, subjects UWA167-1 and UWA184-1 developed multiple cutaneous neurofibromas before age 10, while UWA183-1 developed multiple tumors between the ages of 6 and 12.5 years. The additional manifestations of abnormal CNS findings, pulmonary stenosis, and atrial septal defect observed in 3 of the deleted

patients in this study have also been observed in some of our previously described microdeletion patients. Of particular note, patient UWA176-1 is the second *NF1* microdeletion patient that also had Madelung deformity (Leppig et al. 1996). To date, there is no correlation between extent of the deletion and any of these additional findings.

NF1 gene dosage assays will facilitate a number of critically important studies. First, screening patients regardless of phenotype will permit a direct test of our hypothesis that deletion of a contiguous gene, rather than simply the *NF1* gene itself, causes premature onset of dermal neurofibromas. Second, a cohort of microdeletion patients will be identified for a prospective study of the frequency of malignancies. Third, the ability to screen all *NF1* patients regardless of phenotypic features will determine the spectrum and frequency of clinical findings associated with *NF1* microdeletions. Fourth, the identification and mapping of additional microdeleted patients will address the biological importance of the BCRs.

PCR-based gene dosage assays would provide a powerful strategy define phenotype/genotype correlations of any contiguous gene deletion syndrome. The choice of the primers for amplification of a target locus is restricted only by the requirements that they amplify a unique genomic sequence and are not positioned over known, or suspected, polymorphic sites that could affect annealing and amplification efficiency. In our assay, sequence polymorphism did not appear to be an issue; both the *NF1* and *APP* primer pairs amplified DNA from all the individuals efficiently. In theory, monitoring ratios of genomic DNA to I.S. could identify abnormal results from changes in amplification efficiency due to a DNA polymorphism and/or from genomic deletion of the disomic control gene in particular patients. The power of gene dosage analyses is illustrated in the following *NF1* microdeletion example. Development of additional assays for specific 5' and 3' *NF1* sequences, in addition to

the exon 32 assay described here, could rapidly categorize NF1 patients as (1) non-deleted, (2) deleted for 5' *NF1* sequences and possibly novel genes centromeric to *NF1*, (3) deleted for an intragenic *NF1* region involving at least exon 32 but not contiguous genes, (4) deleted for 3' *NF1* sequences, and possibly novel genes telomeric to *NF1*, or (5) deleted for the entire *NF1* gene and 5' and 3' contiguous sequences. Such a coarse screening would identify the chromosomal regions deleted, estimate deletion frequency, permit an initial assessment of possible genotype/phenotype correlations, and identify the most informative patients for further analyses. Deletion mapping at a finer level could be accomplished by a second series of gene dosage assays for critical loci. Such a mapping approach would be rapid, sensitive, efficient, widely applicable to any microdeletion syndrome and require only genomic DNA of the patients. As an automated alternative to the assay described here, kinetic PCR analysis monitoring real-time DNA amplification reactions is now available (Heid et al. 1996).

Acknowledgements

This research was supported in part by grant EDT17A from the American Cancer Society (K.S.) and in part by Grant NF960043 from the U.S. Army Medical Research and Materiel Command (K.S.). We thank all the patients for their participation in this study, the many clinicians who referred patients that tested negative in this study, Doug Marchuk for sharing his *NFI* YAC end clones, and Mike Mikiska of the PhosphorImaging Analysis Facility, Markey Molecular Medicine Center, University of Washington.

Electronic Database Information

Genome Database: <http://gdbwww.gdb.org/>

Marshfield Medical Research Foundation: <http://www.marshmed.org/genetics/>

National Center for Biotechnology Information: <http://www.ncbi.nlm.gov/cgi-bin/Entrez/efetch?gi=17&db=Genome>.

Online Mendelian Inheritance in Man: <http://www.ncbi.nlm.nih.gov/omim>.

Appendix

Theory of the method. The theoretical aspect of gene dosage PCR is explored briefly. In this method, two alternative strategies of quantitative PCR, competitive PCR and reference gene, are used in combination (Celi et al. 1994). Although the method may be justified intuitively, the experimental conditions must be elucidated under which the method is valid. In general, the exponential phase of the PCR process is expressed by the following equation.

$$N_n = N_0 (1 + E)^n \quad (1)$$

Efficiency of amplifications is denoted by E, where $0 < E < 1$. N_0 and N_n denote the number of molecules before amplification and after n cycles. For the genomic and internal standard, the amplification process is described by:

$$(Nt.g)_n = (Nt.g)_0 (1 + E)^n \quad (2)$$

$$(Nt.s)_n = (Nt.s)_0 (1 + E)^n \quad (3)$$

Where $(Nt.g)_0$ and $(Nt.g)_n$ are the number of genomic target molecules before amplification and after n cycles, respectively. Likewise, $(Nt.s)_0$ and $(Nt.s)_n$ are the number of internal standard molecules for the target gene before amplification and after n cycles.

If it is assumed that E is the same for the internal standard and genomic target gene,

$$(Nt.g)_0 / (Nt.s)_0 = (Nt.g)_n / (Nt.s)_n \quad (4)$$

Since $(Nt.s)_0$ is known and, $(Nt.g)_n$ and $(Nt.s)_n$ are obtained from the experiment,

$$(Nt.g)_0 = (Nt.s)_0 * (Nt.g)_n / (Nt.s)_n \quad (5)$$

For both the target and reference genes,

$$(Nref.g)_0 / (Nref.s)_0 = (Nref.g)_n / (Nref.s)_n \quad (6)$$

$$(Nt.g)_0 / (Nt.s)_0 = (Nt.g)_n / (Nt.s)_n \quad (7)$$

Where $(N_{ref.g})_0$ and $(N_{ref.s})_0$ denote the initial number of reference gene molecules and internal standard for reference gene, and $(N_{ref.g})_n$ and $(N_{ref.s})_n$ denote the number of genomic and internal standard molecules for the reference gene after n cycles. Likewise, $(N_{t.g})_0$ and $(N_{t.s})_0$ denote the number of genomic and internal standard molecules for the target gene before amplification whereas $(N_{t.g})_n$ and $(N_{t.s})_n$ indicate number of genomic and internal standard molecules for the target gene after n cycles.

If the same amounts of two internal standards are used, $(N_{ref.s})_0 = (N_{t.s})_0$. Therefore,

$$(N_{ref.g})_0 * (N_{ref.s})_n / (N_{ref.g})_n = (N_{t.g})_0 * (N_{t.s})_n / (N_{t.g})_n \quad (8)$$

$$(N_{t.g})_0 / (N_{ref.g})_0 = ((N_{t.g})_n / (N_{t.s})_n) / ((N_{ref.g})_n / (N_{ref.s})_n) \quad (9)$$

Because a normal individual has two copies of both the *NFI* and *APP* genes, the ratio $((N_{t.g})_0 / (N_{ref.g})_0)$ is expected to be unity. For individuals hemizygous for *NFI*, it is expected to be 0.5. In this model, the amplification process has to be stopped at the exponential phase before the plateau is reached because it is essential that the ratio of target (*NFI*) to reference gene (*APP*) remains constant. Moreover, the efficiency of replication, E , is the same for both the genomic gene targets and their respective internal standards though it does not have to be the same for the target and reference genes. It is also essential that an equal molar quantity of both internal standards are used in the reaction; the absolute quantity of genomic DNA or internal standards is not critical.

FIGURE LEGENDS

Figure 1. Example of the *NF1* gene dosage PCR assay. The four products of the assay are 310 bp *NF1* and 232 bp *APP* fragments amplified from the subject's genomic DNA and 290 and 212 bp fragments amplified from the internal standard (I.S.) sequences in plasmids pKM204 and pKM201, which were spiked into the reaction. An autoradiograph is shown for illustration purposes only, products were quantitated by phosphorimage analysis. The ratio of genomic to I.S. product for each gene (boxed values) and the *NF1* gene dosage (bold value), which is the quotient of the ratio of *NF1* products over the ratio of *APP* products (Celi et al. 1994), were calculated.

Figure 2. Effect of cycle number on the reaction kinetics of gene dosage PCR. Products from amplification of *NF1* sequences (A) and *APP* sequences (B). Products amplified from genomic DNA (closed triangle), products amplified from I.S. plasmids (open boxes). Results of replicate experiments are graphed. Thirty-three identical reaction tubes were prepared and, beginning with cycle 18, three tubes were sampled and their reactions terminated at the end of each subsequent cycle. Products were resolved by electrophoresis and quantitated.

Figure 3. Effect of cycle number on amplification of genomic and internal standard sequences. (A) the ratio of *NF1* products amplified from genomic sequences to internal standard sequences (I.S), (B) the ratio of *APP* products amplified from genomic sequences to internal standard sequences, (C) the *NF1* gene dosage. Data are from the same experiment depicted in Figure 2.

Figure 4. Distinct distributions of gene dosage values of *NF1* disomic and monosomic control subjects. Genomic DNA from 21 unaffected individuals (presumed disomic at *NF1*) and from 11 individuals monosomic for *NF1* were assayed as described in Materials and Methods. Although duplicate reactions were carried out for all samples, Figure 3 shows one randomly selected outcome per subject. Box plot indicators are: arithmetic mean (closed square), median (50%; horizontal line bisecting open box), upper and lower quartile (75% and 25%; top and bottom boundaries of open box, respectively), upper and lower decile (90% and 10%; upper and lower limits of vertical line); outlying data points (dots extending from vertical line).

Figure 5. *NF1* microdeletions identified by the gene dosage assay. The top line is a non-scaled schematic of loci in the chromosome 17 *NF1* region; the relative positions of D17S795 and CRYB1 are unknown. Estimates of physical distances include the YAC contig at 700 kb (Marchuk et al. 1992) and the location of UT172, estimated at about 1.5 Mb centromeric to *NF1* (Shannon et al. 1994). A schematic of the deleted chromosome 17 homolog is shown for each patient. Thin lines are deleted regions, thick lines are not deleted, and vertical marks indicate the loci assayed by PCR amplification of somatic hybrid cell lines carrying the single deleted chromosome 17 homolog. Data showing the presence of all loci in the hybrid line carrying the undeleted chromosome 17 for each patient are not shown. *NF1* exon 32 was assayed by the gene dosage assay. P1-9, a 65 kb probe spanning *NF1* exons 2-11 assayed by FISH was deleted in all patients (data not shown).

Figure 6. The phenotype of young *NF1* microdeletion patients. Patient UWA167-1 is shown in (A) at 10 months and (B) at 20 months of age. Patient UWA183-1 is shown in (C) at 20 months and in (D,E) at 12.5 years of age.

References

- Ainsworth PJ, Chakraborty PK, Weksberg R (1997) Example of somatic mosaicism in a series of de novo neurofibromatosis type 1 cases due to a maternally derived deletion. *Hum Mutation* 9:452-7
- Ainsworth PJ, Rodenhiser DI (1991) Rapid nonradioactive detection by PCR of pHHH202/RsaI RFLP linked to neurofibromatosis type I [letter]. *Am J Hum Genet* 49:1098-9
- Allanson JE (1987) Noonan syndrome. *J Med Genet* 24:9-13
- Basu TN, Gutmann DH, Fletcher JA, Glover TW, Collins FS, Downward J (1992) Aberrant regulation of ras proteins in malignant tumour cells from type 1 neurofibromatosis patients [see comments]. *Nature* 356:713-5
- Bollag G, Clapp DW, Shih S, Adler F, Zhang YY, Thompson P, Lange BJ, et al (1996) Loss of NF1 results in activation of the Ras signaling pathway and leads to aberrant growth in haematopoietic cells. *Nature Genet* 12:144-8
- Brannan CI, Perkins AS, Vogel KS, Ratner N, Nordlund ML, Reid SW, Buchberg AM, et al (1994) Targeted disruption of the neurofibromatosis type-1 gene leads to developmental abnormalities in heart and various neural crest-derived tissues. *Genes Dev* 8:1019-29
- Cawthon RM, P OC, Buchberg AM, Viskochil D, Weiss RB, Culver M, Stevens J, et al (1990) Identification and characterization of transcripts from the neurofibromatosis 1 region: the sequence and genomic structure of EVI2 and mapping of other transcripts. *Genomics* 7:555-65
- Cawthon RM, Weiss R, Xu GF, Viskochil D, Culver M, Stevens J, Robertson M, et al (1990) A major segment of the neurofibromatosis type 1 gene: cDNA sequence, genomic structure,

and point mutations [published erratum appears in Cell 1990 Aug 10;62(3):following 608]. Cell 62:193-201

Celi F, Cohen M, Antonarakis S, Wertheimer E, Roth J, Shuldiner A (1994) Determination of gene dosage by a quantitative adaptation of the polymerase chain reaction (gd-PCR): rapid detection of deletions and duplications of gene sequences. Genomics 21:304-310

Celi FS, Zenilman ME, Shuldiner AR (1993) A rapid and versatile method to synthesize internal standards for competitive PCR. Nucleic Acids Res 21:1047

Chance PF, Abbas N, Lensch MW, Pentao L, Toa BB, Patel PI, Lupski JR (1994) Two autosomal dominant neuropathies result from reciprocal DNA duplication/deletion of a region on chromosome 17. Hum Mol Genet 3:223-228

Chen K-S, Manian P, Koeuth T, Potocki L, Zhao Q, Chinault AC, Lee CC, et al (1997) Homologous recombination of a flanking repeat gene cluster is a mechanism for a common contiguous gene deletion syndrome. Nature Genet 17:154-163

Cnossen MH, van der Est MN, Breuning H, van Asperen CJ, Breslau-Siderius EJ, van der Ploeg AT, de Goede-Bolder A, et al (1997) Deletions spanning the neurofibromatosis type 1 gene: implications for genotype-phenotype correlations in neurofibromatosis type 1? Human Mutation 9:458-464

Colman SD, Rasmussen SA, Ho VT, Abernathy CR, Wallace MR (1996) Somatic mosaicism in a patient with neurofibromatosis type 1. Am J Hum Genet 58:484-90

Colman SD, Williams CA, Wallace MR (1995) Benign neurofibromas in type 1 neurofibromatosis (NF1) show somatic deletions of the NF1 gene. Nature Genet 11:90-2

Cummings LM, Trent JM, Marchuk DA (1996) Identification and mapping of type 1 neurofibromatosis (NF1) homologous loci. Cytogenet Cell Genet 73:334-40

- DeClue J, Papageorge A, Fletcher J, Diehl S, Ratner N, Vass W, Lowy D (1992) Abnormal regulation of mammalian p21ras contributes to malignant tumor growth in von Recklinghausen (type 1) neurofibromatosis. *Cell* 69:265-267
- Gutmann DH, Collins FS (1995) von Recklinghausen neurofibromatosis. In: Scriver C (ed) *The Metabolic and Molecular Bases of Inherited Disease*. Vol. 1. McGraw-Hill, Inc., New York, pp 677-696
- Heid CA, Stevens J, Livak KJ, Williams PM (1996) Real time quantitative PCR. *Genome Res* 6:986-94
- Heim R, Kam M, Binnie C, Corns D, Cayouette M, Farber R, Aylsworth A, et al (1995) Distribution of 13 truncating mutations in the neurofibromatosis 1 gene. *Hum Mol Genet* 4:975-981
- Hoffmeyer S, Assum G (1994) An *RsaI* polymorphism in the transcribed region of the neurofibromatosis (NF1) gene. *Hum Genet* 93:481-2
- Huson S, Harper P, Compston D (1988) Von Recklinghausen neurofibromatosis: a clinical and population study in south-east Wales. *Brain* 111:1355-1381
- Huson SM (1994) Neurofibromatosis 1: a clinical and genetic overview. In: Huson SM, Hughes RAC (eds) *The Neurofibromatoses: A Pathogenetic and Clinical Overview*. Chapman & Hall Medical, London, pp 160-203
- Jacks T, Shih TS, Schmitt EM, Bronson RT, Bernards A, Weinberg RA (1994) Tumour predisposition in mice heterozygous for a targeted mutation in *Nf1*. *Nature Genet* 7:353-61

- Kamei T, Fukushima Y, Shibata A, Hayashi Y, Tachibana N, Takeda I, Niikawa N, et al (1992)
DNA deletion in patients with von Recklinghausen neurofibromatosis [letter]. *Clin Genet*
42:53-4
- Kayes LM, Burke W, Riccardi VM, Bennett R, Ehrlich P, Rubenstein A, Stephens K (1994)
Deletions spanning the neurofibromatosis 1 gene: identification and phenotype of five
patients. *Am J Hum Genet* 54:424-36
- Kayes LM, Riccardi VM, Burke W, Bennett RL, Stephens K (1992) Large de novo DNA
deletion in a patient with sporadic neurofibromatosis 1, mental retardation, and
dysmorphism. *J Med Genet* 29:686-90
- Kayes LM, Schroeder WT, Marchuk DA, Collins FS, Riccardi VM, Duvic M, Stephens K
(1992) The gene for a novel epidermal antigen maps near the neurofibromatosis 1 gene.
Genomics 14:369-76
- Kim HA, Rosenbaum T, Marchionni MA, Ratner N, DeClue JE (1995) Schwann cells from
neurofibromin deficient mice exhibit activation of p21ras, inhibition of cell proliferation
and morphological changes. *Oncogene* 11:325-35
- Lazaro C, Gaona A, Xu G, Weiss R, Estivill X (1993) A highly informative CA/GT repeat
polymorphism in intron 38 of the human neurofibromatosis type 1 (NF1) gene. *Hum*
Genet 92:429-30
- Legius E, Marchuk DA, Collins FS, Glover TW (1993) Somatic deletion of the
neurofibromatosis type 1 gene in a neurofibrosarcoma supports a tumour suppressor gene
hypothesis. *Nature Genet* 3:122-6
- Legius E, Marchuk DA, Hall BK, Andersen LB, Wallace MR, Collins FS, Glover TW (1992)
NF1-related locus on chromosome 15. *Genomics* 13:1316-8

- Leppig K, Kaplan P, Viskochil D, Weaver M, Orterberg J, Stephens K (1997) Familial neurofibromatosis 1 gene deletions: cosegregation with distinctive facial features and early onset of cutaneous neurofibromas. *Am J Med Genet* 73:197-204
- Leppig KA, Viskochil D, Neil S, Rubenstein A, Johnson VP, Zhu XL, Brothman AR, et al (1996) The detection of contiguous gene deletions at the neurofibromatosis 1 locus with fluorescence in situ hybridization. *Cytogenet Cell Genet* 72:95-8
- Li Y, O'Connell P, Breidenbach HH, Cawthon R, Stevens J, Xu G, Neil S, et al (1995) Genomic organization of the neurofibromatosis 1 gene (NF1). *Genomics* 25:9-18
- Marchuk DA, Saulino AM, Tavakkol R, Swaroop M, Wallace MR, Andersen LB, Mitchell AL, et al (1991) cDNA cloning of the type 1 neurofibromatosis gene: complete sequence of the NF1 gene product. *Genomics* 11:931-40
- Marchuk DA, Tavakkol R, Wallace MR, Brownstein BH, Taillon Miller P, Fong CT, Legius E, et al (1992) A yeast artificial chromosome contig encompassing the type 1 neurofibromatosis gene. *Genomics* 13:672-80
- Martin GA, Viskochil D, Bollag G, McCabe PC, Crosier WJ, Haubruck H, Conroy L, et al (1990) The GAP-related domain of the neurofibromatosis type 1 gene product interacts with ras p21. *Cell* 63:843-9
- Martinsson T, Sjoberg RM, Hedborg F, Kogner P (1997) Homozygous deletion of the neurofibromatosis-1 gene in the tumor of a patient with neuroblastoma. *Cancer Genet Cytogenet* 95:183-9
- Miles D, Freedman M, Stephens K, Pallavicini M, Sievers E, Weaver M, Grunberger T, et al (1997) Patterns of hematopoietic lineage involvement in children with neurofibromatosis, type 1 and malignant myeloid disorders. *Blood* 88:4314-4320

- Mulvihill JJ (1994) Malignancy: epidemiologically associated cancers. In: Huson SM, Hughes RAC (eds) *The Neurofibromatoses: A pathogenetic and Clinical Overview*. Chapman & Hall Medical, London, pp 487
- Pizzuti A, pieretti M, Fenwick RG, Gibbs RA, Caskey CT (1992) A transposon-like element in the deletion-prone region of the dystrophin gene. *Genomics* 13:594-600
- Purandare S, Breidenbach H, Li Y, Zhy X, Sawada S, Neil S, Brothman A, et al (1995) Identification of neurofibromatosis 1 (NF1) homologous loci by direct sequencing, fluorescence in situ hybridization, and PCR amplification of somatic cell hybrids. *Genomics* 30:476-485
- Regnier V, Meddeb M, Lecointre G, Richard F, Duverger A, Nguyen VC, Dutrillaux B, et al (1997) Emergence and scattering of multiple neurofibromatosis (NF1)-related sequences during hominoid evolution suggest a process of pericentromeric interchromosomal transposition. *Hum Mol Genet* 6:9-16
- Reiter LT, Hastings PJ, Nelis E, De Jonghe P, Van Broeckhoven C, Lupski JR (1998) Human meiotic recombination products revealed by sequencing a hotspot for homologous strand exchange in multiple HNPP deletion patients. *Am J Hum Genet* 62:1023-1033
- Reiter LT, Murakami T, Koeuth T, Pentao L, Muzny DM, Gibbs RA, Lupski JR (1996) A recombination hotspot responsible for two inherited peripheral neuropathies is located near a *mariner* transposon-like element. *Nature Genet* 12:288-297
- Riccardi VM (1992) *Neurofibromatosis, Phenotype, Natural History, Pathogenesis*. The Johns Hopkins University Press., Baltimore

- Riva P, Castorina P, Manoukian S, Dalpra L, Doneda L, Marini G, denDunnen J, et al (1996) Characterization of a cytogenetic 17q11.2 deletion in an NF1 patient with a contiguous gene syndrome. *Human Genetics* 98:646-650
- Rodenhiser DI, Ainsworth PJ, Coulter Mackie MB, Singh SM, Jung JH (1993) A genetic study of neurofibromatosis type 1 (NF1) in south-western Ontario. II. A PCR based approach to molecular and prenatal diagnosis using linkage. *J Med Genet* 30:363-8
- Sawada S, Florell S, Purandare S, Ota M, Stephens K, D V (1996) Identification of NF1 mutations in both alleles of a dermal neurofibroma. *Nature Genet* 14:110-112
- Serra E, Puig S, Otero D, Gaona A, Kruyer H, Ars E, Estivill X, et al (1997) Confirmation of a double-hit model for the NF1 gene in benign neurofibromas. *American Journal Of Human Genetics* 61:512-519
- Shannon K, O'Connell P, Martin G, Paderanga D, Olson K, Dinndorf P, McCormick F (1994) Loss of the normal NF1 allele from the bone marrow of children with type 1 neurofibromatosis and malignant meloid disorders. *N Engl J Med* 330:597
- Shen MH, Harper PS, Upadhyaya M (1996) Molecular genetics of neurofibromatosis type 1 (NF1). *J Med Genet* 33:2-17
- Side L, Taylor B, Cayouette M, Conner E, Thomspson P, Luce M, Shannon K (1997) Homozygous inactivation of the NF1 gene in bone marrow cells from children with neurofibromatosis type 1 and malignant myeloid disorders. *N Eng J Med* 336:1713-1720
- Skuse GR, Kosciolk BA, Rowley PT (1989) Molecular genetic analysis of tumors in von Recklinghausen neurofibromatosis: loss of heterozygosity for chromosome 17. *Genes Chromosomes Cancer* 1:36-41

The I, Murthy AE, Hannigan GE, Jacoby LB, Menon AG, Gusella JF, Bernards A (1993)

Neurofibromatosis type 1 gene mutations in neuroblastoma. *Nature Genet* 3:62-6

Tischler AS, Shih TS, Williams BO, Jacks T (1995) Characterization of pheochromocytomas in

a mouse strain with a targeted disruptive mutation of the neurofibromatosis gene NF1.

Endocrine Pathology 6:323-335

Upadhyaya M, Osborn MJ, Maynard J, Kim MR, Tamanoi F, Cooper DN (1997) Mutational and

functional analysis of the neurofibromatosis type 1 (NF1) gene. *Hum Genet* 99:88-92

Valero MC, Pascual Castroviejo I, Velasco E, Moreno F, Hernandez Chico C (1997)

Identification of de novo deletions at the NF1 gene: no preferential paternal origin and phenotypic analysis of patients. *Hum Genet* 99:720-6

Viskochil D, Buchberg AM, Xu G, Cawthon RM, Stevens J, Wolff RK, Culver M, et al (1990)

Deletions and a translocation interrupt a cloned gene at the neurofibromatosis type 1 locus. *Cell* 62:187-92

Wallace MR, Marchuk DA, Andersen LB, Letcher R, Odeh HM, Saulino AM, Fountain JW, et

al (1990) Type 1 neurofibromatosis gene: identification of a large transcript disrupted in three NF1 patients [1749]. *Science* 249:181-6

Wu BL, Schneider GH, Korf BR (1997) Deletion of the entire NF1 gene causing distinct

manifestations in a family. *Am J Med Genet* 69:98-101

Wu B-L, Austin M, Schneider G, Boles R, Korf B (1995) Deletion of the entire NF1 gene

detected by FISH: four deletion patients associated with severe manifestations. *Am J Med Genet* 59:528-535.

- Xu GF, Lin B, Tanaka K, Dunn D, Wood D, Gesteland R, White R, et al (1990) The catalytic domain of the neurofibromatosis type 1 gene product stimulates ras GTPase and complements ira mutants of *S. cerevisiae*. *Cell* 63:835-41
- Xu GF, Nelson L, P OC, White R (1991) An Alu polymorphism intragenic to the neurofibromatosis type 1 gene (NF1). *Nucleic Acids Res* 19:3764
- Xu HM, Gutmann DH (1997) Mutations in the GAP-related domain impair the ability of neurofibromin to associate with microtubules. *Brain Research* 759:149-152
- Xu W, Mulligan LM, Ponder MA, Liu L, Smith BA, Mathew CG, Ponder BA (1992) Loss of NF1 alleles in pheochromocytomas from patients with type I neurofibromatosis. *Genes Chromosomes Cancer* 4:337-42
- Zoller M, Rembeck B, Akesson HO, Angervall L (1995) Life expectancy, mortality and prognostic factors in neurofibromatosis type 1. A twelve-year follow-up of an epidemiological study in Goteborg, Sweden. *Acta Derm Venereol* 75:136-40
- Zoller MET, Rembeck B, Oden A, Samuelsson M, Angervall L (1997) Malignant and benign tumors in patients with neurofibromatosis type 1 in a defined Swedish population. *Cancer* 79:2125-2131

Table 1. Results of screening patients for deletions using the NF1 gene dosage assay.

No. Patients Screened	Phenotypic Class	Findings present in patients of each phenotypic class ¹					No. of patients with NF1 zygosity as predicted by the gene dosage assay ²		
		NF1 diagnostic criteria fulfilled ³	Additional findings ⁴	Facial anomalies	Sporadic NF1	Familial NF1	Disomic	Intermediate	Monosomic
13	A	+		+	+		8	2	3
4	B	+		+		+	4	0	0
6	C	+	+	+/-	+		2	1	3
7	D	-	+/-	+	+		7	0	0
Total	30						21	3	6

¹ Feature(s) present (+) or absent (-) in all patients in the category: (+/-) present in some patients in the category.

² NF1 gene dosage values for disomy (0.82 - 1.14), monosomy (0.37 - 0.53), and intermediate (0.54- 0.81).

³ Diagnostic criteria from NIH Consensus Development Conference, 1988. Patients in category D were less than 6 years of age and had presumptive NF1 based primarily on presence of café au lait spots.

⁴ One or more of documented mental retardation, abnormal CNS findings, multiple congenital anomalies, dramatically excessive tumor burden, additional findings consistent with a second genetic disorder, or malignancy at less than age 25.

Fig. 1

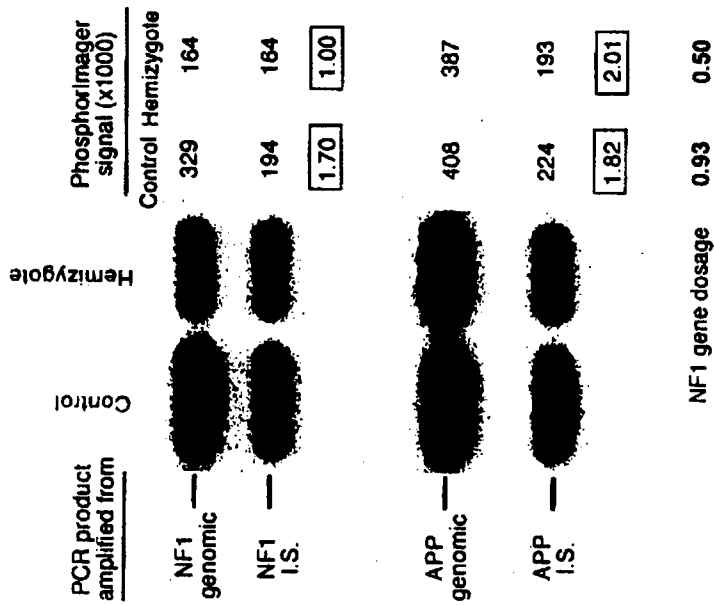


Fig. 2

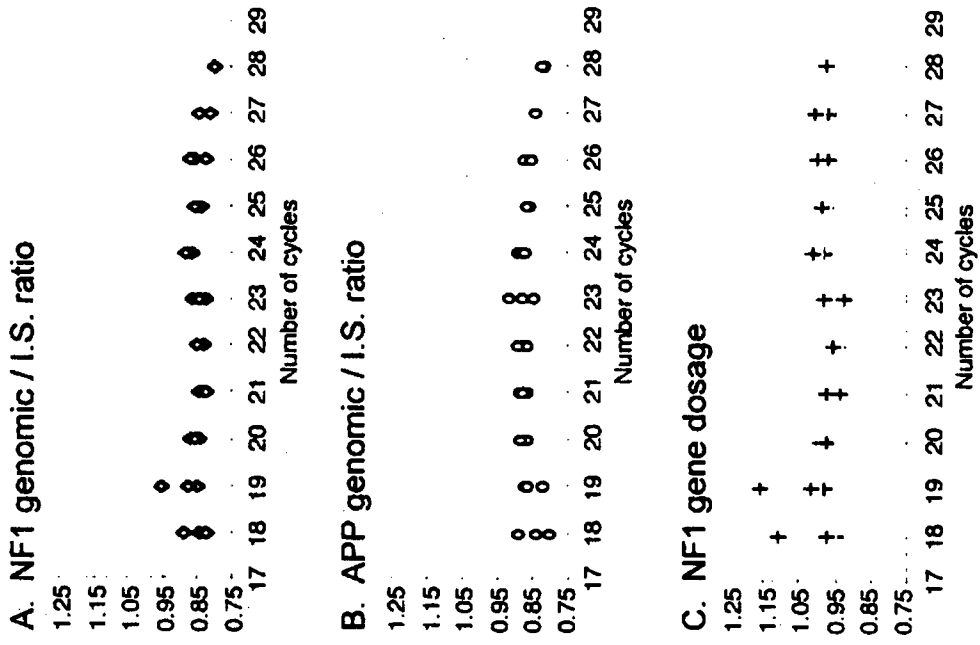


Fig. 3

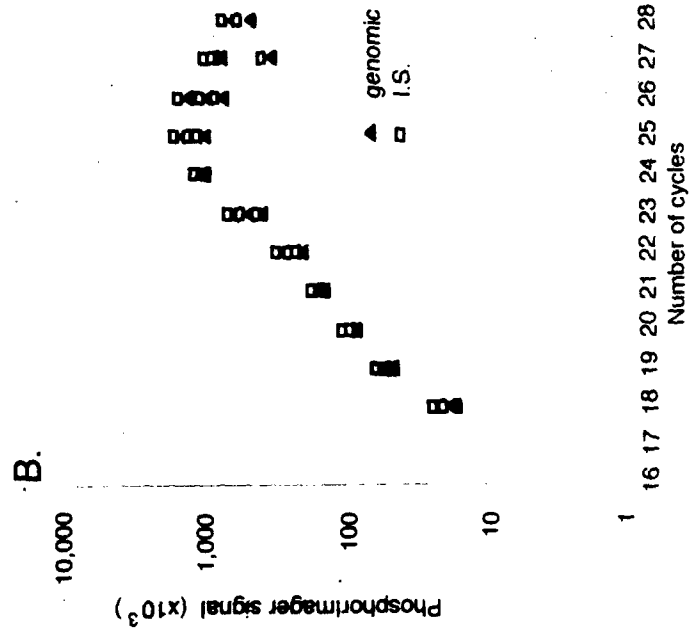
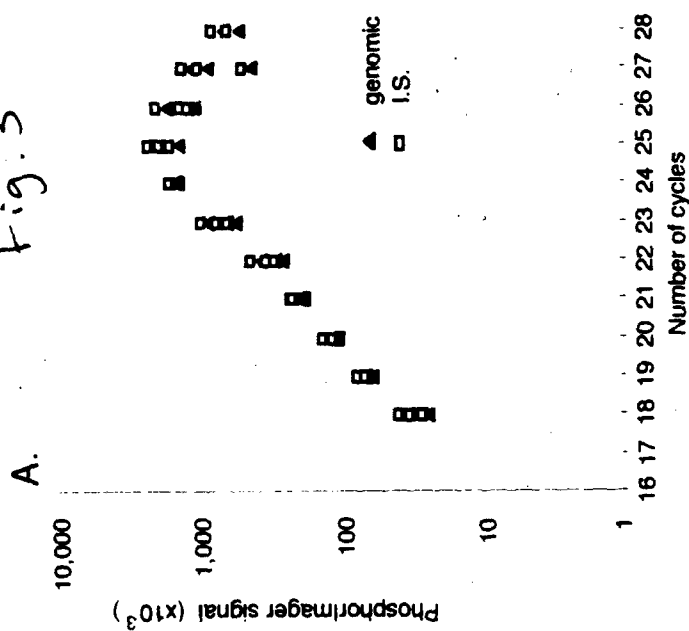
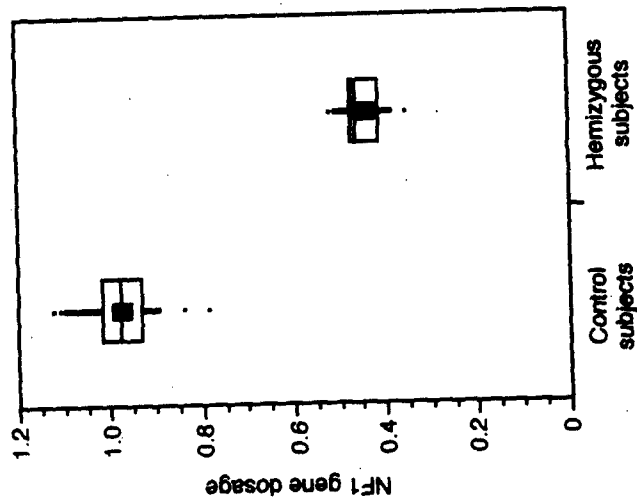


Fig. 4



proprietary information

Figure 5

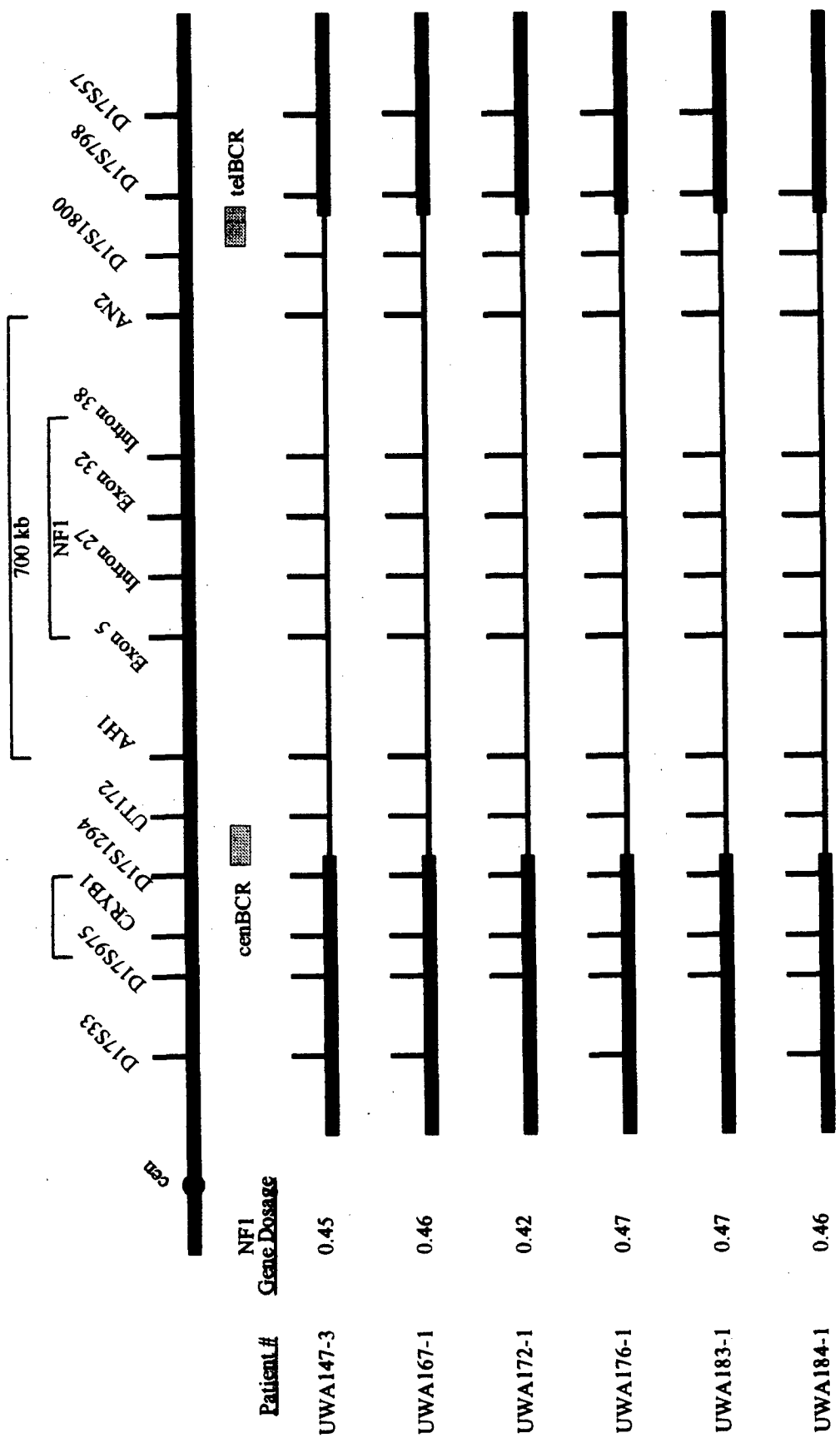


Figure 6



(Near Completion)

APPENDIX C.

Tumor suppressor inactivation by double mitotic recombination at clustered breakpoints

Proposed order of authors

Karen Stephens^{1,2,3}, Molly Weaver¹, Kathy Leppig⁴, Kyoko Maruyama¹, Elizabeth M. Davis⁵,
Rafael Espinosa III⁵, Melvin H. Freedman⁶, Peter Emanuel⁷, Lucy Side⁸, Michelle M. LeBeau⁵,
Kevin Shannon⁸

Departments of Medicine¹, Laboratory Medicine², Pathology³, Pediatrics⁴, University of
Washington, Seattle, Washington 98195-7720

⁵Department of Medicine, Section of Hematology/Oncology, University of Chicago, Chicago,
Illinois *zip code*

⁶Division of Hematology Oncology, Hospital for Sick Children, Toronto, Ontario, M5G1X8
Canada

⁷University of Alabama

⁸Department of Pediatrics, University of California, San Francisco, California 94143-0519.

Communicating author:

Karen Stephens, PhD

University of Washington

Medical Genetics 357720

Seattle, WA 98195

Introduction

Somatic inactivation of tumor suppressor genes is a fundamental mechanism of tumorigenesis. Somatic inactivating mutations commonly result in loss of constitutional heterozygosity (LOH) at multiple contiguous loci. Therefore, mapping chromosomal regions that show LOH is a powerful strategy to identify genes with tumor suppressor activity and to unravel the molecular mechanisms underlying somatic gene inactivation (reviewed in¹⁻³). This strategy has been applied to the analysis of a variety of tumors from patients with neurofibromatosis type 1 (NF1), an autosomal dominant tumor-susceptibility disorder affecting about 1 in 3500 individuals. LOH at *NF1*, along numerous flanking chromosome 17 loci, has been detected in benign neurofibromas, which develop in virtually all affected subjects, and in pheochromocytomas, neurofibrosarcomas, pilocytic astrocytomas, and childhood myeloid leukemias, which are less common NF1-associated tumors⁴⁻⁸. Although multiple loci showed LOH, genetic and biochemical evidence strongly suggest that a critical event in development of these tumors is LOH specifically at *NF1* leading to inactivated neurofibromin protein product. Tumors from patients who had inherited an inactive *NF1* allele from an affected parent showed loss of the remaining normal *NF1* allele inherited from their other unaffected parent (REFS). LOH typically did not occur at the *TP53* tumor suppressor locus on the short arm of chromosome 17 implying that changes in *TP53* expression play little, if any, role in development of at least some NF1-associated tumors. The identification of discrete intragenic *NF1* somatic mutations in some primary tumors provided compelling evidence that functional inactivation of *NF1* was sufficient for tumor development.⁹⁻¹³

The identification of patients with germline *NF1* microdeletions demonstrated that the increased risk of developing tumors, and the additional manifestations of pigmentary and bony abnormalities and learning disabilities, is due to neurofibromin haploinsufficiency (reviewed in^{14, 15, 16, 17}). The majority (~70%) of *NF1* patients have inactivating mutations that predict premature transcription termination of neurofibromin^{18, 19}. An internal domain of neurofibromin has sequence and functional homology with the catalytic domains of yeast *IRA* and mammalian p120 GAP, which are negative regulators of Ras proteins^{20, 21}. The GAP (GTP-ase activating protein) domain of neurofibromin bound to and negatively regulated p21 Ras by accelerating the conversion of active GTP-Ras to inactive GDP-Ras^{22, 23}. These data implied that functional inactivation of neurofibromin could deregulate Ras in a progenitor cell, thereby perturbing signal transduction, the cell cycle, and proliferation²⁴ *include Ras gen review*. The strongest data in support of this hypothesis is from genetic and biochemical analyses of malignant myeloid disorders (reviewed in ref.²⁵). Children with *NF1*, but not adults, are at an estimated 200-500 increased risk for these disorders, which include juvenile myelomonocytic leukemia (JMML), monosomy 7 syndrome (Mo7), and acute myeloid leukemia (AML)^{6, 26}. Primary leukemic cells from *NF1* children showed a selective decrease of neurofibromin-like GAP activity for Ras, an increased percentage of activated GTP-Ras, and abnormal proliferative activity upon exposure to low concentrations of GM-CSF²⁷. Similarly, neurofibromin-deficient myeloid progenitors, isolated from livers of *Nf1*^{-/-} knockout mice prior to embryonic death, showed proliferative changes in colony growth upon cytokine stimulation and caused a chronic

myeloproliferative syndrome when transplanted into irradiated recipient mice²⁷⁻²⁹. The constitutive activation of the Ras-dependent mitogen-activated protein kinase signaling pathway in *Nf1*^{-/-} hematopoietic cells from mice, which is further stimulated by cytokines, suggests a possible mechanism for the pathogenesis of myeloid leukemia in NF1 children²⁸.

Previously, we proposed that haploinsufficiency for a gene contiguous with *NF1* was responsible for the early onset and increased burden of neurofibromas observed in patients with germline *NF1* microdeletions^{16, 17, 30, 31}. In the present study, we sought to determine if LOH in leukemic cells of NF1 children was due to a somatic *NF1* microdeletion that involved similar sequences. Instead, we found that a predominant mechanism of LOH was double mitotic recombination at clustered breakpoints. This rearrangement led to interstitial isodisomy for a large segment of chromosome 17 harboring the inactivated *NF1* allele. Although this is the first report of interstitial isodisomy as a mechanism of somatic inactivation of a tumor suppressor gene, it may have gone unrecognized in many previous LOH studies.

RESULTS

Delineation of a Large Region of LOH in an NF1-Associated Leukemia

In a previous study, genetic analysis of JMML bone marrow samples from children with NF1 revealed LOH at *NF1* in the CD34⁺ subpopulation of immature myeloid cells¹⁰. In contrast, lymphoblasts from these patients typically retained both *NF1* alleles in lymphoblastoid cell lines immortalized by Epstein-Barr virus³⁴. A single exception was found in a 9 month old boy with sporadic NF1 and an unusual myeloproliferative syndrome (Table 1, patient no. 1), whose unfractionated bone marrow and immortalized lymphoblastoid cells both showed loss of the maternal *NF1* allele^{10, 34}. Therefore, this malignant clone was derived from a progenitor cell capable of producing both myeloid and lymphoid cells. While normal lung tissue showed both maternal and paternal *NF1* alleles (Figure 5 in ⁶), primary tumor tissue showed LOH for the maternal allele and an R1276X mutation in the paternal allele that predicted a truncated, inactive neurofibromin^{12, 34}. In addition, leukemic cells of patient no. 1 retained both parental copies of the TP53 tumor suppressor gene at chromosome 17p13.1(ref. ^{10, 34}). Together, these data were consistent with patient no.1 carrying a germline R1276X mutation in the paternal allele and a normal maternal *NF1* allele, which was subsequently lost in the tumor tissue.

The patient's bone marrow was examined to determine if other chromosome 17 loci also showed LOH. Genotypic analysis revealed that multiple loci in an interstitial region of the q arm showed LOH for maternally-derived alleles (Figures 1,2). The length of the LOH region was estimated at 76 cM on a sex-averaged genetic map and approximately 46-54 Mb on the chromosome 17 physical map (see Methods). LOH of this region was not due to an interstitial deletion; cytogenetic analyses of unstimulated bone marrow and immortalized lymphoblasts revealed two normal chromosome 17s (data not shown).

LOH is the result of interstitial isodisomy in patient no. 1

To determine if the patient's leukemic cells had one or two *NF1* alleles, FISH was performed with the *NF1* P1-12 probe. *NF1* hybridization signals were detected on both chromosome 17 homologs (Figure 3A). This data, along with the LOH analyses and normal karyotype, indicated that the maternal homolog of chromosome 17 was comprised of a p arm, centromere, q proximal

segment, and a short q subterminal segment all of maternal origin (Figure 2, patient no. 1, open bar). The interstitial q arm, however, was paternally-derived and carried the R1276X *NF1* mutation (Figure 2, patient no. 1, closed bar). The leukemic clone, therefore, had a normal paternal chromosome 17 homolog and a recombinant maternal homolog, resulting in interstitial paternal isodisomy for a 50 Mb region (Figure 4A). The leukemic cells were homozygous not only for the *NF1* R1276X allele, but also for all genes and sequences located in the isodisomic region.

NF1 Gene Copy Number in Other Leukemias of NF1 Children

To determine if LOH resulted from interstitial isodisomy of chromosome 17 in other cases, bone marrows were obtained from additional *NF1* children whose leukemias showed LOH at *NF1*. To determine if any of these samples were disomic for *NF1*, we utilized an *NF1* gene dosage PCR assay. Because this assay was originally developed by us for copy number determination in normal tissues (Maruyama et al., submitted), we first confirmed that it accurately measured *NF1* gene dosage in both normal and malignant tissues of patient 1 and his parents. In 2 independent experiments, an *NF1* gene segment amplified from peripheral blood DNA of the unaffected parents and from bone marrow and immortalized lymphoblastoid cell DNA of patient 1 gave scores ranging from 0.91 - 1.08 (Table 2, patient no. 1). These values predicted that all samples were disomic at *NF1* (see Methods; ³⁵), which was consistent with the previous FISH and genotypic studies for this family.

Because this assay gave the expected results in test tissues, it was used to assay bone marrow DNA samples from additional children with malignant myeloid disorders with LOH at *NF1*. As shown in Table 2, leukemic cells from 8 patients had gene dosage values consistent with *NF1* disomy, while the leukemias from the 3 remaining patients had values consistent with *NF1* monosomy. These data demonstrated that 8 out of 11 leukemias showed both LOH and disomy at *NF1* indicating that parental isodisomy was a predominant feature of malignant myeloid cells with *NF1* LOH.

FISH of Leukemic Cells Confirms NF1 Copy Number

Because the *NF1* gene dosage assay was validated using peripheral blood from nonleukemic subjects, FISH was performed to confirm the results obtained with leukemic cells. Cryopreserved bone marrow specimens were available from 5 of the children studied. In each case, FISH with an *NF1* probe confirmed the gene copy number as predicted by the *NF1* gene dosage assay. These cases included 4 with LOH at *NF1* in conjunction with *NF1* disomy (patients no. 2,3,5,6 in Tables 1 and 2) and 1 case with LOH at *NF1* and *NF1* monosomy (patient no. 11). With the exception of patient 11, the percentages of cells with two signals for the chromosome 17-specific centromeric probe Cep@17 and the *NF1* probes were comparable to those observed for the P263P1 control probe, which was co-hybridized with the *NF1* probes. Consistent with the prediction of *NF1* monosomy for patient 11, we observed a population of cells with only one *NF1* signal (29%), but two signals for both the control probes Cep@17 and P263P1 (95% and 97%, respectively). The leukemia cells also had two signals for the chromosome 17 centromere-specific probe (95%). Control samples, including leukemic cells from 4 children with *NF1* that retained heterozygosity at *NF1* and a bone marrow sample from a patient with AML in complete remission, were disomic at the *NF1* locus as expected.

To confirm that the cells being examined represented the malignant clone, a chromosome 7-specific probe (Cep@7) was hybridized to bone marrow cells of patient no. 3, who had monosomy 7 syndrome, LOH at *NF1*, a gene dosage score of 0.93, and 2 *NF1* alleles by FISH (Tables 2,3). As expected, FISH revealed one copy of chromosome 7 in cells that had 2 signals with the *NF1* probes (Table 2; Figure 3B).

Clustering of LOH genetic breakpoints

In addition to patient no. 1, DNA was available from primary leukemic cells of 9 patients to map the extent of chromosome 17 LOH. As depicted in Figure 2, the patient bone marrow constituted two distinct subsets. One was comprised of 8 cases with large LOH regions, while the second subset consisted of 2 cases with restricted LOH regions. The maximum estimated sex-averaged genetic length of the large LOH region from D17S959 to D17S928 was 89 cM (Figure 2). The smaller, restricted LOH regions had a maximum length of 22 cM, as estimated from D17S1294 to D17S250.

The q terminal marker, D17S928, was informative and retained heterozygosity in four of the cases with large LOH regions (Figure 2, patients no. 1-3, 6). This data, along with the *NF1* gene copy number analyses and normal karyotype of bone marrow cells, provided compelling evidence that the leukemic cells had interstitial isodisomy for an ~ 50 Mb region of chromosome 17, as depicted in Figure 3A. The isodisomic regions in the additional 4 cases (patients no. 4, 5, 7, 8) were of similar size and extent, but because D17S928 was uninformative, it is not known if they were interstitial in nature.

Among the 8 isodisomic cases, both the proximal and distal LOH breakpoints were clustered (Figure 2). The centromeric breakpoint in all cases mapped to a maximum interval bounded by D17S959 and D17S975/D17S1294, a distance estimated at 2.7 cM. All distal breakpoints mapped near the telomere. The leukemic cells of patients no. 1-3 and 6 with interstitial isodisomy, had telomeric breakpoints between D17S1822/D17S1830 and D17S928, a distance of about 9.6 cM. The distal breakpoints of the remaining 4 patients mapped telomeric to D17S1822/D17S1830, but were not localized to a specific interval.

The 2 cases with restricted LOH regions, patients no. 9 and 11 (Figure 2) also had breakpoints mapping within the same intervals. The centromeric breakpoints between D17S1294 and *NF1* intron 38, while the telomeric breakpoints were localized between D17S1800 and D17S250. The size of the centromeric interval was less than 11.7 cM, the sex-averaged genetic distance from D17S1294 to D17S1800. The telomeric breakpoint interval was from D17S1800 to D17S250 is 22 cM in length. The restricted LOH region in these 2 cases apparently arose by interstitial deletion of the normal *NF1* allele because the leukemic cells were monosomic for *NF1* (Tables 1 and 2, Figure 3A).

Parental origin of LOH regions

Leukemic cells of patients no. 1-3, and 8 were isodisomic for paternally-derived sequences, while the tumor cells of patients 4-7 were isodisomic for maternally-derived sequences of the same regions (Figure 2, Figure 4A). In each patient with familial NF1, the region of isodisomy was derived from the affected parent. Patients no. 2 and 8, who inherited a defective *NF1* allele from their fathers (Table 1), had leukemic cells that were isodisomic for sequences of paternal origin and had lost the normal maternal *NF1* allele. Similarly, patients no. 4-7, who inherited a maternally-derived mutant *NF1* allele (Table 1), showed maternal isodisomic regions in their

bone marrows and had lost the normal paternal *NF1* allele. The tumor of patient no.1 was shown to have an R1726X inactivating mutation in the paternal *NF1* allele and loss of the normal maternal allele¹². Therefore, each of the tumors had lost the normal *NF1* allele and instead carried 2 copies of the dysfunctional *NF1* allele. The leukemic cells of patients no. 9 and 11 that had undergone interstitial deletion had a related pattern. The normal *NF1* allele was lost and one copy of the dysfunctional *NF1* allele was retained, which in these 2 cases was derived from either parent (Table 1, Figure 2, Figure 4A).

DISCUSSION

The patterns of LOH at chromosome 17 loci were analyzed to gain insight into the mechanisms leading to allelic loss of *NF1* in primary leukemia cells of NF1 children. Analysis of bone marrows from 11 unselected cases showed that LOH occurred by two distinct mechanisms, each of which resulted in loss of the normal *NF1* allele. Three tumors (30%) had interstitial microdeletions between D17S1294 and D17S250, an estimated distance of 22 cM or 17 Mb that spanned the normal *NF1* gene at chromosome 17q11.2 (Figures 2, 4A, Table 1). The remaining 8 cases (70%) resulted from isodisomy for a 50 Mb chromosomal segment harboring a defective *NF1* allele. In at least 4 of these cases, the isodisomic segment was interstitial to the chromosome 17q arm (Figures 2,3) and estimated to be 55 Mb in length (distance from D17S1878 to D17S1822/D17S1830; see Methods).

Although somatic isodisomy of varying extent commonly leads to LOH in tumors, we believe this is the first report of interstitial isodisomy. Isodisomy for an entire chromosome has been observed in retinoblastomas and many other tumor types (Table 3 and references therein). The underlying mechanism is attributed to chromosomal nondisjunction with reduplication (or duplication followed by nondisjunction), which results in homozygosity at all loci along the length of the chromosome. Partial isodisomy for a chromosomal arm has also been detected in many tumors, presumably due to a single mitotic recombination. This results in homozygosity at all loci between the site of recombination and the telomere. Somatic mosaicism for isodisomy of chromosome 11p, apparently the result of mitotic recombination early in development, has been detected in patients with Beckwith-Wiedemann syndrome, a disorder of the overgrowth, cancer predisposition³⁶. In addition to somatic isodisomy, presumed germline rearrangements leading to constitutive uniparental isodisomy for an entire chromosome have been reported (reviewed in³⁷). We are not, however, aware of any reports of germline interstitial isodisomy.

Although our sample size was small, the detection of only two mechanisms of LOH at *NF1* with clustered breakpoints, was unexpected. Using the paradigm of the *Rb1* tumor suppressor, somatic inactivation occurs by any one of numerous rearrangements and mutational events, without evidence of breakpoint clustering. Examples of RB1 inactivation in retinoblastomas include every mechanism listed in Table 1, with the exceptions of double mitotic recombination and illegitimate V(D)J recombination (reviewed in³⁸ and another later review). Due to tissue-restricted expression of V(D)J recombinase, the later mechanism would not be expected in most tumor types. These data provide compelling evidence that the critical genetic alteration in retinoblastomas is the functional inactivation of Rb1 and that the mechanism employed makes little or no contribution to tumorigenesis. Our data suggest that *NF1* loss in malignant myeloid disorders may not follow this paradigm.

Mechanisms of LOH at NF1 in leukemic cells

To explain our findings, we propose that interstitial isodisomy arose by a double mitotic recombination event between non-sister chromatids during the S/G2 phase of the cell cycle of a ancestral cell (Figure 4B). One of 4 possible segregants would have homozygous inactivation of *NF1* from replacement of an interstitial maternal segment carrying a functional *NF1* allele with a homologous paternal segment with a dysfunctional *NF1* allele. A tumor arising from this

segregant would, like the tumors of patients no. 1-8, have a normal karyotype, show LOH at all loci in the 50 Mb interstitial isodisomic region, and have 2 copies of the *NF1* gene. For patient no. 6 with interstitial maternal isodisomy, the parental origin of the segments would be reversed from those depicted in Figure 4B. Tumors with the genotypes of any of the other three possible segregants were not detected, presumably because homozygous inactivation of *NF1* is essential for development of malignant myeloid leukemias in *NF1* children. An alternate mechanism underlying interstitial isodisomy would be a double recombination during the G1 cycle of an ancestral cell. This is, however, considered less likely because of the additional requirement for chromosome duplication (Figure 4C). In addition, we cannot rule out the possibility that the large interstitial isodisomic regions arose in a stepwise manner by sequential single recombination events during S/G2 in a series of precursor cells. However, because the genotype of a tumor is a reflection of both somatic mutation and selection, it seems highly unlikely that selection would favor proliferation of each of several "intermediate" cells. The lack of an informative qter locus in the tumors of patients no. 4,5,7, and 8 precluded determining if the isodisomic regions were interstitial. If homozygosity extends through the telomere, then these malignant clones probably arose by a single recombination event in the same 17q proximal breakpoint region as the other clones.

Besides mitotic recombination, it is theoretically possible that the isodisomic regions arose by gene conversion, which is the non-reciprocal transfer of genetic information from donor to recipient chromosome. Although considerable circumstantial evidence has been reported for gene conversion-like events in germline and somatic tissues of mammals³⁹ [*Strachan, Nat Gen article?*]^{40, 41}, conversion of a 50 Mb segment would dramatically exceed previous reports. In humans only small segments of several kilobases or less appear to be converted^{42 43 44 45 46 47}. In some cases, however, reliance on the polymerase chain reaction may have precluded detection of larger conversion tracts. Apparent large-scale conversion-like events, like those involving the ___ kb steroid 21-hydroxylase gene in some patients with congenital adrenal hyperplasia, are thought to arise by a series of independent crossovers, involving at least one unequal sister chromatic exchange⁴⁸.

The interstitial somatic microdeletions observed in patients no. 9 and 11 clearly arose by an independent, rather than a reciprocal, mechanism from that of the isodisomic cases. Although little is known at the sequence level about somatic microdeletion breakpoints, clues can be garnered from molecular analysis of germline microdeletions that cause human genetic disease. Although presumed to be meiotic in origin, many human germline mutations may actually occur during the ≥ 30 mitoses that occur in germ cells before each meiotic event⁴⁹. Evidence is mounting that germline microdeletions result from homologous recombination between flanking low copy number repeat sequences (reviewed in ref. ⁵⁰). Examples include the dystrophin deletion hotspot in Duchenne muscular dystrophy (*Pizzatti, 1992, Genomics, look for more recent ref?.*) and the ~5 Mb deletion responsible for Smith-Magenis syndrome⁵¹. The strongest evidence is from the analysis recombination between CMT1A-REP repeats that generates reciprocal products carrying a duplication or a deletion of the intervening 1.5 Mb region. Within the 24 kb CMT1A-REPs, about 75% of the deletion breakpoints map to a 456 bp region near a *mariner* transposon-like element, which is postulated as the site of a double strand break that initiates the recombination event^{52, 53}. The recombination products cause different inherited neuropathies; a

duplication results in Charcot-Marie-Tooth disease type 1A, while a deletion causes hereditary neuropathy with liability to pressure palsies (*Chance et al. Hum Mol Genet 3, 223, 1994*).

Clustering of LOH breakpoints

LOH breakpoints in the isodisomic cases were clustered, as were those in the microdeletion cases. The microdeletion breakpoints in patient nos. 9 and 11 mapped to the same proximal and distal genetic intervals estimated at 11.7 and 10.3 cM, respectively (Figure 2). Although the physical length of these intervals is unknown, estimates from the Genome Data Base are 5 Mb for the centromeric interval and 11 Mb for the distal (see Methods). The isodisomic breakpoints in all 8 cases examined were in a 2.7 cM centromeric interval between D17S959 and D1294, an estimated physical length of 5.3 Mb (Figure 2, Methods). The distal breakpoints in 4 cases mapped to a 9.6 cM interval flanked by D17S1822/D17S1830 and D17S928. The physical length of this interval is estimated at 7.2 Mb. [Karen--may need a note that Mb estimates are very crude; unclear to what extent male/female recombination freq differences specific to chr 17 are taken into consideration in conversion; waiting for reply from GDB]. To determine if recombination occurred at specific sequences, the LOH breakpoints could be mapped using single nucleotide polymorphisms. The availability of immortalized cell lines for the parents and the malignant clone of patient no. 1 would facilitate cloning the breakpoints in this case, which could subsequently be analyzed in the leukemic cells of other patients with isodisomy.

The existence of putative recombinogenic sequences in the somatic microdeletion breakpoint intervals defined by patients no 9 and 11, is consistent with recent data from the analysis of germline *NF1* microdeletions. We now have identified 8 additional *NF1* microdeletion patients to add to the 9 cases reported previously^{17, 30, 31} (K. Maruyama et al., submitted; K. Stephens et al., unpublished data). Analysis of somatic cell hybrids have mapped both the proximal and distal germline deletion breakpoints in all 17 patients to the same marker intervals as the somatic breakpoints in patients no. 9 and 11 (Figure 2; K. Stephens et al, unpublished data). These data imply the existence of recombinogenic sequences, perhaps low copy number repeats, that predispose to both germline and somatic microdeletions in the intervals of D17S1294 to *NF1* exon 38 and D17S1822/D17S1830 to D17S928. Fine mapping and cloning of the germline microdeletion breakpoints is in progress to identify the recombination sites. These data will provide the opportunity to determine if LOH microdeletion breakpoints in leukemic cells occur in the same or related sequences.

The variety of LOH mechanisms and patterns may be restricted to either small interstitial deletions or large isodisomic segments in order to maintain biallelic expression of an gene on the q arm that is essential for survival of hematopoietic cells. Reduction to hemizyosity by nondisjunction, large deletion events, and other mechanisms, would be lethal. This putative essential gene would also be expected to maintain biallelic expression in the ~50% of bone marrows from leukemic *NF1* children that do not show LOH at the *NF1* locus¹⁰. Presumably in these tumors, neurofibromin was inactivated by a mechanism that retained heterozygosity (Table 1) or these tumors carry an undefined mutation in the Ras pathway that is functionally equivalent to neurofibromin-deficiency. Mitotic recombination at preferential sites may occur due to a selection of two different functions on the same chromosome: loss of neurofibromin function and retention of biallelic expression from an essential gene. Similar to the way we select for recombination in mammalian cells in vitro. Findbest ref?? It may be possible to test this hypothesis directly by analyzing the extent of LOH at chromosome 11 loci in the leukemic cells of *Nf*^{+/-}

mice with myeloid malignancies. Because synteny of human chromosome 17q loci is maintained with mouse chromosome 11 (<http://www.informatics.jax.org/bin/oxfordgrid>), this hypothesis would predict comparable LOH regions. Intriguingly, we have recently demonstrated that therapy-related myeloid leukemias in *Nf*^{+/-} mice show both LOH and disomy at the *NF1* locus (N. Mahgoub et al, submitted).

How do the LOH regions observed in malignant bone marrow cells compare to those previously reported in other tumors of NF1 patients? Most of the early LOH studies showed either a significant number of tumors with LOH at 17p loci^{4, 54} or were analyzed with an insufficient number of markers to detect similarities. However, two reports of LOH in benign neurofibromas suggests that these cases have LOH regions similar in extent to those observed in the present study. Serra et al.⁹ observed LOH at *NF1* in 15 (n=60) neurofibromas. Six tumors showed restricted LOH regions similar in extent to the leukemic microdeletion cases (Figure 2, patients no. 9,11). Seven neurofibromas had large LOH regions with centromeric breakpoints in a region comparable to the leukemic isodisomy cases (Figure 2, patients 1-8), and 2 tumors showed LOH only for *NF1* intragenic markers (not observed in the present study). In an independent analysis, 8 out of 22 neurofibromas had LOH regions that could be grouped into the same subsets. Three cases showed restricted LOH regions, 4 had large LOH regions with centromeric breakpoints in comparable regions, and 1 showed LOH only at an *NF1* intragenic marker⁷. In these studies, it was not determined whether heterozygosity was retained near the 17q telomere in the cases with large LOH regions. The most telomeric locus tested that was informative was D17S785 or D17S21, which are located about 15-20 Mb centromeric to D17S928, the locus that retained heterozygosity in our study. In addition, it is not known if loci in the LOH regions of neurofibromas are monosomic or disomic. Perhaps the *NF1* gene dosage PCR assay could address this question, particularly for that subset of neurofibromas with a limited admixture of non-tumor tissues, as determined by little or no amplification of the normal allele. Ascertainment of the LOH mechanism(s) in neurofibromas will be a direct test of whether the mitotic recombination we observed is specific to, and selected for, only in hematopoietic stem cells or if they also contribute to tumor development in other tissues of NF1 patients.

Clustering of recombination breakpoints could also be due to physical proximity or specific features of chromosome 17 regions. It has been shown that individual chromosomes occupy discrete territories within the interphase nucleus and that chromosome arms move in a cell cycle-dependent manner (reviewed in ⁵⁵). The proximity of subchromosomal regions could facilitate recombination either during G1 or S/G2 phase of the cell cycle. The breakpoint regions could also contain chi-like sequences or unknown elements that are prone to double-strand breaks, both of which are implicated in regions with increased recombination in mammalian cells [Ref of DSB and Marshall B. et al, 1996, *Gene* 174:175-179].

Implications of somatic NF1 microdeletion and isodisomy in leukemogenesis

The remarkable nature of our findings prompts the question of whether attenuation of normal neurofibromin function in a precursor cell is sufficient for development of childhood leukemia? Or, are there additional functional consequences of the underlying genetic mechanism of *NF1* inactivation that may be important in leukemogenesis? Data from the present study do not identify any putative genetic or functional factors that may contribute to onset of leukemia.

Neither the isodisomic nor the microdeletion rearrangements were specific to any one type of leukemia; obvious differences in disease course in these two sets of patients were not detected (Table 1). Leukemias that retained maternally- or paternally-derived chromosome 17q sequences were observed among both the isodisomic and microdeletion cases (Figure 2). This excluded the possibility of an imprinted gene whose normal mono-allelic, parental-specific expression pattern was perturbed. While the microdeletions resulted in loss of sequences and, in theory, could generate a novel fusion gene product, loss of sequences at the recombination sites of the isodisomic cases would be considered less likely. Although during *recBCD*-mediated recombination in *E. coli*, the exonuclease activity of the *recBCD* enzyme destroys DNA between its entry point at a double strand break and the chi element, which is thought to inhibit the exonuclease and reveal the recombinase activity (reviewed in⁵⁶).

While functional inactivation of neurofibromin is apparently sufficient for the myeloproliferative phenotype, there is evidence that modifying genes may contribute to the development of acute leukemia. Modifying loci are implicated in the decreased latency of leukemia observed in *Nf1*^{+/-} mice in the BXH-2 genetic background, which is permissive for horizontal transmission of an ecotropic virus²⁹. In addition to an *NF1* targeted disruption, these mice carried an average 3.8 somatically acquired proviruses. The authors postulated that proviral insertional mutagenesis altered expression of other loci, which, in concert with *Nf1* haploinsufficiency, caused an earlier onset of leukemia^{29, 57}. Some myeloid leukemias of *NF1* children also have monosomy 7, which is presumed to be secondary to LOH of the normal *NF1* allele^{6, 58}. It is interesting that *Nf*^{+/-} mice do not develop leukemia until their second year of life, while in humans it is affected children, but not adults who are at risk. Although this may be attributed to general interspecies differences, it could also reflect differences in expression of a specific *NF1*-modifying locus in the mouse.

It is possible that *NF1* children who tend to develop leukemias have inherited an *NF1* disease allele (familial or *de novo*) on a specific haplotype that predisposes to hematopoietic malignancies. Unexpectedly, virtually complete linkage disequilibrium is maintained across the ~350 kb *NF1* locus^{59, 60}. As expected for a disorder with a high mutation frequency⁶¹, however, there was no association of a specific haplotype with the *NF1* disease allele in 30 patients analyzed⁵⁹. Perhaps if the patient cohort was comprised of *NF1* children that developed malignant myeloid leukemias a specific haplotype would be predominant. This hypothesis is consistent with our observations of leukemic cells that retain either one or two copies of the dysfunctional *NF1* locus, irregardless of parent of origin. The low frequency of leukemia in *NF1* children could reflect a low prevalence of this haplotype.

This hypothesis becomes more tenable due to the existence of 3 genes within the *NF1* gene that could have gain-of-function or loss-of-function alleles in disequilibrium with *NF1*. These genes, *EVI2A*, *EVI2B*, and *OMG*, are embedded within *NF1* intron 27b and are transcribed in the direction opposite that of the *NF1* gene (*ref*). In addition to their intriguing location, other features make them candidates as putative modifiers of *NF1*-associated tumorigenesis. *EVI2A* and *EVI2B* are genes of unknown function that are highly expressed in human bone marrow and myeloid cells⁶². Although these 2 genes are in close proximity to sites of frequent proviral integration in BXH2 mice with leukemia, it is actually the *NF1* gene that is inactivated by their insertion⁵⁷. No consistent changes in expression of *EVI2A* or *EVI2B* were detected in these mice suggesting that these genes are not involved in myeloid tumor induction in this mouse

model. Overexpression of OMG in fibroblasts suppresses growth presumably by inhibition of PDGF-induced mitogenesis [Habib et al *Oncogene* *need volume*:525-1531, 1998]. Although expression of OMG is thought to be restricted primarily to tissues of the central nervous system, the expression level in bone marrow is unknown. A specific haplotype that predisposes a neurofibromin-deficient hematopoietic precursor cell to proliferate into a myeloid tumor does not require that the modifying allele be in disequilibrium with the *NF1* disease allele. It could simply be that the *NF1* disease allele and the modifying allele are coincidentally in *cis* on certain haplotypes and are therefore both altered by the rearrangements leading to LOH.

Broad implications of interstitial isodisomy

Interstitial isodisomy as a mechanism of LOH may have gone unrecognized in many previous studies. Genotyping only the tumor suppressor locus and/or a few flanking loci would not necessarily have revealed the interstitial nature of the LOH region. Furthermore, LOH studies alone, without accompanying physical analyses, can not distinguish between LOH arising from interstitial isodisomy or from deletion, nondisjunction, and other mechanisms where alleles are physically lost. For example, two recent LOH studies reported data strikingly similar to ours. Intestinal tumor epithelium in mice that were *cis*-compound heterozygotes at *Apc* and *Dpc4* loci showed LOH of both normal alleles in conjunction with disomy at these loci, which are 30 cM apart⁶³. Gupta et al⁶⁴ demonstrated that the majority of clones from T lymphocytes of *APRT* heterozygotes that underwent *in vivo* multilocus LOH at 16q exhibited normal diploid karyotypes and were disomic for *APRT*. Analysis of additional loci on these chromosomes may reveal a region of interstitial isodisomy. In the present study, the retention of heterozygosity at the D17S928 close to the telomere (Figures 2, 4A) is intriguing. It is unclear if this was coincidental or if recombinant chromosomes in other tumors also preferentially maintain their original maternal or paternal subtelomeric sequences. This could be tested directly by genotyping telomeric loci in a collection of tumors that previously showed multilocus LOH due to a presumed single mitotic recombination event. This would include for example 80% of retinoblastomas (*karen, check percentage again and reference*).

A broad implication of our study is that the power of genetic LOH studies can be increased significantly when performed in concert with physical analyses for gene copy number determination. This provides the opportunity to detect a putative modifying gene, a unique genetic mechanism leading to somatic mutation, a sequence that may be recombination-prone in certain tissues, an imprinted gene whose expression is altered, or a correlation between LOH genotype and tumor/disease phenotype. In addition to increasing our understanding of somatic mutation in tumorigenesis, such information could affect the design and efficacy of putative therapeutic agents.

METHODS

Patients. Clinical descriptions and the results of *NF1* mutation detection and LOH studies have been reported for most of the patients included in this report^{10, 12, 34}. Selected demographic and laboratory data are summarized in Table 1.

***NF1* gene dosage assay.** A PCR gene dosage assay, originally developed to detect germline deletions of *NF1*, was performed as described previously (Maruyama et al., submitted)⁶⁵. The

assay measures the copy number of a segment of exon 32 of the *NF1* gene by quantitating the *NF1* product relative to the product of a competitively-amplified segment of a disomic control locus on chromosome 21. Disomic control individuals had a mean *NF1* gene dosage value of 0.98 ± 0.08 sd., while *NF1* subjects with germline microdeletions had a mean gene dosage value of 0.45 ± 0.04 sd. (sd., one standard deviation). To approximate a 95% confidence interval, the range of values indicating either germline disomy or monosomy was set at the mean ± 2 sd. This established a gene dosage value range of 0.82 - 1.14 for *NF1* disomy and a range of 0.37 - 0.53 for *NF1* monosomy.

Fluorescence In Situ Hybridization. Metaphase chromosome preparations of immortalized lymphoblastoid cells of patient no. 1 were prepared and hybridized to the *NF1* bacteriophage P1 probe P1-12, which contains ~55 kb of *NF1* intron 27B^{30, 66}. Cryopreserved bone marrow samples were thawed and cultured at 1×10^6 cells/ml for 24 hr (90% RPMI 1640/10% fetal bovine serum, 100 U/ml penicillin, 100 μ g/ml streptomycin, 10 mM HEPES) at 37°C in 95% air/5% CO₂. Following incubation, the cells were exposed to hypotonic KCl (0.75 M, 8 min, 37°C), fixed in absolute methanol:glacial acetic acid (3:1), and air dried on slides. *NF1* probes were P1 bacteriophage clone P1-9, which spans ~65 kb of the *NF1* gene including exons 2-11, and clone P1-12 (ref.³⁰). A centromere-specific probe for chromosome 17 (CEP@17-Spectrum Green™, Vysis, Inc., Downer's Grove, IL), and a P1 artificial chromosome (PAC) clone, P263P1 (Genome Systems Inc., St. Louis, MO), were hybridized as control probes. P263P1 was isolated by screening the PAC library using primers for D5S479, and contains an insert of 70 kb derived from 5q31. Labeled PAC and P1 probes were prepared by nick-translation using Bio-11-dUTP (Enzo Diagnostics, New York, NY) or digoxigenin-11-dUTP (Boehringer Mannheim, Indianapolis, IN). Interphase FISH was performed as described previously⁶⁷. Hybridization of probes labeled with either biotin or digoxigenin was detected with fluorescein-conjugated avidin (Vector Laboratories, Burlingame, CA) and rhodamine-conjugated anti-digoxigenin antibodies (Boehringer Mannheim), respectively. Nuclei were counterstained with 4,6-diamidino-2-phenylindole-dihydrochloride (DAPI). The slides were randomized and examined by two observers in a blinded fashion (500 cells were scored by each observer for each probe). The distribution of hybridization signals per nucleus for the CEP@17 probe was determined in bone marrow cells from healthy control individuals (Table 3, N=10). We, and other investigators, have observed an increased number of cells with one or no signals in bone marrow cells that have been cryopreserved, presumably due to the presence of inviable cells. For this reason, we hybridized the CEP@17 probe to a control, cryopreserved, bone marrow sample, and co-hybridized the *NF1*-specific probes with a control probe for chromosome 5 (P263P1), which is typically not involved in chromosomal abnormalities in these childhood myeloid leukemias. The slides were randomized and analyzed by two observers (500 cells each) in a blinded fashion

[reference]

Mapping LOH regions. Polymorphic loci were genotyped by PCR amplification using primers described previously (<http://gdbwww.gdb.org/>). LOH at the *NF1* locus was evaluated by PCR of at least one informative intragenic marker including exon 5, intron 27B AluI/AluII, and intron 38 as described³¹. LOH at chromosome 17 loci was determined by comparing the genotypes in peripheral blood DNA of the patient's parents to those detected in tumor DNA of the patient. For patients no. 1, 8 (which others.??), normal tissue was available to confirm a constitutional genotype that included biparental inheritance of *NF1* alleles (Figure 5 in ref. ^{34, 58}). Segregation

of alleles from parents to child for multiple informative loci on autosomes other than 17 was consistent with parentage as stated for each case (data not shown). Genetic distances are from the chromosome 17 sex-averaged map of the Center for Medical Genetics, Marshfield Medical Research and Education Foundation (<http://www.marshmed.org/genetics/>). Physical distances for chromosome 17 intervals were as estimated by the Genome Data Base (<http://gdbwww.gdb.org/>).

ACKNOWLEDGMENTS

Thanks to Dr. Virginia P. Sybert and Dr. Eric Sievers for referral of patient no. 1. This research was supported in part by U.S. Army Medical Research and Materiel Command grant NF960043 (K.S.) and UPS grant PO1 CA40046 (M.M.L, K.M.S).

FIGURE LEGENDS

Figure 1. A chromosome 17 interstitial LOH region in leukemic cells. The results of genotypic analysis of selected loci in the tumor of patient no. 1 are shown. The loci, arranged in their unique order on the q arm of chromosome 17, document the interstitial nature of the LOH region. The flanking loci D17S33 and D17S928 retained heterozygosity, while loci in between lost the paternal allele.

Figure 2. Chromosomal 17 loci with LOH in malignant myeloid cells of NF1 children. For each patient, a schematic of the chromosome 17 that showed loss of constitutional heterozygosity is depicted. The region of LOH is shaded, informative loci are designated with a dash to the left of the bar depicting the chromosome, and the parental origin of the LOH region is indicated below as P, paternal and M, maternal. Locus order with estimated interlocus distances in cM from sex-averaged genetic map are given to left of each interval (<http://www.marshmed.org/genetics/>). D17S1878, D17S975, and D17S1294 were mapped centromeric to *NF1* between D17S635 and D17S33, while D17S1800 was localized telomeric to *NF1* using a panel of somatic cell hybrids carrying segments of chromosome 17^{17, 30, 31, 68, 69}, Stephens, unpublished data). This mapping panel also confirmed the previously reported localization of D17S635, alias UT172^{10, 31}, as centromeric to *NF1* (<http://www.marshmed.org/genetics/>; <http://gdbwww.gdb.org/>).

Find reference & evidence that D17S 959 is on q arm.

Figure 3. Fluorescence in situ hybridization of tumor cells with *NF1* probes. Panel (A), metaphase spread of immortalized lymphoblastoid cells of patient no.1 hybridized with a bacteriophage P1 *NF1* probe, P1-12. Each of 20 metaphases examined had signals on both chromosome 17 homologues. As expected, FISH of cells of an *NF1* hemizygous control individual showed 48 of 50 metaphases with signals on only one chromosome 17 homologue, with the remaining 2 spreads showing no labeling (data not shown). The chromosome 17 homologues were identified by the Hoechst/actinomycin D staining (data not shown), which reveals a Q-banding like pattern⁶⁶.

Panels (B-x), Choose other FISH figures and write legends.

Dual-color FISH was performed by co-hybridizing biotin-labeled *NF1* probes and a control probe, digoxigenin-labeled P263P1, a PAC clone derived from 5q31. The *NF1* probes (P1-9 and P1-12) were co-hybridized with the control probe in independent experiments. An α -satellite probe specific for the centromere of chromosome 17 (CEP^R17) was hybridized in a third independent experiment to enumerate the number of copies of chromosome 17 in each sample. Figure 4. Somatic interstitial isodisomy in leukemic cells of NF1 children.

A) The 2 different chromosome 17 karyotypes observed in the patients studied. Paternally-derived sequences are shaded; maternally-derived sequences are not. Two of the possible mechanisms for double mitotic recombination leading to interstitial isodisomy in a progenitor cell are diagrammed in B) double recombination during G2/S phase.

REFERENCES

1. Brown, M.A. Tumor suppressor genes and human cancer. *Adv-Genet* **36**, 45-135 (1997).
2. Tischfield, J.A. Loss of heterozygosity or: How I learned to stop worrying and love mitotic recombination. *Am J Hum Genet* **61**, 995 -- (1997).
3. Qian, F. & Germino, G.G. "Mistakes happen": Somatic mutation and disease. *Am J Hum Genet* **61**, 1000-1005 (1997).
4. Xu, W. *et al.* Loss of NF1 alleles in pheochromocytomas from patients with type I neurofibromatosis. *Genes Chromosomes Cancer* **4**, 337-42 (1992).
5. Skuse, G.R., Kosciulek, B.A. & Rowley, P.T. Molecular genetic analysis of tumors in von Recklinghausen neurofibromatosis: loss of heterozygosity for chromosome 17. *Genes Chromosomes Cancer* **1**, 36-41 (1989).
6. Shannon, K. *et al.* Monosomy 7 myeloproliferative disease in children with neurofibromatosis type 1: epidemiology and molecular analysis. *Blood* **79**, 1311 (1992).
7. Colman, S.D., Williams, C.A. & Wallace, M.R. Benign neurofibromas in type 1 neurofibromatosis (NF1) show somatic deletions of the NF1 gene. *Nat Genet* **11**, 90-2 (1995).
8. von Deimling, A. *et al.* Deletions on the long arm of chromosome 17 in pilocytic astrocytoma. *Acta Neuropathol* **86**(1993).
9. Serra, E. *et al.* Confirmation of a double-hit model for the NF1 gene in benign neurofibromas. *American Journal Of Human Genetics* **61**, 512-519 (1997).
10. Shannon, K. *et al.* Loss of the normal NF1 allele from the bone marrow of children with type 1 neurofibromatosis and malignant myeloid disorders. *N Engl J Med* **330**, 597 (1994).
11. Sawada, S. *et al.* Identification of NF1 mutations in both alleles of a dermal neurofibroma. *Nature Genet* **14**, 110-112 (1996).
12. Side, L. *et al.* Homozygous inactivation of the NF1 gene in bone marrow cells from children with neurofibromatosis type 1 and malignant myeloid disorders. *New England Journal Of Medicine* **336**, 1713-1720 (1997).
13. Legius, E., Marchuk, D.A., Collins, F.S. & Glover, T.W. Somatic deletion of the neurofibromatosis type 1 gene in a neurofibrosarcoma supports a tumour suppressor gene hypothesis. *Nat Genet* **3**, 122-6 (1993).
14. Riccardi, V.M. *Neurofibromatosis, Phenotype, Natural History, Pathogenesis.*, (The Johns Hopkins University Press., Baltimore, 1992).
15. Mulvihill, J.J. Malignancy: epidemiologically associated cancers. in *The Neurofibromatoses: A pathogenetic and Clinical Overview* First edn (eds Huson, S.M. & Hughes, R.A.C.) 487 (Chapman & Hall Medical, London, 1994).
16. Kayes, L.M., Riccardi, V.M., Burke, W., Bennett, R.L. & Stephens, K. Large de novo DNA deletion in a patient with sporadic neurofibromatosis 1, mental retardation, and dysmorphism. *J Med Genet* **29**, 686-90 (1992).
17. Kayes, L.M. *et al.* Deletions spanning the neurofibromatosis 1 gene: identification and phenotype of five patients. *Am J Hum Genet* **54**, 424-36 (1994).
18. Heim, R. *et al.* Distribution of 13 truncating mutations in the neurofibromatosis 1 gene. *Hum Mol Genet* **4**, 975-981 (1995).
19. Upadhyaya, M. *et al.* Mutational and functional analysis of the neurofibromatosis type 1 (NF1) gene. *Hum Genet* **99**, 88-92 (1997).

20. Ballester, R. *et al.* The NF1 locus encodes a protein functionally related to mammalian GAP and yeast IRA proteins. *Cell* **63**, 851-9 (1990).
21. Xu, G.F. *et al.* The neurofibromatosis type 1 gene encodes a protein related to GAP. *Cell* **62**, 599-608 (1990).
22. Xu, G.F. *et al.* The catalytic domain of the neurofibromatosis type 1 gene product stimulates ras GTPase and complements ira mutants of *S. cerevisiae*. *Cell* **63**, 835-41 (1990).
23. Martin, G.A. *et al.* The GAP-related domain of the neurofibromatosis type 1 gene product interacts with ras p21. *Cell* **63**, 843-9 (1990).
24. Downward, J. Cell cycle: Routine role for Ras. *Current Biology* **7**, R258-R260 (1997).
25. O'Marcaigh, A.S. & Shannon, K.M. Role of the NF1 gene in leukemogenesis and myeloid growth control. *J Pediatr Hematol Oncol* **19**, 551-554 (1997).
26. Stiller, C.A., Chessells, J.M. & Fitchett, M. Neurofibromatosis and childhood leukemia/lymphoma: a population-based UKCCSG study. *Br J Cancer* **70**, 969-972 (1994).
27. Bollag, G. *et al.* Loss of NF1 results in activation of the Ras signaling pathway and leads to aberrant growth in haematopoietic cells. *Nat Genet* **12**, 144-8 (1996).
28. Zhang, B.Y.-Y. *et al.* *Nf1* regulates hematopoietic progenitor cell growth and ras signaling in response to multiple cytokines. *J Exp Med* **187**, 1893-1902 (1998).
29. Largaespada, D.A., Brannan, C.I., Jenkins, N.A. & Copeland, N.G. *Nf1* deficiency causes Ras-mediated granulocyte/macrophage colony stimulating factor hypersensitivity and chronic myeloid leukaemia. *Nat Genet* **12**, 137-43 (1996).
30. Leppig, K.A. *et al.* The detection of contiguous gene deletions at the neurofibromatosis 1 locus with fluorescence in situ hybridization. *Cytogenet Cell Genet* **72**, 95-8 (1996).
31. Leppig, K. *et al.* Familial neurofibromatosis 1 gene deletions: cosegregation with distinctive facial features and early onset of cutaneous neurofibromas. *Am J Med Genet*, submitted (1997).
32. Jacks, T. *et al.* Tumour predisposition in mice heterozygous for a targeted mutation in *Nf1*. *Nat Genet* **7**, 353-61 (1994).
33. Tischler, A.S., Shih, T.S., Williams, B.O. & Jacks, T. Characterization of pheochromocytomas in a mouse strain with a targeted disruptive mutation of the neurofibromatosis gene *NF1*. *Endocrine Pathology* **6**, 323-335 (1995).
34. Miles, D. *et al.* Patterns of hematopoietic lineage involvement in children with neurofibromatosis, type 1 and malignant myeloid disorders. *Blood*, in press. (1997).
35. Maruyama, K., Weaver, M., Leppig, K. & Stephens, K. Gene dosage assay based on competitive PCR to detect large de novo DNA deletion in the neurofibromatosis 1 gene region. (submitted).
36. Henry, I. *et al.* Somatic mosaicism for partial paternal isodisomy in Wiedemann-Beckwith syndrome: a post-fertilization event. *Eur J Hum Genet* **1**, 19-29 (1993).
37. Hurst, L.D. & McVean, G.T. growth effects of uniparental disomies and the conflict theory of genomic imprinting. *Trends Genet* **13**, 436-443 (1997).
38. Cavenee, W.K. *et al.* Expression of recessive alleles by chromosomal mechanisms in retinoblastoma. *Nature* **305**, 779- (1983).
39. Howard, J. Not all converted yet. *Nat Genet* **10**, 371-373 (1995).
40. Bohme, J. & Hogstrand, K. Timing and effects of template number for gene conversion of major histocompatibility complex genes in the mouse. *Hereditas* **127**, 11-18 (1997).

41. Hogstrand, K. & Bohme-J. A determination of the frequency of gene conversion in unmanipulated mouse sperm. *Proc Natl Acad Sci, USA* **91**, 9921-9925 (1994).
42. Jeffreys, A.J., Tamaki, K., MacLeod, A., Monckton, D.G. & Neil, D.L., Armour, J.A.L. Complex gene conversion events in germline mutation at human minisatellites. *Nat Genet* **6**, 136-145 (1994).
43. Zangenberg, G., Huang, M.-M., Arnheim, N. & Erlich, H. New HLA-DPB1 alleles generated by interallelic gene conversion detected by an analysis of sperm. *Nat Genet* **10**, 407-414 (1995).
44. Collier, S., Tassabehji, M. & Strachan, T. A *de novo* pathological point mutation at the 21-hydroxylase locus: implications for gene conversion in the human genome. *Nat Genet* **3**, 260-265 (1993).
45. Huang, C.-H., Chen, Y., Reid, M. & Ghosh, S. Genetic recombination at the human *RH* locus: A family study of the red-cell Evans phenotype reveals a transfer of exons 2-6 from the *RHD* to the *RHCE* gene. *Am J Hum Genet* **59**, 825-833 (1996).
46. Giordano, M., Marchetti, C., Chiorboli, E., Bona, G. & Richiardi, P.M. Evidence for gene conversion in the generation of extensive polymorphism in the promoter of the growth hormone gene. *Hum Genet* **100**, 249-255 (1997).
47. Reyniers, E. *et al.* Gene conversion between red and defective green opsin gene in blue cony monochromacy. *Genomics* **29**, 323-328 (1995).
48. Strachan, T. Molecular pathology of 21-hydroxylase deficiency. *J Inherit Metab Dis* **17**, 430-41 (1994).
49. Hall, J.G. Somatic mosaicism: observations related to clinical genetics. *Am J Hum Genet* **43**, 355-363 (1988).
50. Cooper, D.N. & Krawczak, M. *Human Gene Mutation*, 402 (BIOS Scientific Publishers Limited, 1993).
51. Chen, K.-S. *et al.* Homologous recombination of a flanking repeat gene cluster is a mechanism for a common contiguous gene deletion syndrome. *Nat Genet* **17**, 154-163 (1997).
52. Reiter, L.T. *et al.* Human meiotic recombination products revealed by sequencing a hotspot for homologous strand exchange in multiple HNPP deletion patients. *Am J Hum Genet* **62**, 1023-1033 (1998).
53. Reiter, L.T. *et al.* A recombination hotspot responsible for two inherited peripheral neuropathies is located near a *mariner* transposon-like element. *Nat Genet* **12**, 288-297 (1996).
54. Menon, A.G. *et al.* Chromosome 17p deletions and p53 gene mutations associated with the formation of malignant neurofibrosarcomas in von Recklinghausen neurofibromatosis. *Proc Natl Acad Sci U S A* **87**, 5435-9 (1990).
55. Lamond, A.I. & Earnshaw, W.C. Structure and function in the nucleus. *Science* **280**, 547-553 (1998).
56. Stahl, F. & Myers, R. Old and new concepts for the role of chi in bacterial recombination. *J Heredity* **86**, 327-329 (1995).
57. Largaespada, D.A., Shaughnessy, J., J.D., Jenkins, N.A. & Copeland, N.G. Retroviral integration at the *Evi-2* locus in BXH-2 myeloid leukemia cell lines disrupts *Nf1* expression without changes in steady-state Ras-GTP levels. *J Virol* **69**, 5095-5102 (1995).
58. Luna-Fineman, S., Shannon, K.M. & Lange, B.J. Childhood monosomy 7: epidemiology, biology, and mechanistic implications. *Blood* **85**, 1985-1999 (1995).

59. Purandare, S.M. *et al.* Genotyping of PCR-based polymorphisms and linkage-disequilibrium analysis at the NF1 locus. *Am J Hum Genet* **59**, 159-66 (1996).
60. Jorde, L.B., Watkins, W.S., Viskochil, D., P, O.C. & Ward, K. Linkage disequilibrium in the neurofibromatosis 1 (NF1) region: implications for gene mapping. *Am J Hum Genet* **53**, 1038-50 (1993).
61. Huson, S.M., Compston, D.A., Clark, P. & Harper, P.S. A genetic study of von Recklinghausen neurofibromatosis in south east Wales. I. Prevalence, fitness, mutation rate, and effect of parental transmission on severity. *J Med Genet* **26**, 704-11 (1989).
62. Cawthon, R.M. *et al.* cDNA sequence and genomic structure of EV12B, a gene lying within an intron of the neurofibromatosis type 1 gene. *Genomics* **9**, 446-60 (1991).
63. Takaku, K. *et al.* Intestinal tumorigenesis in compound mutant mice of both *Dpc4 (Smad4)* and *Apc* genes. *Cell* **92**, 645-656 (1998).
64. Gupta, P.K. *et al.* High frequency *in vivo* loss of heterozygosity is primarily a consequence of mitotic recombination. *Cancer Res* **57**, 1188-1193 (1997).
65. Celi, F. *et al.* Determination of gene dosage by a quantitative adaptation of the polymerase chain reaction (gd-PCR): rapid detection of deletions and duplications of gene sequences. *Genomics* **21**, 304-310 (1994).
66. Chance, P.F. *et al.* DNA deletion associated with hereditary neuropathy with liability to pressure palsies. *Cell* **72**, 143-51 (1993).
67. Le Beau, M.M. *et al.* Cytogenetic and molecular delineation of a region of chromosome 7 commonly deleted in malignant myeloid diseases. *Blood* **88**, 1930-1935 (1996).
68. Ledbetter, D.H., Rich, D.C., P, O.C., Leppert, M. & Carey, J.C. Precise localization of NF1 to 17q11.2 by balanced translocation. *Am J Hum Genet* **44**, 20-4 (1989).
69. van Tuinen, P., Rich, D.C., Summers, K.M. & Ledbetter, D.H. Regional mapping panel for human chromosome 17: application to neurofibromatosis type 1. *Genomics* **1**, 374-81 (1987).

Table 1. NF1 gene dosage in bone marrows of NF1 children with malignant myeloid disorders.

Patient		Age at		Origin of		LOH at	NF1 Gene	Predicted NF1
No.	Sex	Onset	Diagnosis	NF1 mutation	NF1 Locus		Dosage Value ^{a,b}	Gene Copy No. ^a
1	M	9 mo	MPS	<i>de novo</i> (paternal)	maternal		0.99	disomy
2	M	10 mo	AML	paternal	maternal		0.93	disomy
3	M	24 mo	monosomy 7	unknown	maternal		0.96	disomy
4	M	14 mo	JMML	maternal	paternal		0.86	disomy
5	F	30 mo	JMML	maternal	paternal		0.94	disomy
6	M	10 mo	JMML	maternal	paternal		0.87	disomy
7	M	5 mo	monosomy 7	maternal	paternal		0.90	disomy
8	F	18 mo	MPS	paternal	maternal ^a		0.85	disomy
9	M	5 yr	JMML	maternal	paternal		0.57	monosomy
10	F	18 mo	JMML	unknown	probable		0.44	monosomy
11	M	19 mo	monosomy 7	<i>de novo</i>	maternal ^a		0.48	monosomy

^aData from this manuscript.

^bMeasured in unfractionated bone marrow cells, except patients 3, 9 for which leukemic cells in peripheral blood were used.

Table 2. Interphase fluorescence *in situ* hybridization analysis of bone marrow samples.

Patient	Chr. 17	Number of Hybridization Signals					Control	Number of Hybridization Signals				
		0	1	2	3	>4		0	1	2	3	>4
3	Ccp®17	0	6	87	3	4						
	P1-9	0.6	14	84	1	0.4	263P1	0	7.6	90	2	0.4
	P1-12	1	13	80	6	0	263P1	0	9	88	2	1
3	P1-9	4	4	92	0	0	Ccp®7	0	92	8	0	0
	P1-12	2	4	94	0	0	Ccp®7	0	89	11	0	0
4	Ccp®17	0	5	90	2	3						
	P1-9	0.5	10	86	3	0.5	263P1	0	12	84	2	1.5
	P1-12	0.5	13	78	8	0/5	263P1	0.4	7	92	0.6	0
5	Ccp®17	0	6	93	0	1						
	P1-9	6	7	82	4	1	263P1	1	4	90	4	1
	P1-12	0.4	6	90	2.6	1	263P1	0.2	4.8	93	0.5	1.5
6	Ccp®17	0	2	97	1	0						
	P1-9	1	5	95	0	0	263P1	0	25	74	1	0
	P1-12	1	9	76	12	2	263P1	0	15	84	0	1
11	Ccp®17	0.8	3.6	95	0.6	0						
	P1-12	4	29	67	0	0	263P1	0	3	97	0	0
C1 [†]	Ccp®17	0	6.4	93	0.6	0						
	P1-9	3	7	89	1	0	263P1	2	3	86	5	4
	P1-12	2	5	89	2	2	263P1	0	7	90	1.5	1.5
C2 [†]	Ccp®17	1	3	95	1	0						
	P1-9	2	22	76	0	0	263P1	1	19	79	1	0
	P1-12	0.5	7	86	5	1.5	263P1	1.6	6	88	3	1.4
C3 [†]	Ccp®17	0	5	94	0	0						
	P1-9	1.5	12	81	4	1.5	263P1	0	8	90	2	0
	P1-12	0	9	85	3.4	2.6	263P1	0	8	89	2	1
C4 [†]	Ccp®17	0	4	96	0	0						
	P1-9	0.5	11	83	1.5	2	263P1	0.5	9	88	2	0.5
	P1-12	0.5	9.5	85	4	1	263P1	0.5	17	82	0.5	0
C5 [†]	Ccp®17	0	6	93	1	0						
	P1-9	1	6	92	0.5	0.5	263P1	0.6	4	95	0.2	0.2
	P1-12	0	5	94	1	0	263P1	0	3	96	0.8	0.2
Control [*] N=10	Ccp®17											
	Mean	0.15	4.5	95	0.24	0.15						
	S.D.	0.19	0.79	0.83	0.25	0.16						

*Probe 263P1 is a 70 kb PAC clone containing D5S479 (chromosome band 5q31 : Ccp®17 and Ccp®7 are centromere-specific probe for chromosomes 17 and 7, respectively. [†] C1 is a cryopreserved bone marrow sample from a patient with AML-M4 in complete remission. C2-C5 are cryopreserved bone marrow samples from 4 children with myeloid leukemias that retained heterozygosity at the *NF1* locus. ^{*} The distribution of signals for the chromosome 17 centromere-specific probe was determined by the interphase analysis of bone marrow cells from 10 healthy individuals.

Table 3. Genetic mechanisms leading to somatic inactivation of tumor suppressor genes^a.

Constitutional heterozygosity at tumor suppressor	LOST		RETAINED
	Hemizygous	Homozygous (Disomic)	
Tumor Genotype			Heterozygous
Single Locus LOH	<ul style="list-style-type: none"> • intragenic deletion • illegitimate V(D)J recombination 	<ul style="list-style-type: none"> • gene conversion 	<ul style="list-style-type: none"> • compound heterozygosity • methylation → transcriptional silencing
Multilocus LOH	<ul style="list-style-type: none"> • multilocus deletion • mitotic nondisjunction → chromosome loss • unbalanced chromosome abnormalities → e.g., translocation, isochromosome 	<ul style="list-style-type: none"> • chromosome loss with reduplication → chromosomal isodisomy • homologous single mitotic recombination → partial isodisomy • homologous double mitotic recombination → interstitial isodisomy 	<ul style="list-style-type: none"> • [none reported]

^aSelected references [Tischfield, 1997 #813; Sawada, 1996 #702; Schroeder, 1997 #827; Honma, 1997 #834; Herman, 1994 #828; Cayuela, 1997 #831; Caron, 1994 #826; Cavence, 1983 #825][Qian, 1997 #847].

FIGURE 2.

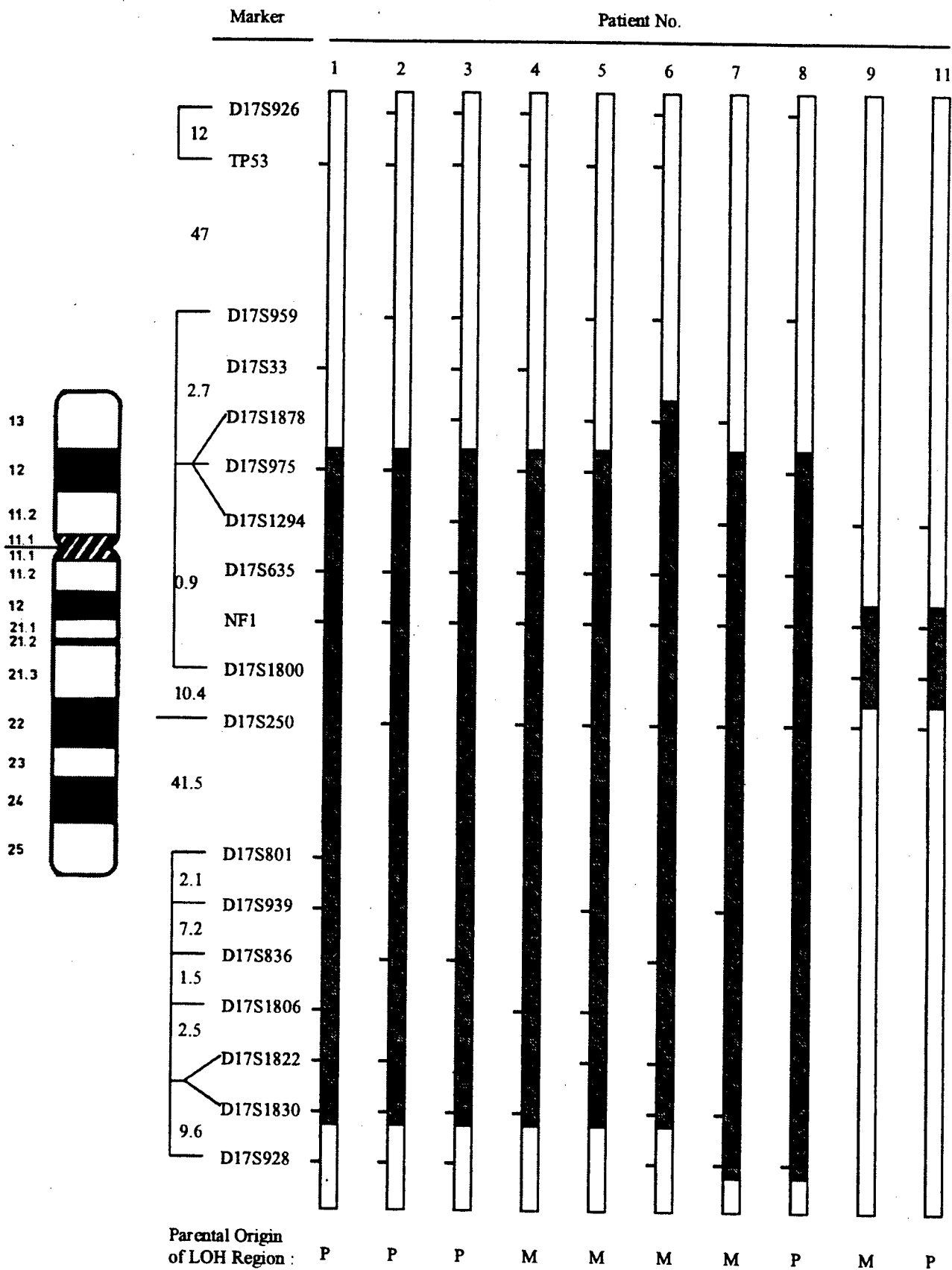


FIG. 4

B.

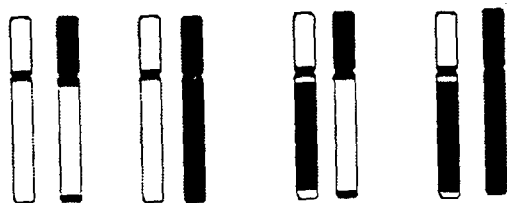
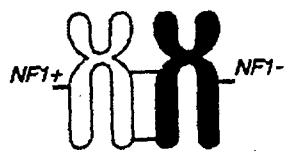
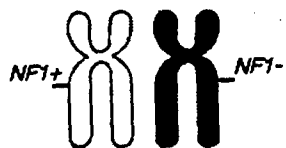
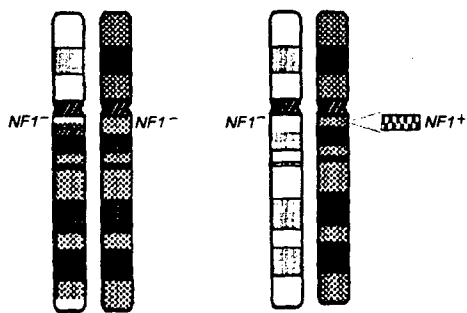


Figure in progress.

A.



Interstitial paternal isodisomy Interstitial paternal deletion

FIGURE 4

APPENDIX D.

**Mapping of the human serotonin transporter and
carboxypeptidase D genes to a 1Mb YAC/PAC contig
on 17q11.1: hemizyosity in a patient with a deletion
spanning the adjacent neurofibromatosis 1 gene**

**Sanbing Shen^{*1}, Sharon Battersby¹, Molly Weaver², Elma Clark¹,
Eve M. Lutz¹, Karen Stephens^{2,3,4} and Anthony J. Harmar¹**

¹MRC Brain Metabolism Unit, Royal Edinburgh Hospital, Morningside Park,
Edinburgh EH10 5HF, Scotland

²Departments of Medicine, ³Laboratory Medicine and ⁴Pathology, University of
Washington, Seattle, WA 98195

* corresponding author:

MRC Brain Metabolism Unit,
Royal Edinburgh Hospital
Morningside Park
Edinburgh
EH10 5HF
Scotland

Tel: 44-131-5376527

Fax: 44-131-5376110

Email: sshen@srv1.bmu.mrc.ac.uk

Running Title: Hemizyosity of SLC6A4 and CPD in a NF1 patient

*DRAFT of 10/22/98
in preparation*

ABSTRACT

The SLC6A4 gene encodes a protein (the serotonin transporter) that is the target of an important class of antidepressant drugs, the serotonin selective reuptake inhibitors. Polymorphic variation in the SLC6A4 gene has been reported to be associated with susceptibility to depression and other psychiatric disorders. We have constructed a 1 Mb YAC and PAC contig which harbours the SLC6A4 gene and also the gene encoding carboxypeptidase D (CPD), a recently discovered membrane-bound metalloproteinase. The order of STS markers within the contig was cen-D17S975-D17S1549-D17S1294-SLC6A4-CPD-D17S2009-S17S2004-D17S1863-D17S2120-ter. A patient (NF106-3) with neurofibromatosis type I (NF1) resulting from a large deletion in chromosome 17q11.2 was hemizygous for both SLC6A4 and CPD genes. Our data should facilitate studies of contribution of the SLC6A4, CPD and other contiguous genes to susceptibility to developmental and psychiatric disorders and to the distinct phenotype seen in NF1 deletion patients.

INTRODUCTION

The endogenous indoleamine serotonin (5-hydroxytryptamine, 5-HT) is a neurotransmitter in the central and peripheral nervous systems. The actions of serotonin released into the synaptic cleft are terminated by reuptake into pre-synaptic nerve terminals by a high-affinity, Na⁺-dependent serotonin transporter (SERT) encoded by the SLC6A4 ('solute carrier family 6, member 4') gene. The SERT is the target for an important class of antidepressant drugs, the serotonin selective reuptake inhibitors (Anderson and Tomenson, 1994) and also of certain drugs of abuse including 3,4-Methylenedioxyamphetamine (MDMA or "ecstasy": Rudnick and Wall, 1992). Polymorphic variation in the SLC6A4 gene has been reported by several laboratories to be associated with susceptibility to affective disorder (Battersby *et al.*, 1996; Collier *et al.*, 1996a, 1996b; Harmar *et al.*, 1996; Ogilvie *et al.*, 1996; Rees *et al.*, 1997), may influence personality traits (Lesch *et al.*, 1996) and may be a risk factor for late onset Alzheimer's disease (Li *et al.*, 1997) and autistic disorder (Cook *et al.*, 1997; Klauck *et al.*, 1997). The human SLC6A4 gene, which encompasses >30 kb (Bradley and Blakely, 1997), has been mapped to 17q12 using a restriction fragment length polymorphism (RFLP) in the 3' untranslated region (3'-UTR) of the gene (Gelernter *et al.*, 1995) and to 17q11.2 - 17q12 using fluorescence *in situ* hybridization (FISH) and somatic cell hybrids (Ramamoorthy *et al.*, 1993).

Human carboxypeptidase D (CPD) is a newly discovered membrane-bound metallo-carboxypeptidase that has been proposed to be involved in the post-translational processing of peptides and proteins that transit the secretory pathway (Ishikawa *et al.*, 1998; Tan *et al.*, 1989). The human gene for carboxypeptidase D has been localized to chromosome 17p11.1-q11.1/11.2, using the polymerase chain reaction (PCR) with gene-specific primers and DNA derived from somatic cell hybrids (Riley *et al.*, 1998).

edit
expand

The Neurofibromatosis type I (NF1) gene has been mapped to chromosome 17q11.2 between D17S33 and D17S57. Defects in the NF1 gene result in an autosomal dominant disorder, affecting approximately 1/1000^{pop} of the population, characterized by the development of multiple neurofibromas, cafe au lait spots, and Lisch nodules of the iris (for review see Shen *et al.*, 1996). There is marked variation and severity in clinical expression of the disease depending on the nature of the defect in the NF1 gene. Patients with large deletions in 17q11 exhibit facial dysmorphism, mental retardation, and/or learning disabilities (Cnossen *et al.*, 1997; Kayes *et al.*, 1992, 1994; Wu *et al.*, 1995).

Previously, six NF1 patients with mild facial dysmorphism, mental retardation, and/or learning disabilities were extensively examined for DNA rearrangements within the NF1 region (Kayes *et al.*, 1994). Analyses of somatic hybrid cell lines demonstrated that each of the five patients carried a deletion >700 kb in size, including the entire 350- kb NF1 gene, three genes (EVI2A, EV12B, and OMG-t) nested within an intron of the NF1 gene and considerable flanking DNA. These patients displayed a variable number of physical anomalies that were not correlated with the extent of their deletions, suggesting that unknown gene (s) in the NF1 region may influence tumour initiation and/or development (Kayes *et al.*, 1994).

Edit

We report here (i) the isolation of YAC/PAC clones encompassing the human SLC6A4 and CPD genes, (ii) the construction of a 1 Mb YAC contig from 17q11.1 with 7 STS markers flanking the two genes, (iii) hemizyosity of the SLC6A4 and CPD genes in the patient NF106-3 who carries the most extensive deletion and (iv) localization of the centromeric breakpoint of the deletion to a <15 kb region between D17S1294 and the 3'-UTR of the SLC6A4 gene.

MATERIALS AND METHODS

Screening of PAC and YAC libraries

Full length human SLC6A4 cDNA (200 µg) was excised from the pGEM-T vector, labeled with [α -³²P]dCTP using Ready-To-Go DNA labeling beads (Pharmacia) and applied to high density gridded filters of 4 libraries: the RPC-1 human PAC library (Ioannou *et al.*, 1994), the ICI (Anand *et al.*, 1990), ICRF (Larin *et al.*, 1991) and CEPH (Chumakov *et al.*, 1992) human YAC libraries. Hybridization was performed at 55°C for 20 hours in a buffer containing 0.5 M phosphate pH7.2, 7% SDS, 1% BSA and 1 mM EDTA. After hybridization, filters were washed in 40 mM phosphate/1% SDS/1 mM EDTA and exposed to autoradiography film (Fuji RX) at -70°C overnight. Positive clones were obtained from UK MRC HGMP Resource Centre.

Patient and somatic cell hybrid lines

The patient NF106-3, who has a large deletion at 17q11.2, has been described previously by Kayes *et al.* (Kayes *et al.*, 1992, 1994). The somatic hybrids were established by fusing immortalized lymphoblasts from the patient to hamster hypoxanthine ribosyltransferase-deficient RJK cells. The line NF106-3-#36 carries the deleted chromosome 17 and NF106-3-#41 the non-deleted chromosome 17 of the patient (Kayes *et al.*, 1994).

Fluorescence in situ hybridization (FISH)

DNA from PAC clone 50G6 was labeled with biotin-11-dATP by nick-translation (Gibco BRL). Chromosome metaphase spreads from the lymphoblastoid cell line (NF106-3) were prepared using standard methodology. Hybridization was carried out as previously described by Edelhoff *et al.* (1994) and signals were detected using a commercial system (Vector). The chromosomes were banded using Hoechst 33258-actinomycin D staining and counterstained with propidium-iodide. The chromosomes and signals were visualized by fluorescence microscope using a dual band pass filter (Omega).

PCR and primers

PCR primers for the SLC6A4 and NF1 genes are listed in Table 1. The T_m for each primer oligonucleotide was calculated using the formula:

$T_m = 69.3 + 41 \times N_{GC} / N_{total} - 650 / N_{total}$ (where N_{GC} is the number of G and C residues in a primer of total length N_{total} residues) and the lower T_m value for each primer pair was used as the annealing temperature. Extension times were chosen according to the expected size of individual PCR products (approximately 1 min per 500 bp). PCR was performed for 30 or 35 cycles.

Preparation of YAC and PAC DNA

Yeast DNA was prepared with a modification of the combined methods of Schedl *et al.* (1993) and Bellis *et al.* (1987). YAC clones were inoculated into 15 ml of medium (Ura⁻/Trp⁻) with 2% of glucose as the carbon source. When cells had grown to late log phase after 2 - 4 days, low melting point (LMP) agarose plugs were made and subjected to novozyme (Novo Biolabs) digestion for 4 - 6 hours. Plugs were then washed in 50 mM EDTA (2 x 30 min) and digested with proteinase K (2 mg/ml) at 55°C overnight, in a buffer containing 0.5 M NaCl, 0.125 M Tris pH 8.0, 0.25 M Na₂EDTA, 1% (w/v) lithium sulphate, and 0.5 M β-mercaptoethanol. Plugs were washed with TE and stored at 4°C in 0.5 M EDTA.

Pulsed-field gel electrophoresis (PFGE)

Agarose plugs containing YAC DNA were washed in TE (3 x 30 min), loaded onto 1% agarose gels and sealed with 1% LMP agarose in 0.5 x TBE buffer. Gels were run in 0.5 x TBE buffer at 6V/cm for 24 hours at 14°C with 60 seconds switch time. After running, gels were stained with ethidium bromide and photographed.

Southern blotting and probes

DNA was fragmented by soaking gels in 0.25 M HCl for 15 min to facilitate efficient transfer, denatured in 0.4 M NaOH for 3 x 20 min and blotted onto Appligene Positive Membrane overnight. Filters were neutralized with 25 mM phosphate pH 6.8/1 mM EDTA for 10 min and fixed for 2 min at full power (650W) in a microwave oven. Labeling of DNA probes, hybridization and autoradiography were performed using the same methods employed for library screening. Four probes were used for construction of the contig: (i) a 854 bp Pst I fragment of SLC6A4 cDNA (corresponding to bp 785 - 1639, GenBank accession no. L05568), (ii) a 2.3 kb Eco RI - Pvu II fragment of pBR322 to detect the long YAC arm, (iii) 28L, a 3.2 kb Not I - Eco RI fragment of PAC clone 50G6, which is ~35 kb upstream of the SLC6A4 gene, (iv) 24R, a 8.4 kb Not I - Hind III fragment of PAC clone 50G6, containing sequences ~15 kb downstream of the SLC6A4 coding sequence. For probes 28L and 24R, labeled DNA was pre-hybridized to human Cot-1 DNA (Gibco) for 15 min at 55°C before application to blots.

RESULTS

Characterization of the SLC6A4 gene and PAC clone 50G6

The size of the SLC6A4 gene was determined by long-range PCR of human genomic DNA with 6 pairs of primers which cover the entire SLC6A4 gene from exon 1 to 14 (43084/43085, 43088/43089, 26373/2B, 54073/54074, 5A/5B, and 6A/P3, Table 1). PCR products of 10, 3.5, 5, 4, 4 and >12 kb were obtained, respectively. We conclude that the SLC6A4 gene contains at least 15 exons and spans approximately 40 kb of genomic DNA.

To isolate genomic clones encoding the SLC6A4 gene, we screened the RPC-1 human PAC library by hybridization with full length human SLC6A4 cDNA. Five PAC clones (228M22, 295J12, 297L15, 64L1 and 50G6) were identified and further screened by PCR with primers (Table I) flanking exons 2 (26373/26374) and 14 (26375/26376)

of the SLC6A4 gene. Four of the 5 clones contained the 5' end of the SLC6A4 gene but lacked the 3'-UTR (data not shown). However, the PAC clone 50G6 appeared to contain the entire coding sequence of the SLC6A4 gene, since PCR products of the expected sizes were obtained with both pairs of primers. FISH analysis of 50G6 PAC DNA to human metaphase chromosomes indicated that the clone was not chimeric (Table II).

To acquire probes for genomic mapping, we subcloned Not I - Eco RI and Not I - Hind III digests of PAC clone 50G6 into pBluescript SK⁻ and identified fragments flanking the cloning site of 50G6 by DNA sequencing. Clone 24R contained a 8.4 kb Not I-Hind III fragment of the insert of 50G6 together with the cloning site and the SP6 promoter sequence of the PAC vector pCYPAC2N. Clone 28L contained a 3.2 kb Not I-Eco RI fragment of 50G6 adjacent to the T7 promoter sequence of pCYPAC2N. Not I digestion of 50G6 DNA generated three fragments of 16 kb (corresponding to PAC vector), 40 kb and 55 kb. Southern blot analysis revealed that subclone 28L hybridized to the 40 kb Not I fragment whereas both SLC6A4 cDNA and subclone 24R hybridized to the 55 kb Not I fragment (data not shown). These results indicated that the PAC clone 50G6 contains approximately 40 kb upstream sequence, the entire SLC6A4 gene (40 kb) and approximately 15 kb downstream sequence.

Identification of SLC6A4-containing YAC clones

High density gridded filters of the ICI, ICRF and CEPH human YAC libraries were screened by hybridization with full length human SLC6A4 cDNA and eleven positive clones were identified (Table II). YAC DNA was prepared from each positive clone and the size of each YAC was determined by PFGE and subsequent hybridization with pBR322 DNA (Fig. 1). All YAC clones were examined by PCR with 6 sets of primers (Table I) spanning the entire SLC6A4 gene and by Southern hybridization using probes (28L and 24R) derived from 50G6 PAC DNA (Fig. 1). Three ICRF clones (49A9, 35D8, 132C6) and 5 CEPH clones (765D1, 782E2, 793F2, 923F8 and 704F1) were showed to carry the entire coding region of the SLC6A4 gene (Table II).

YAC/PAC clones were analysed for polymorphisms in the promoter (Heils *et al.*, 1996) and in intron 2 (Ogilvie *et al.*, 1996). The 10 repeat form of the VNTR in intron 2 was present in all clones tested. Interestingly, the ICRF clones carried the short form and the CEPH clones the long form of the polymorphism in the promoter region (Table II).

Close linkage of the SLC6A4 gene to D17S1294 marker

Seventeen STS markers from the region 17cen - 17q11.2 were used to analyse the SLC6A4-containing YAC/PAC clones. No clones analysed carried the markers D17S1543, TIGR-A004R11, TIGR-A007E42, D17S1317, D17S1873, SHGC37126, SHGC36334, D17S1824, or D17S1837. One or more clones were found to harbour the following markers WI-9201, D17S975, D17S1549, D17S1294, D17S2009, D17S2004, D17S1863 and D17S2120 (Table II). On the basis of Southern blotting of the YAC and PAC clones (Fig. 1), together with data on the presence or absence of STS markers, we were able to construct a 1 Mb contig encompassing the SLC6A4 gene (Fig. 2). This analysis also enabled us to determine the orientation of the SLC6A4 gene. Clone 704F1 lacked the first exon of the gene but was positive for exons 1b - 14 of the gene and the more centromeric markers (D17S1294 and D17S1549) whilst clone 947G11, which contained only the promoter region and first exon of the gene, was positive for more telomeric markers (D17S2009, D17S2004, D17S1863 and D17S2120: Collins *et al.*, 1996a). These data indicated that the 3' end of the SLC6A4 gene is oriented towards the centromere.

D17S1294 was found to be present in the majority (6/11) of the YAC clones containing the SLC6A4 gene and in the 95 kb PAC clone 50G6 (Table II), suggesting that D17S1294 lies close to, or within the SLC6A4 gene. We ruled out the possibility that D17S1294 might be located 5' of the SLC6A4 gene since clone 704F1, which was negative for the 5' flanking region and first exon of the gene (28L and 1AP, Table II), was positive for the marker. D17S1294 was not located within the SLC6A4 gene since clones 793F2 and 49A9, spanning the entire SLC6A4 gene, did not contain the marker. These results indicated that D17S1294 is located within a <15 kb fragment centromeric to the 3' end of the SLC6A4 gene. In agreement with this assignment, those YAC clones (765D1, 782E2, 923F8 and 35D8, 132C6, 793F2, 704F1), which were positive for both exon 14 and for the probe 24R (which lies <15kb downstream of exon 14), were also positive for D17S1294, and clones (793F2 and 641D5) negative for the 24R probe were also negative for D17S1294.

Mapping of the CPD gene within the SLC6A4 YAC contig

In the process of constructing the SLC6A4-containing YAC contig, we found that a number of YAC clones (35D8, 765D1, 49A9 and 947G11) were positive for the STS markers D17S2009 and D17S2004 (Table II). D17S2004 corresponds to bp 1283 - 1564 of an expressed sequence tag (GenBank accession no. U90914) isolated from infant

brain (Andersson *et al.*, 1996). Nucleotides 1-651 of the U90914 were identical to nucleotides 5125-5775 of the published cDNA sequence of human carboxypeptidase D (GenBank accession no. U65090: Tan *et al.*, 1997), which lie in the 3'-UTR of the cDNA immediately adjacent to the polyadenylation signal. U90914 appeared to be an alternatively polyadenylated form of human carboxypeptidase D mRNA containing an additional 1300 bp of 3' sequence. Subsequently, we found that the sequences of D17S2004 and D17S2009 were present in a 96 kb genomic sequence which contains 8 un-ordered pieces of genomic sequence from human chromosome 17 (GenBank accession no. AC002317: sequence of human BAC clone HCIT7H10, Whitehead Institute/MIT Center for Genome Research, Human Genome Sequencing Project). By sequence alignment with human CPD cDNA, we were able to order and orient three large fragments from AC002317 (approx. 60 kb) to predict the exon structure of the last 20 exons of the human CPD gene.

Based on the re-ordered 60 kb genomic sequence from AC002317, we predicted that the distance between D17S2009 and D17S2004 would be approximately 2 kb. By using both forward primers of D17S2009 and D17S2004, a 2.1 kb PCR product was obtained by using either human genomic or YAC (35D8, 765D1, 49A9 and 947G11) DNA. Direct sequencing of the 2.1 kb PCR product confirmed its identity to the corresponding sequence in AC002317. To confirm the presence of the CPD gene in our YAC/PAC contig, two pairs of primers (cpd6740F/cpd6858R, and cpd1065F/cpd1768R) were designed from the cDNA sequence of CPD. Primers cpd6740F and cpd6858R are 1 kb downstream of D17S2004 within the 3'-UTR of the CPD gene and amplified the expected 118 bp product from YAC clones 35D8, 765D1, 49A9, 947G11 and from human genomic DNA. Primers cpd1065F and cpd1768R were approximately 44 kb upstream (5') of D17S2009 based on the re-ordered genomic sequence of AC002317. The predicted 2.7 kb PCR product was also detected from YAC clones 35D8, 765D1, 49A9 and 947G11 and from human genomic DNA.

All YAC clones positive for D17S2009 and D17S2004 were also positive for markers D17S1963 and D17S2120, which are telomeric to the SLC6A4 gene. However, not all of these clones contained the entire SLC6A4 gene (Table II). We concluded that the CPD gene lies further from the centromere than the SLC6A4 gene.

Hemizygotic deletion of the SLC6A4 and CPD genes in a NF1 patient

The STS marker WI-9201 derived from exon 10 of the NF1 gene appeared in 132C6 but not in the other YAC clones. To examine the possibility that the NF1 gene might lie within our YAC contig, three pairs of PCR primers, from exons 1, 27 and 49 of the

NF1 gene (Li *et al.*, 1995), were designed (Table I). Surprisingly, none of the YAC/PAC clones was positive for these primer pairs, indicating that the contig does not contain the NF1 gene. The presence of the WI-9201 marker in clone 132C6 suggests that this YAC is chimeric. Although FISH analysis did not provide evidence for chimerism (data not shown), the NF1 and SLC6A4 genes may be so close that FISH analysis may not be adequate to reveal the chimerism.

Kayes *et al.* (1992, 1994) have described a NF1 patient (NF106-3) with a large deletion in 17q11.2 which encompasses markers that have been mapped closer to the centromere than the SLC6A4 gene (Collins *et al.*, 1996a). To test the possibility that the SLC6A4 gene might be deleted in this patient, we examined metaphase chromosomes prepared from the patient by FISH using the SLC6A4-containing PAC 50G6 as probe. Only a single copy of the SLC6A4 gene was detected in this patient (Fig. 3).

DNA samples from hybrid cell lines carrying the deleted (NF106-3-#36) and non-deleted (NF106-3-#41) chromosome 17 of the patient were analysed by PCR to determine the extent of the deletion. As shown in Fig. 4, the CPD gene was hemizygotically deleted in the patient, along with D17S1863 and D17S2120 (Fig. 4). The entire SLC6A4 gene, from the promoter region to exon 14 was deleted in cell line NF106-3-#36. However, the centromeric markers D17S1294 and D17S1549 were detected in both cell lines NF106-3-#36 and NF106-3-#41. We conclude that the centromeric breakpoint of the deletion in the patient lies in a <15kb region between exon 14 of the SLC6A4 gene and D17S1294.

DISCUSSION

We report here the construction of a 1 Mb YAC/PAC contig encompassing the SLC6A4 and CPD genes which are flanked by seven STS markers. We determined that SLC6A4 is <15 kb telomeric to D17S1294 and the 3' end of the gene is oriented towards the centromere. The order of STS markers (cen-D17S975-D17S1549-D17S1294-SLC6A4-CPD-D17S2004/D17S2009-D17S1863-D17S2120-ter.) is in general agreement with the data in the Genetic Location Database (Collins *et al.*, 1996b), the Genethon human linkage map (Dib *et al.*, 1996), the GDB Human Genome Database (Fasman *et al.*, 1997) and in the database published by the Center for Medical Genetics, Marshfield, WI (Broman *et al.*, 1998).

In previous studies the SLC6A4 gene has been mapped by Ramamoorthy *et al.* (1993) to chromosome 17q11.2 - 17q12 using FISH and

somatic cell hybrids, and by Gelernter *et al.* (1995) to 17q12 (flanked by D17S58 and D17S73) using a RFLP in the 3'-UTR (for which 'SLC6A4' and 'HTT' are synonyms in the Genome Database). Our results are consistent with those of Esterling *et al.* (1998), who found close linkage of HTT to D17S1294, but differ in the order of D17S1294 and D17S2120. Surprisingly, these authors assigned different map positions to two markers (HTT and SGHC-11022) which should be coincident: the sequence of SGHC-11022 is nested within that of HTT.

The appearance of the markers D17S2009 and D17S2004 markers in our YAC contig suggested that the CPD gene might be present in this region. This was confirmed by PCR with primers from other regions of the CPD gene. Our results are in agreement with those of Riley *et al.* (1998), who recently localised the gene to 17p11.1-q11.1/11.2 by use of a regional mapping panel derived from somatic cell hybrids containing different portions of chromosome 17. Although no disorder has directly been linked with the CPD gene, it is possible that deficiency in this gene might affect the processing of secreted proteins. A mutation in the closely related carboxypeptidase E (CPE) gene has been reported to result in defective proinsulin processing leading to obesity and hyperglycaemia in *fat/fat* mice (Naggert *et al.*, 1995).

The NF1 gene is located on chromosome 17q11.2, close to the SLC6A4 gene. In a patient with neurofibromatosis type 1 resulting from a large deletion on 17q11.2 flanking the NF1 gene (Kayes *et al.*, 1992, 1994), the deletion included D17S120 and D17S117, which map closer to the centromere than SLC6A4 in the genome databases. In four other patients described by Kayes *et al.* (1994) and in the five cases reported by Cnossen *et al.* (1997), D17S117 defined the centromeric boundary of the possible extent of the deletions. This led us to predict and subsequently confirm that the SLC6A4 and CPD genes were hemizygotically deleted together with the NF1 gene in the patient NF106-3.

Editor
Neurofibromatosis type 1 is characterized by remarkable variation in the nature and severity of symptoms dependent on the mutations present. Hemizygoty of the SLC6A4 and/or CPD genes might account for some of the additional symptoms seen in NF1 patients with large chromosomal deletions, e.g. facial dysmorphology, mental retardation, and/or learning disabilities (Cnossen *et al.*, 1997; Kayes *et al.*, 1994; Leppig *et al.*, 1996, 1997; Riva *et al.*, 1996; Wu *et al.*, 1995, 1997). The SLC6A4 gene is transiently expressed in craniofacial epithelial structures during development, suggestive of a role for serotonin in craniofacial morphogenesis (Lauder *et al.*, 1988; Lauder and Zimmerman, 1988; Shuey *et al.*, 1993). Exposure of

mouse embryos in culture to inhibitors of the serotonin transporter caused craniofacial malformations consistent with a direct action at serotonin uptake sites (Shuey *et al.*, 1992). Polymorphic variation in the SLC6A4 gene has been reported to be associated with susceptibility to affective disorder (Battersby *et al.*, 1996; Collier *et al.*, 1996a,b; Harmar *et al.*, 1996; Kunugi *et al.*, 1997; Ogilvie *et al.*, 1996; Rees *et al.*, 1997) and to be a risk factor for late onset Alzheimer's disease (Li *et al.*, 1997) and autistic disorder (Cook *et al.*, 1997; Klauck *et al.*, 1997). It is possible that both the craniofacial malformations and the psychiatric disabilities exhibited by patients with large NF1 deletions may be due in part to hemizyosity of the SLC6A4 gene.

The identification of seven polymorphic STS markers flanking the SLC6A4 gene in our YAC contig will facilitate future studies of the role of the gene in susceptibility to developmental and psychiatric disorders. This contig will also provide centromeric anchor for chromosomal walking towards the NF1 gene which may lead to the discovery of other genes contiguous to NF1. Functional analysis of these genes should play an role in understanding of neurofibromatosis as well as other developmental/psychiatric disorders.

FIGURE LEGENDS

Figure 1: Analysis of YAC clones by pulsed-field gel electrophoresis and Southern blotting. (a) Resolution of YAC DNA by ethidium bromide staining. The sizes of yeast chromosomes from *S. cerevisiae* are shown in kb at the left. Lanes 1 to 8 are DNA from 793F2, 765D1, 923F8, 704F1, 782E2, 641D5, 35D8 and 132C6 respectively; The blot was sequentially hybridized with (b) a 854 bp Pst I fragment of SLC6A4 cDNA; (c) a 2.3 kb Eco RI - Pvu II fragment of pBR322 DNA; (d) the subclone 28L and (e) the subclone 24R.

Figure 2: Mapping of the SLC6A4 and CPD genes to 17q11.1 in a YAC/PAC contig.

(a) Physical map (not to scale) of the region of chromosome 17 between the centromere and D17S54 (b) diagram illustrating the extent of the deletion (---) in the patient NF106-3. The centromeric breakpoint (arrow head) of the deletion lies between D17S1294 and the last exon of the SLC6A4 gene, (c) the positions of the SLC6A4 (■) and CPD (▣) genes, STS markers and other probes in the eight YAC clones and one PAC clone (50G6) used in construction of the contig. Sizes of the clones are indicated in brackets. The orientations of the YAC vector arms for clones 35D8 and 132C6 are indicated with L (for long arm) and S (for short arm).

Orientation of the genomic insert in the PAC clone 50G6 is shown relative to the SP6 and T7 promoters of the PAC vector. The 3' end of the SLC6A4 gene is oriented towards the centromere. Circles represent the presence of STS markers, detected by PCR and probes 28L and 24R, detected by Southern hybridization, in the patient NF106-3 and in YAC/PAC clones.

Figure 3: Detection by FISH of hemizygotic deletion of the SLC6A4 gene in the patient NF106-3. Metaphase chromosomes were prepared from the NF106-3 cell line and hybridized with 50G6 PAC DNA. The two chromosomes 17 are arrowed: SLC6A4 is present in only one of them.

Figure 4: Localization by PCR of the centromeric breakpoint of the deletion in patient NF106-3. DNA templates were as follows: (lane 1) YAC 765D1; (lane 2) genomic DNA from patient NF106-3; (lane 3) cell line NF106-3-#36 carrying the deleted chromosome 17; (lane 4) cell line NF106-3-#41 carrying the non-deleted chromosome 17; (line 5) the control RJK cell line. The primers pairs used (Table 1) and the size of the PCR product in bp are indicated at the right. The specific PCR product of the E2F and 2B primer pair is arrowed. Note that the centromeric breakpoint of the deletion lies between D17S1294 and exon 14 (defined by primer P3) of the SLC6A4 gene.

REFERENCES

- Anand, R., Riley, J. H., Butler, R., Smith, J. C., and Markham, A. F. (1990). A 3.5 genome equivalent multi access YAC library: construction, characterisation, screening and storage. *Nucleic Acids Res.* 18: 1951-6.
- Anderson, I. M., and Tomenson, B. M. (1994). The efficacy of selective serotonin re-uptake inhibitors in depression: a meta-analysis of studies against tricyclic antidepressants. *J. Psychopharmacol.* 8: 238-249.
- Andersson, B., Wentland, M. A., Ricafrente, J. Y., Liu, W., and Gibbs, R. A. (1996). A "double adaptor" method for improved shotgun library construction. *Anal. Biochem.* 236: 107-13.
- Battersby, S., Ogilvie, A. D., Smith, C. A. D., Blackwood, D. H. R., Muir, W. J., Quinn, J. P., Fink, G., Goodwin, G. M., and Hammar, A. J. (1996). Structure of a VNTR of the serotonin transporter gene and association with affective disorder. *Psychiatr. Genet.* 6: 177-181.
- Bellis, M., Pages, M., and Roizes, G. (1987). A simple and rapid method for preparing yeast chromosomes for pulsed field gel electrophoresis. *Nucleic Acids Res.* 15: 6749.
- Bradley, C. C., and Blakely, R. D. (1997). Alternative splicing of the human serotonin transporter gene. *J. Neurochem.* 69: 1356-67.
- Broman, K. W., Murray, J. C., Sheffield, V. C., White, R. L., and Weber, J. L. (1998). Comprehensive Human Genetic Maps: Individual and Sex-Specific Variation in Recombination. *Am. J. Hum. Genet.* 63: 861-9.
- Chumakov, I. M., Le Gall, I., Billault, A., Ougen, P., Soularue, P., Guillou, S., Rigault, P., Bui, H., De Tand, M. F., Barillot, E., Abderrahim, H., Cherif, D., Berger, R., Lepaslier, D., and Cohen, D. (1992). Isolation of chromosome 21-specific yeast artificial chromosomes from a total human genome library. *Nat. Genet.* 1: 222-5.
- Cnossen, M. H., van der Est, M. N., Breuning, M. H., van Asperen, C. J., Breslau-Siderius, E. J., van der Ploeg, A. T., de Goede-Bolder, A., van den Ouweland, A. M., Halley, D. J., and Niermeijer, M. F. (1997). Deletions spanning the neurofibromatosis type 1 gene: implications for genotype-phenotype correlations in neurofibromatosis type 1? *Hum. Mutat.* 9: 458-64.
- Collier, D. A., Arranz, M. J., Sham, P., Battersby, S., Vallada, H., Gill, P., Aitchison, K. J., Sodhi, M., T., L., Roberts, G. W., Smith, B., Morton, J., Murray, R. M., Smith, D., and Kirov, G. (1996a). The serotonin transporter gene is a potential susceptibility factor for bipolar affective disorder. *Neuroreport* 7: 1675-1679.
- Collier, D. A., Stoeber, G., Li T, Hiels, A., Catalano, M., Di Bella, D., Arranz, M. J., Murray, R. M., Smith, D., and Kirov, G. (1996b). A novel functional polymorphism within the promoter of the serotonin transporter gene: possible role in susceptibility to affective disorders. *Mol. Psychiatry* 1: 453-460.
- Collins, A., Frezal, J., Teague, J., and Morton, N. E. (1996a). A metric map of humans: 23,500 loci in 850 bands. *Proc Natl Acad Sci U S A* 93: 14771-5.
- Collins, A., Teague, J., Keats, B. J., and Morton, N. E. (1996b). Linkage map integration. *Genomics* 36: 157-62.
- Cook, E. H., Jr., Courchesne, R., Lord, C., Cox, N. J., Yan, S., Lincoln, A., Haas, R., Courchesne, E., and Leventhal, B. L. (1997). Evidence of linkage between the serotonin transporter and autistic disorder. *Mol. Psychiatry* 2: 247-50.

- Dib, C., Faure, S., Fizames, C., Samson, D., Drouot, N., Vignal, A., Millasseau, P., Marc, S., Hazan, J., Seboun, E., Lathrop, M., Gyapay, G., Morissette, J., and Weissenbach, J. (1996). A comprehensive genetic map of the human genome based on 5,264 microsatellites. *Nature* 380: 152-4.
- Edelhoff, S., Ayer, D. E., Zervos, A. S., Steingrimsson, E., Jenkins, N. A., Copeland, N. G., Eisenman, R. N., Brent, R., and Distèche, C. M. (1994). Mapping of two genes encoding members of a distinct subfamily of MAX interacting proteins: MAD to human chromosome 2 and mouse chromosome 6, and MXI1 to human chromosome 10 and mouse chromosome 19. *Oncogene* 9: 665-8.
- Esterling, L. E., Yoshikawa, T., Turner, G., Badner, J. A., Bengel, D., Gershon, E. S., Berrettini, W. H., and Detera-Wadleigh, S. D. (1998). Serotonin transporter (5-HTT) gene and bipolar affective disorder. *Am. J. Med. Genet.* 81: 37-40.
- Fasman, K. H., Letovsky, S. I., Li, P., Cottingham, R. W., and Kingsbury, D. T. (1997). The GDB Human Genome Database Anno 1997. *Nucleic Acids Res.* 25: 72-81.
- Gelernter, J., Pakstis, A. J., and Kidd, K. K. (1995). Linkage mapping of serotonin transporter protein gene SLC6A4 on chromosome 17. *Hum. Genet.* 95: 677-80.
- Harmar, A. J., Ogilvie, A. D., Battersby, S., Smith, C. A. D., Blackwood, D. H. R., Muir, W. J., Fink, G., and Goodwin, G. M. (1996). The serotonin transporter gene and affective disorder. *Cold Spring Harb. Symp. Quant. Biol.* 61: 791-795.
- Heils, A., Teufel, A., Petri, S., Stober, G., Riederer, P., Bengel, D., and Lesch, K. P. (1996). Allelic variation of human serotonin transporter gene expression. *J. Neurochem.* 66: 2621-2624.
- Ioannou, P. A., Amemiya, C. T., Garnes, J., Kroisel, P. M., Shizuya, H., Chen, C., Batzer, M. A., and de Jong, P. J. (1994). A new bacteriophage P1-derived vector for the propagation of large human DNA fragments. *Nat. Genet.* 6: 84-9.
- Ishikawa, T., Murakami, K., Kido, Y., Ohnishi, S., Yazaki, Y., Harada, F., and Kuroki, K. (1998). Cloning, functional expression, and chromosomal localization of the human and mouse gp180-carboxypeptidase D-like enzyme. *Gene* 215: 361-70.
- Kayes, L. M., Burke, W., Riccardi, V. M., Bennett, R., Ehrlich, P., Rubenstein, A., and Stephens, K. (1994). Deletions spanning the neurofibromatosis 1 gene: identification and phenotype of five patients. *Am. J. Hum. Genet.* 54: 424-36.
- Kayes, L. M., Riccardi, V. M., Burke, W., Bennett, R. L., and Stephens, K. (1992). Large de novo DNA deletion in a patient with sporadic neurofibromatosis 1, mental retardation, and dysmorphism. *J. Med. Genet.* 29: 686-90.
- Klauck, S. M., Poustka, F., Berner, A., Lesch, K. P., and Poustka, A. (1997). Serotonin transporter (5-HTT) gene variants associated with autism? *Hum. Mol. Genet.* 6: 2233-8.
- Kunugi, H., Hattori, M., Kato, T., Tatsumi, M., Sakai, T., Sasaki, T., Hirose, T., and Nanko, S. (1997). Serotonin transporter gene polymorphisms: ethnic difference and possible association with bipolar affective disorder. *Mol. Psychiatry* 2: 457-62.
- Larin, Z., Monaco, A. P., and Lehrach, H. (1991). Yeast artificial chromosome libraries containing large inserts from mouse and human DNA. *Proc Natl Acad Sci U S A* 88: 4123-7.
- Lauder, J. M., Tamir, H., and Sadler, T. W. (1988). Serotonin and morphogenesis. I. Sites of serotonin uptake and -binding protein immunoreactivity in the midgestation mouse embryo. *Development* 102: 709-20.

- Lauder, J. M., and Zimmerman, E. F. (1988). Sites of serotonin uptake in epithelia of the developing mouse palate, oral cavity, and face: possible role in morphogenesis. *J. Craniofac. Genet. Dev. Biol.* 8: 265-76.
- Leppig, K. A., Kaplan, P., Viskochil, D., Weaver, M., Ortenberg, J., and Stephens, K. (1997). Familial neurofibromatosis 1 microdeletions: cosegregation with distinct facial phenotype and early onset of cutaneous neurofibromata. *Am. J. Med. Genet.* 73: 197-204.
- Leppig, K. A., Viskochil, D., Neil, S., Rubenstein, A., Johnson, V. P., Zhu, X. L., Brothman, A. R., and Stephens, K. (1996). The detection of contiguous gene deletions at the neurofibromatosis 1 locus with fluorescence in situ hybridization. *Cytogenet. Cell Genet.* 72: 95-8.
- Lesch, K. P., Bengel, D., Heils, A., Sabol, S. Z., Greenberg, B. D., Petri, S., Benjamin, J., Müller, C. R., Hamer, D. H., and Murphy, D. L. (1996). Association of anxiety related traits with a polymorphism in the serotonin transporter gene. *Science* 274: 1527-1531.
- Li, T., Holmes, C., Sham, P. C., Vallada, H., Birkett, J., Kirov, G., Lesch, K. P., Powell, J., Lovestone, S., and Collier, D. (1997). Allelic functional variation of serotonin transporter expression is a susceptibility factor for late onset Alzheimer's disease. *Neuroreport* 8: 683-6.
- Li, Y., O'Connell, P., Breidenbach, H. H., Cawthon, R., Stevens, J., Xu, G., Neil, S., Robertson, M., White, R., and Viskochil, D. (1995). Genomic organization of the neurofibromatosis 1 gene (NF1). *Genomics* 25: 9-18.
- Naggert, J. K., Fricker, L. D., Varlamov, O., Nishina, P. M., Rouille, Y., Steiner, D. F., Carroll, R. J., Paigen, B. J., and Leiter, E. H. (1995). Hyperproinsulinaemia in obese fat/fat mice associated with a carboxypeptidase E mutation which reduces enzyme activity. *Nat. Genet.* 10: 135-42.
- Ogilvie, A. D., Battersby, S., Bubb, V. J., Fink, G., Goodwin, G. M., Harmar, A. J., and Smith, C. A. D. (1996). A polymorphism of the serotonin transporter gene is associated with susceptibility to major affective disorder. *Lancet* 347: 731-733.
- Ramamoorthy, S., Bauman, A. L., Moore, K. R., Han, H., Yang-Feng, T., Chang, A. S., Ganapathy, V., and Blakely, R. D. (1993). Antidepressant- and cocaine-sensitive human serotonin transporter: molecular cloning, expression, and chromosomal localization. *Proc Natl Acad Sci U S A* 90: 2542-6.
- Rees, M., Norton, N., Jones, I., McCandless, F., Scourfield, J., Holmans, P., Moorhead, S., Feldman, E., Sadler, S., Cole, T., Redman, K., Farmer, A., McGuffin, P., Owen, M. J., and Craddock, N. (1997). Association studies of bipolar disorder at the human serotonin transporter gene (hSERT; 5HTT). *Mol. Psychiatry* 2: 398-402.
- Riley, D. A., Tan, F., Miletich, D. J., and Skidgel, R. A. (1998). Chromosomal localization of the genes for human carboxypeptidase D (CPD) and the active 50-kilodalton subunit of human carboxypeptidase N (CPN1). *Genomics* 50: 105-8.
- Riva, P., Castorina, P., Manoukian, S., Dalpra, L., Doneda, L., Marini, G., den Dunnen, J., and Larizza, L. (1996). Characterization of a cytogenetic 17q11.2 deletion in an NF1 patient with a contiguous gene syndrome. *Hum. Genet.* 98: 646-50.
- Rudnick, G., and Wall, S. C. (1992). The molecular mechanism of "ecstasy" [3,4-methylenedioxy-methamphetamine (MDMA)]: serotonin transporters are targets for MDMA- induced serotonin release. *Proc Natl Acad Sci U S A* 89: 1817-21.
- Schedl, A., Montoliu, L., Kelsey, G., and Schutz, G. (1993). A Yeast Artificial Chromosome Covering the Tyrosinase Gene Confers Copy Number-Dependent Expression In Transgenic Mice. *Nature* 362: 258-261.

Shen, M. H., Harper, P. S., and Upadhyaya, M. (1996). Molecular genetics of neurofibromatosis type 1 (NF1). *J. Med. Genet.* 33: 2-17.

Shuey, D. L., Sadler, T. W., and Lauder, J. M. (1992). Serotonin as a regulator of craniofacial morphogenesis: site specific malformations following exposure to serotonin uptake inhibitors. *Teratology* 46: 367-78.

Shuey, D. L., Sadler, T. W., Tamir, H., and Lauder, J. M. (1993). Serotonin and morphogenesis. Transient expression of serotonin uptake and binding protein during craniofacial morphogenesis in the mouse. *Anat Embryol (Berl)* 187: 75-85.

Tan, F., Chan, S. J., Steiner, D. F., Schilling, J. W., and Skidgel, R. A. (1989). Molecular cloning and sequencing of the cDNA for human membrane-bound carboxypeptidase M. Comparison with carboxypeptidases A, B, H, and N. *J. Biol. Chem.* 264: 13165-70.

Tan, F. L., Rehli, M., Krause, S. W., and Skidgel, R. A. (1997). Sequence of human carboxypeptidase D reveals it to be a member of the regulatory carboxypeptidase family with three tandem active site domains. *Biochem. J.* 327: 81-87.

Wu, B. L., Austin, M. A., Schneider, G. H., Boles, R. G., and Korf, B. R. (1995). Deletion of the entire NF1 gene detected by the FISH: four deletion patients associated with severe manifestations. *Am. J. Med. Genet.* 59: 528-35.

Wu, B. L., Schneider, G. H., and Korf, B. R. (1997). Deletion of the entire NF1 gene causing distinct manifestations in a family. *Am. J. Med. Genet.* 69: 98-101.

Table I. Primer pairs used for PCR

Forward Primers (5' - 3')	Reverse Primers (5' - 3')	Product	Size
31013 CACCTAACCCCTAATGTCCCTACT	31014 GGACTGAGCTGGACAACCAC	SLC6A4 5-HTTLPR	458/502 bp
1AP (F) GCTCTAGGTGGACACAGAATC	1AP (R) TCGCGCTTGTGTTCCAGTAC	SLC6A4 Exon 1a	545 bp
43084 CTTGCCAGGAGCGGAGGAGG	43085 AACTCCTCTCCGGTACTAATCG	SLC6A4 Exon 1-Intron 1a	10 kb
44771 CTAGTGACTGACATTTGCCCTGG	44772 TGTCCAGTCTATCTGCCACATG	SLC6A4 Exon 1b	824 bp
43088 GCTTGGCGTTGGCCGCTCTGAATGC	43089 TAGCAGCAGCAGTGGACAGTTACC	SLC6A4 Intron 1a-Exon 2	3.5 kb
26373 ACTAACCCAGCAGGATGGAGAGG	26374 TAGAGTCCCGTGTGTCACTCC	SLC6A4 Exon 2	199 bp
18564 GTCAGTATCACAGGCTGGGAG	18565 TGTTCCTAFTCTTACGCCAGTG	SLC6A4 Intron 2 VNTR	249/266/299 bp
26373 ACTAACCCAGCAGGATGGAGAGG	2B TTAGACCCGGTGGATCTGCAG	SLC6A4 Exons 2-5	5 kb
54073 TGGCAAGGTGAGGAAGGCTCTGG	54074 CCACCTCAGACACATCTCATTTCC	SLC6A4 Exons 5-8	4 kb
5A ATGAAGATGTCTTGAGGTGG	5B ACAGCGACTGCTTCGATCAG	SLC6A4 Exons 8-11	3.8 kb
6A TACGTGGTGAAGCTGCTGGGA	P3 GAGGAGGAGTTGTGGAGAAGCC	SLC6A4 Exons 11-14	>12 kb
26375 AGTTCGTGATGAGGCACGC	26376 TTCATCACCTCCATCCACATCC	SLC6A4 Exon 14	223 bp
60703 ATCACATTAGAAGTGTCTTTGTTGC	60704 AGGTATTCTATGAGGTTCAACACAGC	CPD 1065F + CPD 1768R	2.7 kb
60705 TTATGTAGTTCAGTAAGATGTGCC	60706 GCAAGTATCTTCAACTGGATAGG	CPD 6740F + CPD 6858R	118 bp
2009F TGGCTTTAGTATTTTCTTTGTTTTT	2004F GAAACACTGAAGAAATGCATTTCC	D17S2009F+D17S2004F	2.1 kb
56217 CAGACCCCTCCTTTGCCCTCTT	56218 GGATGGAGGTCGGAGGCTG	NF1 Ex1	438 bp
56219 GTTACAAGTAAAGAAATGTTGTAG	56220 CTAACAAGTGGCCCTGTTGGCAAAC	NF1 Ex27	298 bp
56221 AGCCAGGAAATCGCTTGAACC	56222 CTCCTTACTTCCAGCCTAAGC	NF1 Ex28	218 bp
56223 GCAATGAATTCAGTCTCTGGAAGG	56224 CCCACTTTCTTGGCAGTTGTTCTG	NF1 Ex49	449 bp
62713 CTGGGTTTCTACCAATTATCTTGG	62714 GTGGCGAACACAGATAGCCCATTTA	CRYB1	424 bp

Table II Analyses of YAC/PAC clones containing the SLC6A4 and CPD genes

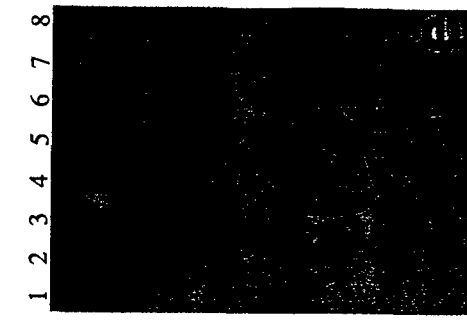
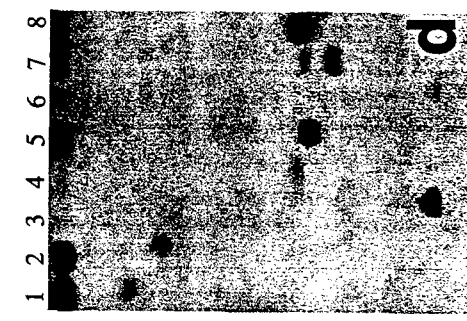
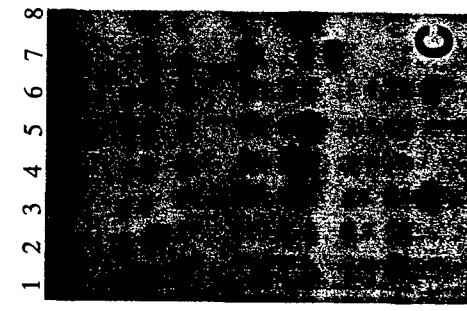
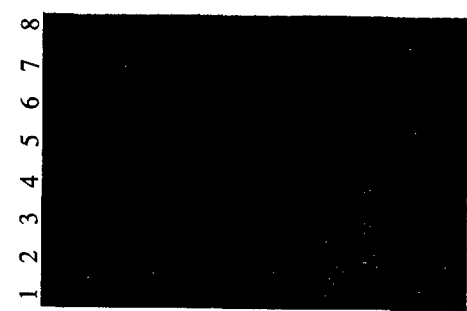
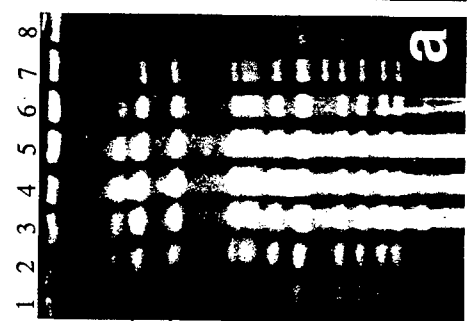
GLD	Markers	704F1 640 kb	50G6 95 kb	78E2 600 kb	132C6 630 k	923F8 160 kb	35D8 500 kb	765D1 1000 kb	49A9 230 kb	793F2 1600 kb	641D5 140 kb	16FC9 820 kb	947G11 600 kb
28.040	D17S1543	-	-	-	-	-	-	-	-	-	-	-	-
	TIGR-A004R11	-	-	-	-	-	-	-	-	-	-	-	-
	TIGR-A007E42	-	-	-	-	-	-	-	-	-	-	-	-
28.061	D17S1317	-	-	-	-	-	-	-	-	-	-	-	-
28.146	D17S1873	-	-	-	-	-	-	-	-	-	-	-	-
	SHGC37126	-	-	-	-	-	-	-	-	-	-	-	-
	SHGC36334	-	-	-	-	-	-	-	-	-	-	-	-
28.191	D17S1824	-	-	-	-	-	-	-	-	-	-	-	-
28.253	D17S975	-	-	-	-	-	-	+	-	-	-	-	-
28.373	D17S1549	+	-	+	-	+	+	+	-	-	-	-	-
	24R (probe)	+	+	+	+	+	+	+	NE	-	-	NE	-
28.318	D17S1294	+	+	+	+	+	+	+	-	-	-	-	-
	EX 14	+	+	+	+	+	+	+	+	+	+	-	-
	EX 5-8	+	+	+	+	+	+	+	+	+	+	-	-
	EX 2-5	+	+	+	+	+	+	+	+	+	+	-	-
	IN 2 VNTR	10	10	10	10	10	10	10	10	10	-	10	-
	EX 2	+	+	+	+	+	+	+	+	+	-	+	-
	EXON 1B	+	+	+	+	+	+	+	+	+	-	+	-
	1AP	-	+	+	+	+	+	+	+	+	-	+	+
	5'HTTLPR	-	+	L	S	L	S	L	+	L	-	NE	L
	28L (probe)	-	+	+	+	+	+	+	NE	+	-	NE	+
	CPD6740/6858	-	-	-	-	-	+	+	+	-	-	-	+
28.454	D17S2009	-	-	-	-	-	+	+	+	-	-	-	+
28.521	D17S2004	-	-	-	-	-	+	+	+	-	-	-	+
	CPD1065/1768	-	-	-	-	-	+	+	+	-	-	-	+
28.587	D17S1863	-	-	-	-	+	-	+	+	-	-	-	+
	D17S2120	-	-	-	-	+	-	+	+	-	-	-	+
28.587	D17S1837	-	-	-	-	-	-	-	-	-	-	-	-
	Chimerism	CS	NCF	NE	NCF	NE	NCF	NE	CF	CS	CS	CS	NE

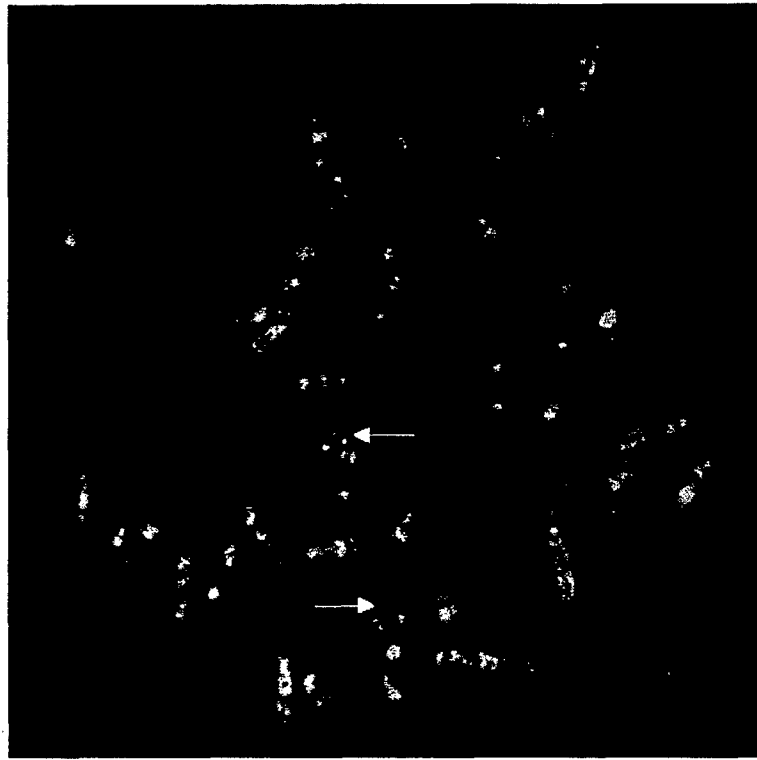
YAC/PAC DNA were analysed by PFGE, hybridisation, FISH, and PCR for STS markers and other primers. NCF: not chimeric demonstrated by FISH; CF: chimeric revealed by FISH; CS: Chimeric determined by Southern hybridization and STS analyses; NE: not examined. (+): positive by PCR or hybridization, (-): negative by PCR or hybridization. Alleles of the polymorphism in the promoter region (5'HTTLPR) are indicated by L (long form) and S (short form), and the VNTR in intron 2 was the 10 repeat allele (10) for all YACs tested. Column 28L and 24R are from hybridisation data. YAC sizes were determined by hybridisation with pBR322 plasmid DNA. Column GLD shows the distances (in Mb) of markers to 17pter in the Genetic Location Database (Collins *et al.*, 1996b).

Lane 1 2 3 4 5 6 7 8

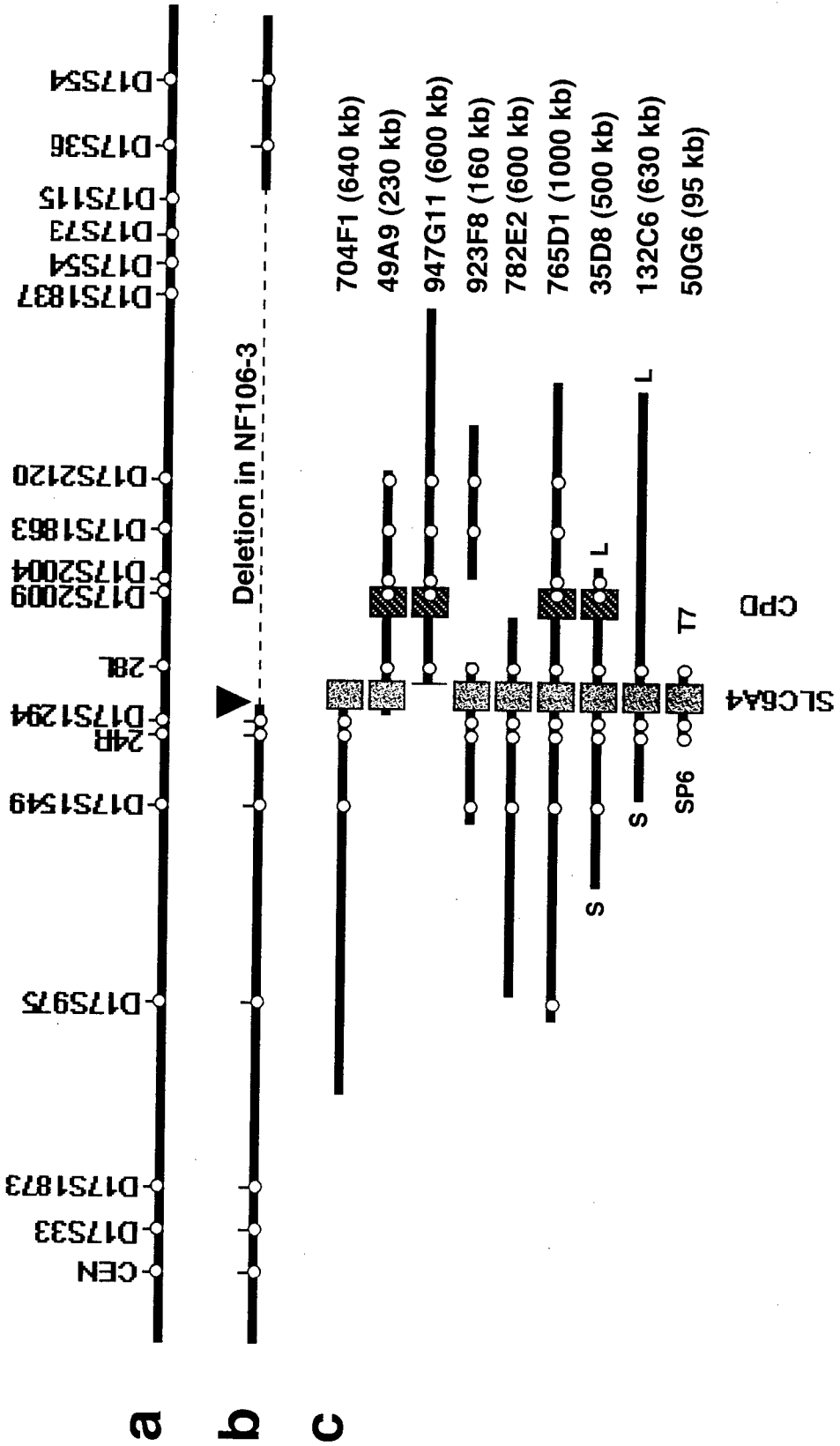
Kb

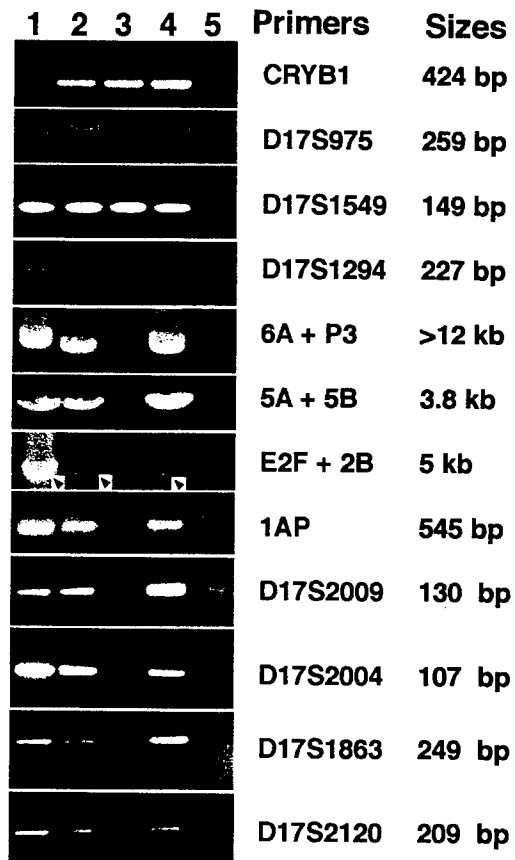
1900/1640
1120/1100
945/915
815
785
745
680
610/555
450
375
295
225





Proprietary Information







DEPARTMENT OF THE ARMY

US ARMY MEDICAL RESEARCH AND MATERIEL COMMAND
504 SCOTT STREET
FORT DETRICK, MARYLAND 21702-5012

REPLY TO
ATTENTION OF:

MCMR-RMI-S (70-1y)

23 Aug 01

MEMORANDUM FOR Administrator, Defense Technical Information
Center (DTIC-OCA), 8725 John J. Kingman Road, Fort Belvoir,
VA 22060-6218


SUBJECT: Request Change in Distribution Statement

1. The U.S. Army Medical Research and Materiel Command has reexamined the need for the limitation assigned to the technical reports listed at enclosure. Request the limited distribution statement for these reports be changed to "Approved for public release; distribution unlimited." These reports should be released to the National Technical Information Service.

2. Point of contact for this request is Ms. Judy Pawlus at DSN 343-7322 or by e-mail at judy.pawlus@det.amedd.army.mil.

FOR THE COMMANDER:

Encl


PHYLIS M. RINEHART
Deputy Chief of Staff for
Information Management

Reports to be Downgraded to Unlimited Distribution

ADB241560	ADB253628	ADB249654	ADB263448
ADB251657	ADB257757	ADB264967	ADB245021
ADB263525	ADB264736	ADB247697	ADB264544
ADB222448	ADB255427	ADB263453	ADB254454
ADB234468	ADB264757	ADB243646	
ADB249596	ADB232924	ADB263428	
ADB263270	ADB232927	ADB240500	
ADB231841	ADB245382	ADB253090	
ADB239007	ADB258158	ADB265236	
ADB263737	ADB264506	ADB264610	
ADB239263	ADB243027	ADB251613	
ADB251995	ADB233334	ADB237451	
ADB233106	ADB242926	ADB249671	
ADB262619	ADB262637	ADB262475	
ADB233111	ADB251649	ADB264579	
ADB240497	ADB264549	ADB244768	
ADB257618	ADB248354	ADB258553	
ADB240496	ADB258768	ADB244278	
ADB233747	ADB247842	ADB257305	
ADB240160	ADB264611	ADB245442	
ADB258646	ADB244931	ADB256780	
ADB264626	ADB263444	ADB264797	